

## ABSTRACT

Title of dissertation: SUB ALFVÉNIC REDUCED EQUATIONS  
IN A TOKAMAK

Wrick Sengupta, Doctor of Philosophy, 2016

Dissertation directed by: Professor Adil B. Hassam  
Department of Physics

Magnetized fusion experiments generally perform under conditions where ideal Alfvénic modes are stable. It is therefore desirable to develop a reduced formalism which would order out Alfvénic frequencies. This is challenging because sub-Alfvénic phenomena are sensitive to magnetic geometries. In this work an attempt has been made to develop a formalism to study plasma phenomena on time scales much longer than the Alfvénic time scales.

In Part I, a reduced set of MHD equations is derived, applicable to large aspect ratio tokamaks and relevant for dynamics sub-Alfvénic with respect to ideal ballooning modes. Our ordering optimally allows sound waves, Mercier modes, drift modes, geodesic-acoustic modes, zonal flows, and shear Alfvén waves. Long to intermediate wavelengths are considered. With the inclusion of resistivity, tearing modes, resistive ballooning modes, Pfirsch-Schluter cells, and the Stringer spin-up are also included. A major advantage is that the resulting system is 2D in space, and the system incorporates self-consistent dynamic Shafranov shifts. A limitation is that the system is valid only in radial domains where the tokamak safety factor,

$q$ , is close to a rational. Various limits of our equations, including axisymmetric and subsonic limits, are considered. In the tokamak core, the system is well suited as a model to study the sawtooth discharge in the presence of Mercier modes.

In Part II, we show that the methods of Part I can be directly applied to derive sub-Alfvénic but supersonic reduced fluid equations, for collisionless plasmas, starting from a drift-kinetic description in MHD ordering.

In Part III, we begin a reduced description of sub-Alfvénic phenomena for collisionless kinetic MHD in the subsonic limit. We limit ourselves to discuss axisymmetric modes, including geodesic acoustic modes (GAMs), sound waves and zonal flows. In axisymmetric geometry it is well known that trapped particles precess toroidally at speeds much exceeding the  $\mathbf{E} \times \mathbf{B}$  speed. This large flow is expected to contribute a large effective inertia. We show that the kinetic analog of the “Pfirsch-Schluter” effective inertia ( $1 + 2q^2$ ) is augmented by the well-known Rosenbluth-Hinton factor  $\approx 1.6q^2/\sqrt{\epsilon}$ .

SUB-ALFVÉNIC REDUCED EQUATIONS  
IN A TOKAMAK

by

Wrick Sengupta

Dissertation submitted to the Faculty of the Graduate School of the  
University of Maryland, College Park in partial fulfillment  
of the requirements for the degree of  
Doctor of Philosophy  
2016

Advisory Committee:

Professor Adil B. Hassam, Chair/Advisor

Professor Thomas Antonsen, Dean's representative

Professor James F. Drake

Professor William Dorland

Dr Jason TenBarge

© Copyright by  
Wrick Sengupta  
2016

## Dedication

To my loving parents,  
whose self-less sacrifice  
made all of this possible.

## Acknowledgments

I would like to take this opportunity to convey my thanks to those individuals who helped me during the last few years of my graduate life. I owe my greatest thanks to my loving parents. They have always encouraged me to pursue my interests in science and made great sacrifices to make that possible. Coming from a middle class family in India means getting the bare minimum education that helps one secure a good paying job. Science is definitely not the top priority. My parents, on the other hand, understood the value of science and have been very supportive throughout. I never had the luxury of being rich, but who cares if one has the luxury of spending one's entire day reading Feynman's lectures? My parents gave me that life and I am really grateful to them. My extended family, particularly my uncles, aunts, and cousins also helped me a lot. I deeply appreciate their love and encouragement.

Just like my parents, I got an equally loving, caring and immensely helpful advisor, Prof. Adilnawaz Badrudin Satchu Hassam, who has a heart commensurate with his name. He has been like a second father to me. He has advised me on so many levels. I have been very fortunate to have TA'd with him before I started working under him. My TA experience was as great as my research experience. He introduced me to the wonders of plasma physics through his lectures. He has not only provided me with interesting research problems but has actually held my hand throughout. He has spent hours doing nitty-gritty algebra on the blackboard. He spent hours helping me write the papers, posters, and finally this thesis. I am

absolutely sure I could not have asked for more. I take this moment to thank him from the core of my heart and wish him and his family the very best. The only way I can truly return his favor is by advising some student in the future, with the same level of patience and commitment. Hopefully I can make that possible through hard work.

I have been also very lucky to have had the pleasure of knowing a few professors closely and they have made a great impact on my graduate life. In stark contrast to my undergraduate years (spent in a so called ‘premiere Indian institute’), my graduate life has been excellent. I couldn’t have hoped for a better grad life! Thanks goes to professors like Bill Dorland who inspired me not only to do good physics but also to be a good human being. I have received a great deal of encouragement and support from him over the last few years and knowing him has definitely been a very high point in my graduate life. He has helped me tremendously in my search for postdoctoral positions. Anyone in the plasma community knows how much of a big shot he is but he has always been very down-to-earth. Thanks Bill for all the time that you have taken out of your busy schedule to hang out with me and others at your house, office, or the Escape Room. I wish you and your family good health and may you always stay as cheerful as you have been. Thanks also to Sarah and Kendall for letting me stay at their house and pet their lovely dog Roxy.

I am also very fortunate to be in the same floor as Prof. Rajarshi Roy. We speak the same language, we love the same type of food, music, and we share similar backgrounds. I have constantly received love and treasures from him including books, music, snacks, advice, and sometimes just his infectious enthusiasm. I wish

I could have stayed in his vicinity for some more time.

The notes that I have received from Prof. Jim Drake and Tom Antonsen speak volumes about their creators. They have a wealth of information which is not easy, if not impossible, to glean from standard text books. The reason why these notes are so great is that Jim and Tom have thought about these problems in their own intuitive and highly creative ways. It has also been a privilege for me to participate in group meetings at UMD attended by stalwarts like them. Thanks also for the reference letters; I deeply appreciate it. I would also like to express my sincere thanks for all the help I received from Dr. Matt Landreman and Dr. Jason TenBarge. Jason has also made valuable suggestions and corrections for the overall improvement of this thesis, for which I am immensely grateful.

I can't end the acknowledgement section on professors and teachers without mentioning my academic grandfather Prof. R.M. Kulsrud! I was extremely lucky last year to be able to finally meet him at an APS conference. We had a very long discussion which went over 6 hours! We discussed plasma physics (his equation mostly). I was overjoyed when he thanked me for letting him know about a certain invariant in his equation. He told me so many stories about famous physicists like Fermi, Chandrasekhar, Spitzer with whom he had one-on-one discussions. If I could do a time loop I would probably go to that day again.

Graduate life would have been very boring and lonely if I didn't have my wonderful friends, colleagues and office mates. I benefited a lot from my discussions with Dr. Ian Abel, Prof. Steve Cowley, Prof. Felix Parra, Prof. Ivan Calvo, Prof. Michael Barnes, Prof. Alex Schekochihin, Prof. István Pusztai, Adam Stahl, Prof.



Tünde Fülöp, Dr. Obioma Ohia, and Dr. Marc Swisdak. I have also been very fortunate to have Lora, George, Joel, Jimmy, Gareth, Qile, Elizabeth, Ching Pui, Anjor, Joe Hart, and Mike as my office mates and Dibyendu, Soumyada, Ranchu, Jonathan, Da, Srimoyee, Ayoti, Ramda, Liz, Tristin, Arthur, Tawfeeq, Mary ,and all IHOPpers and friends at Graduate Hills as my housemates. Everyone brought a different flavor to my life. They laughed at my silly jokes. Not being good actors, their laughs were as fake as Jimmy Fallon's, but nonetheless it made me happy and feel accomplished. So thanks a lot! Special thanks goes to Elizabeth, George, and Amber Wilkie for helping me out so many times with so many things and providing me with valuable advice.

I would also like to acknowledge my gratitude to Prof. Antoine Cerfón and Prof. Harold Weitzner for offering me a postdoc position at Courant Institute of Mathematical Sciences, NYU. It is a new beginning and hopefully the valuable things I learnt here at the University of Maryland, College Park would be helpful. My last thanks goes to the reader who has been patient enough to reach the very end of this.

## Table of Contents

List of Figures	x
List of Abbreviations	xi
1 General Introduction	1
1.1 Reduced MHD	1
1.2 Scope of this work	3
2 Sub-Alfvénic reduced equations: Ideal MHD	6
2.1 Overview	6
2.2 Introduction	7
2.3 Sub-Alfvénic reduced MHD in a cylinder	10
2.3.1 Equations and ordering	11
2.3.2 Asymptotic expansion of the Ideal MHD equations	13
2.3.3 Summary: Closed set in a cylinder	19
2.4 Reduction in Toroidal Geometry	21
2.4.1 Summary: closed set in a torus	27
2.5 Further reduction	28
2.5.1 Summary: closed set in a torus (in new variables)	32
2.6 Resistive MHD	32
2.6.1 Summary: reduced Resistive MHD equations in a torus	34
2.7 Complete set of toroidal sub-Alfvénic equations	35
2.8 Invariants of the Reduced system	37
2.9 Various sub-limits	38
2.9.1 Axisymmetric limit	38
2.9.2 Subsonic limit	40
2.10 Linearized modes	41
2.10.1 Ideal MHD interchange modes without shear	43
2.10.2 Ideal MHD Linear modes with shear	44
2.10.3 Resistive ballooning without shear	45
2.10.4 Resistive MHD modes with shear	46
2.11 Summary and Discussion	47

3	Sub-Alfvénic and supersonic reduced Kinetic MHD	51
3.1	Overview	51
3.2	Kinetic MHD Equations and ordering	51
3.3	Supersonic limit	54
3.4	Summary and discussion	59
4	Sub-Alfvénic Axisymmetric Kinetic MHD	61
4.1	Overview	61
4.2	Introduction	62
4.3	Kinetic Equations	66
4.4	The classic Rosenbluth Hinton problem	68
4.4.1	Rosenbluth-Hinton $\parallel$ flows	70
4.5	Shifted coordinates	71
4.6	The RH problem revisited	73
4.6.1	Sub-bounce limit	73
4.6.2	RH flows	74
4.6.3	RH Effective mass	77
4.6.4	Flows and effective masses for truncated distributions	78
4.7	The role of the barely circulating particles	80
4.8	Effective mass factor in collisional and collisionless axisymmetric dynamics	84
4.9	Summary	88
5	Conclusion	90
0	Various sub-Alfvénic modes	92
A	Operators and Commutators	96
B	Identities satisfied by flutes	99
C	Evaluation of $\{\langle \partial_R \Psi_1, n_0 \rangle\}$	101
D	Evaluation of $\langle \partial_z N_1 \rangle$ in the subsonic limit	103
E	Conserved quantities	104
E.1	Flux and magnetic helicity conservation	104
E.2	Cross helicity	104
E.3	Angular momentum	104
E.4	Energy	105
F	Vorticity equation in $\mathcal{E}$ and $\mathcal{E}_*$ coordinates	107
G	Proof of equivalence of Angular momentum and vorticity equation	108
H	$J_{\parallel}$ invariance	109



## List of Figures

2.1	Interchanges on a rational flux surface . . . . .	8
2.2	Field line following coordinate system . . . . .	15
4.1	Comparison of initial and final RH flows . . . . .	63
4.2	A toy model . . . . .	64
4.3	Comparison of the coordinate systems. [4.3a] standard energy coordinates $(\text{sign}(v_{  }), \mathcal{E}, \theta)$ . [4.3b] the shifted coordinates $(\text{sign}(v_{  *}), \mathcal{E}_*, \theta)$ . The shift is $I\phi'/B$ . . . . .	73
4.4	The distribution function is nonzero only well above the separatrix $\mathcal{E}_* = \mu B_0(1 + \epsilon)$ . . . . .	80
4.5	New toy model with potential $V(\theta)$ . . . . .	81
4.6	driven pendulum phase portrait . . . . .	82

## List of Abbreviations

MHD	Magneto-Hydrodyanmics
RMHD	Reduced Magneto-Hydrodyanmics
KMHD	Kinetic Magneto-Hydrodyanmics
CGL	Chew-Goldberger-Low
$p$	plasma pressure
$n, N$	plasma density
$T$	plasma temperature
$M_i$	ion mass
$\mathbf{E}$	electric field
$E_r$	radial component of electric field
$\mathbf{B}$	magnetic field
$\mathbf{A}$	magnetic vector potential
$\varphi$	electrostatic potential
$\mathbf{j}$	currents
$I$	toroidal plasma current
$\psi, \Psi$	poloidal flux
$\beta$	plasma beta ( $= p/B^2$ )
$U_E$	$\mathbf{E} \times \mathbf{B}$ drift
$c_s$	sound speed
$c_A$	Alfvén speed
$a$	minor radius of a tokamak
$R$	major radius of a tokamak
$\epsilon$	inverse aspect ratio ( $= a/R$ ) of a tokamak
$q$	magnetic safety factor
$\rho_i$	larmor radius
$k_{\parallel}, k_{\perp}$	parallel and perpendicular (to $\mathbf{B}$ ) wavenumbers
$U_{\parallel}, \mathbf{u}_{\perp}$	parallel and perpendicular plasma flows
$\zeta$	toroidal angle in a tokamak
$\theta$	poloidal angle in a tokamak
$\mu$	magnetic moment of a magnetized particle
TP	trapped particle in a magnetic field
CP	circulating particle
GAM	Geodesic Acoustic Mode
RH	Rosenbluth-Hinton
$\mathcal{D}$	effective inertia
$\mathcal{E}$	energy $= 1/2v_{\parallel}^2 + \mu B$
$\mathcal{E}_*$	shifted energy $\mathcal{E} + I\varphi'v_{\parallel}/B$
IREAP	Institute for Research in Electronics and Applied Physics

## Chapter 1: General Introduction

### 1.1 Reduced MHD

Ideal MHD [1] has been often described as the simplest self-consistent model of plasma that can offer quantitative predictions for stability thresholds of plasma confined in a magnetic confinement device like a Tokamak. However, from both analytical and computational points of view, it is almost always beneficial to reduce the complexities associated with the full nonlinear ideal MHD equations, by making simplifying assumptions either about the magnetic geometry or the time scale and length scales associated with the problem.

Several such simplified “reduced” sets of equations have been proposed in the literature, which attempt to simplify the physics by asymptotically retaining the relevant low frequency modes. In all these reduced models, the fast compressional Alfvén waves are eliminated by analytical reduction. Computationally, the maximum time step is not pinned to the fast-wave time scales.

The original ideal reduced MHD (RMHD) equations were obtained by Rosenbluth [2] and generalized and further developed by Strauss [3-5] to study global kink modes for a large aspect ratio tokamak. They used the inverse aspect ratio as the expansion parameter. This reduction has been found very useful to describe quan-

tatively kink, ballooning, tearing, and associated modes. The reduced time scale in all these models are typically of the order of  $\tau_A \equiv R/c_A$ , where  $c_A \equiv B^2/nM_i$  is the Alfvén speed. However, under normal fusion experiment conditions, with plasma  $\beta \equiv p/B^2$  well below ideal ballooning threshold, the characteristic growth time for macroscopic instabilities is longer than  $\tau_A$ . This is a motivation to seek a sub-Alfvénic reduced MHD system.

Some modes that are sub-Alfvénic include interchange (Mercier) modes, resistive interchange and resistive ballooning modes, drift waves, ITG modes, ion acoustic waves, geodesic acoustic modes (GAMs) and zero-frequency zonal flows [6]. A brief description of various sub-Alfvénic modes are provided in Appendix 0. A nonlinear reduced description of all these modes together would constitute a sub-Alfvénic system. As pointed out by Waelbroeck [7], the various sub-Alfvénic modes share some common characteristics, namely: their evolution time scales are slow compared to Strauss' RMHD modes, they have localized structures, and most perturbations are flute-like, i.e, they tend to be highly elongated along the magnetic field line.

The fact that the sub-Alfvénic modes are slowly evolving make them particularly sensitive to magnetic geometries. In the literature most of the analytic calculations involving these modes have been done in the cylindrical limit or by making some ad-hoc simplifications. This is because, even for circular flux surfaces, in a torus, the Shafranov shift leads to mode coupling and geometric intricacies. Correspondingly, in the collisionless limit, to include the effects of Landau damping, trapped particles, and self consistent zonal flows, reduced kinetic models must be used. Thus, a self-consistent nonlinear treatment of fluid and/or drift kinetic



description is quite challenging and is therefore still largely lacking.

## 1.2 Scope of this work

In this thesis, we make an effort to construct a nonlinear fluid as well as a drift kinetic sub-Alfvénic MHD system. The thesis is divided into three parts. In Part I, we shall present an analytic reduction to obtain a complete sub-Alfvénic MHD model in a low beta, large aspect ratio tokamak. In Part II, we use the methods of Part I to derive reduced equations in the collisionless, supersonic MHD limit. In Part III, we examine axisymmetric, subsonic modes in collisionless MHD to elucidate some aspects of trapped ion dynamics in this regime.

In Part I, we shall expand about a low order rational surface and consider modes below the ideal ballooning Alfvén wave. We make use of the standard large aspect ratio expansion and assume circular flux surfaces to lowest order. We allow long to intermediate wavelengths. We also allow resistivity. Our final reduced equations are nonlinear, but two dimensional, and include a dynamic Shafranov shift.

In Part II, we shall generalize our methods of Part I to derive sub-Alfvénic drift-kinetic equations in the supersonic limit. We base our analysis on Kulsrud's [8] Kinetic MHD formulation. We present a nonlinear, closed set of reduced kinetic equations which allow pressure anisotropy. In the supersonic limit, Kulsrud's description reduces to the CGL [9] double adiabatic formalism. Thus, we can also consider this case to be an extension of our isothermal fluid equations to a fluid

described by CGL closure.

In Part III, we consider axisymmetric sub-Alfvénic MHD type motions in a collisionless tokamak. In the collisionless limit, kinetic theory allows particle trapping along the magnetic fields and including their dynamics is important. At this level, one can study GAMs and zonal flows. We explore the effect of trapped ions on zonal flows and show that the well known Rosenbluth-Hinton [6] factor is the kinetic generalization of the “Pfirsch-Schluter” effective mass factor.

In what follows, we present Parts I, II and III. Each part is self contained and begins with a short description in an Overview.

# Part I

Collisional: Sub-Alfvénic Reduced MHD

## Chapter 2: Sub-Alfvénic reduced equations: Ideal MHD

### 2.1 Overview

A reduced set of MHD equations is derived, applicable to large aspect ratio tokamaks and relevant for dynamics that are sub-Alfvénic with respect to ideal ballooning modes. This ordering optimally allows sound waves, Mercier modes, drift modes, geodesic-acoustic modes, zonal flows, and shear Alfvén waves. Wavelengths long compared to gyroradius but comparable to minor radius of a typical tokamak are considered. With the inclusion of resistivity, tearing modes, resistive ballooning modes, Pfirsch-Schluter cells, and the Stringer spin-up are also included. A major advantage is that the resulting system is 2D in space, and the system incorporates self-consistent dynamic Shafranov shifts. A limitation is that the system is valid only in radial domains where the tokamak safety factor,  $q$ , is close to rational. In the tokamak core, the system is well suited to study the sawtooth discharge in the presence of Mercier modes. The systematic ordering scheme and methodology developed is versatile enough to reduce the more general collisional two-fluid equations or possibly the Vlasov-Maxwell system in the MHD ordering.

## 2.2 Introduction

The tokamak is characterized by having a strong axisymmetric toroidal magnetic field and a relatively weak poloidal field, in the geometry of a large aspect ratio toroid. Given this, scale lengths perpendicular to  $\mathbf{B}$  are shorter than along  $\mathbf{B}$ , resulting in a disparate separation of fundamental MHD mode frequencies. In particular, the magnetosonic mode is at higher frequency and separates from the shear Alfvén wave with a frequency ratio of  $O(\epsilon)$ , where  $\epsilon$  is the inverse aspect ratio. This separation allows a reduction of the ideal MHD equations (Rosenbluth [2], Strauss [3, 4]) wherein the reduced system describes shear Alfvén waves and is quasistatic with respect to the magnetosonic modes. Another MHD frequency of interest in tokamaks is that of sound waves. For a typical low beta system like a tokamak, this frequency is below the Alfvén frequency by the square root of  $\beta$ , the ratio of thermal energy to magnetic energy. The sound frequency band is generally also the same order as the frequency of drift waves and of interchange-like modes (which incorporate Mercier modes and geodesic acoustic modes).

This Part of the thesis is concerned with a reduction of the MHD equations to frequencies at the sonic level; in particular, frequencies of interest are below the ballooning Alfvén frequency,  $c_A/qR$ . At sub-Alfvénic frequencies, any MHD convection in the system must be consistent with interchanges of magnetic field lines that, to lowest order, preserve the magnetic structure. The frequencies of interest that can then be studied include sound waves ( $c_s/qR$ ), Mercier interchange modes ( $c_s/R$ )( $a/L_n$ ), geodesic acoustic modes ( $c_s/R$ ), drift waves ( $c_s\rho_i/(aL_n)$ ), and

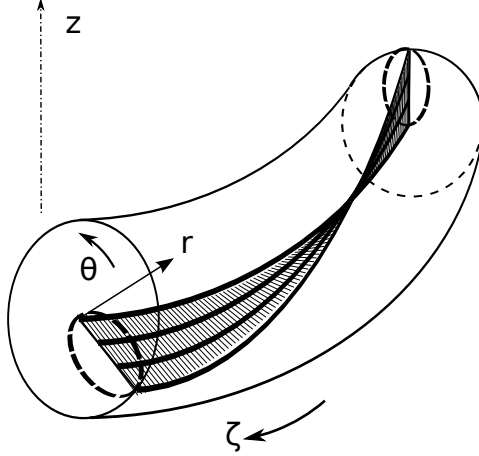


Figure 2.1: Interchanges on a rational flux surface

zonal flows (zero frequency). Here,  $c_A$ ,  $c_s$ ,  $a$ ,  $R$ ,  $L_n$ ,  $\rho_i$  are, respectively, the Alfvén speed, sound speed, minor radius, major radius, density scale length, and ion Larmor radius. An expansion in  $\epsilon \sim a/R$  is made.

To lowest order, the dominant motions are electrostatic convection cells in the cross-field plane as shown pictorially in Fig. 2.1. Thus, to lowest order, the expansion is centered about and in the vicinity of a low order rational surface; in particular, the off-rational part of the magnetic pitch and the magnetic shear are considered weaker than the poloidal magnetic field. In our expansion, these weaker portions are allowed in higher order, thus allowing magnetic shear. We clarify later in the chapter what restrictions these assumptions put on our system of equations. Within the expansion scheme, our system of equations optimally allows sound waves, Mercier modes, drift modes, geodesic-acoustic modes, zonal flows, and shear Alfvén waves. We allow wavelengths long compared to gyroradius but comparable to the size of tokamak. With the inclusion of resistivity, tearing modes, resistive ballooning modes, Pfirsch-Schluter cells, and the Stringer spin-up are also included. Since the

system is largely electrostatic, the magnetic field acts as a “guide” to the convection and, therefore, a major advantage of the reduction is that the resulting system of nonlinear equations is 2-dimensional.

In what follows, we systematically derive, starting from the full ideal MHD equations, reduced equations at sonic frequencies. Since the frequency of interest is two orders below the magnetosonic frequency, we find we have to go to  $O(\epsilon^4)$  to obtain a closed set of equations. Consequently, the required algebra is tedious and several cancellations of terms are found. As a check on the algebra, we find it helpful to motivate the cancellations by proceeding to the WKB limit and comparing with the expected local dispersions based on previous work.

In Sec 2.3, we outline the ordering of the full MHD equations and systematically derive reduced equations in a periodic cylinder. We begin with a cylinder as it serves to establish the basic methodology and allows us to introduce the notation, etc. In Sec 2.4, then, we extend this to a torus. This brings in toroidal curvature effects and, in particular, introduces new variables, with harmonic content, to the system. In Sec 2.5, we show that the toroidal equations of Sec 2.4 can be greatly simplified by a redefinition of variables: with the redefinition, two cancellations, motivated by examining WKB limits, are demonstrated and the resulting system is then rendered physically more transparent.

A rationale for reduction of toroidal MHD equations to the sonic level has been articulated by Waelbroeck [7]. A primary interest is that a reduction to this level allows drift waves and the associated small scale turbulent transport. While we do not include drift waves in this chapter, for simplicity, the ordering and methodology

allow this band of frequencies for wavelengths longer than the ion gyroradius. The ideal RMHD equations were previously generalized and extended self consistently to the resistive MHD case by Drake and Antonsen (DA) [10]. They pointed out that earlier attempts by Schmalz [11], Izzo et. al [12] and Strauss [5] to obtain resistive modes in a large aspect ratio tokamak by simply retaining higher powers of  $\epsilon$  was not self consistent. This is because the sub-Alfvénic modes are sensitive to magnetic geometry and a careful asymptotic analysis is therefore required. The sensitivity of magnetic geometry can be seen from the fact that the magnetic fields in this limit behave like “stiff” rods and the sub-Alfvénic modes would have to quasi statically adjust themselves to avoid bending the field lines. In this chapter, we present a systematic expansion upto 4<sup>th</sup> order in  $\epsilon$ .

### 2.3 Sub-Alfvénic reduced MHD in a cylinder

We begin our reduction of equations for the case of a straight cylinder; this establishes the ordering and methodology. We employ standard  $(r, \theta, \zeta)$  cylindrical geometry with the unit vector  $\hat{\zeta}$  in the direction of the symmetry direction of the cylinder. We assume a periodic cylinder of radius  $a$  and axial length  $2\pi R$ .



### 2.3.1 Equations and ordering

We begin with the Ideal MHD equations:

$$\partial_t n + \nabla \cdot (n\mathbf{u}) = 0 \quad (2.1)$$

$$M_i n (\partial_t + \mathbf{u} \cdot \nabla) \mathbf{u} = -\nabla p + \mathbf{j} \times \mathbf{B}, \quad \mathbf{j} \equiv \nabla \times \mathbf{B} \quad (2.2)$$

$$\partial_t \mathbf{B} = -\nabla \times \mathbf{E} \quad (2.3)$$

$$\nabla \cdot \mathbf{B} = 0 \quad (2.4)$$

Standard notation is used and we have set  $c = 4\pi = 1$  to avoid cumbersome constants. We have  $M_i$  as the ion mass,  $p = nT$  with  $T = T_e + T_i$ , and we assume constant isothermal temperature  $T$ , for simplicity. For ideal MHD,

$$\mathbf{E} = -\mathbf{u} \times \mathbf{B}. \quad (2.5)$$

This forms a complete set for the variables  $\{n, \mathbf{U}, \mathbf{B}\}$ . In this section, it is more convenient to use  $\mathbf{B} \equiv \nabla \times \mathbf{A}$ . This results in

$$\partial_t \mathbf{A} = -\mathbf{E} - \nabla \varphi. \quad (2.6)$$

Equation (2.6) replaces Eqs. (2.3) and (2.4). Thus, the primary equations are (2.1,2.2,2.6). For the asymptotic expansion, we adopt the following ordering:

$$\frac{k_{\parallel}}{k_{\perp}} \sim \frac{|\mathbf{u}_{\perp}|}{c_s} \sim \frac{U_{\parallel}}{c_s} \sim \frac{B_{\theta}}{B_{\zeta}} \sim \frac{c_s}{c_A} \sim \sqrt{\beta} \sim \epsilon \quad (2.7)$$

where  $k_{\parallel}$ ,  $k_{\perp}$  are the wavenumbers parallel and perpendicular to the full magnetic field  $\mathbf{B}$ , with poloidal and toroidal components  $B_{\theta}$  and  $B_{\zeta}$ ,  $c_s$  is the sound speed  $\equiv (T/M)^{1/2}$ , and  $\beta = nT/B^2$ . Since in the large aspect ratio limit the lowest order

magnetic field is toroidal. it is more convenient to define parallel and perpendicular with respect to the toroidal axis. With this ordering, we find that the terms in the  $n$  and  $\mathbf{A}$  equations, (2.1,2.6), each are of the same order. However, the momentum equation is ordered as

$$M_i n (\partial_t + \mathbf{u} \cdot \nabla) \mathbf{u} = -\nabla p + \mathbf{j} \times \mathbf{B}.$$

$$\epsilon^4 \quad : \quad \epsilon^4 : \quad \beta \sim \epsilon^2 : \quad 1$$

Thus, we would need to go to at least 4<sup>th</sup> order to close the system. To systematically apply the asymptotic expansion, we will need annihilation equations for the momentum equations. These are:

$$\mathbf{B} \cdot \left( M_i n \frac{d\mathbf{U}}{dt} + \nabla p \right) = 0 \tag{2.8}$$

$$\begin{aligned} \nabla \cdot \left( M_i n \frac{d\mathbf{U}}{dt} \times \frac{\hat{\mathbf{b}}}{B} \right) &= \mathbf{B} \cdot \nabla \left( \frac{j_{\parallel}}{B} \right) + \frac{1}{B^2} \mathbf{j} \cdot \nabla p \\ &+ 2 \hat{\mathbf{b}} \times \nabla p \cdot \nabla \left( \frac{1}{B} \right) \end{aligned} \tag{2.9}$$

We will also find useful as an annihilator the parallel component of the  $\mathbf{A}$  equation, namely

$$\mathbf{B} \cdot \partial_t \mathbf{A} = -\mathbf{B} \cdot \nabla \varphi. \tag{2.10}$$

This corresponds to the  $E_{\parallel} = 0$  condition of ideal MHD.

In what follows we assume that the magnetic field is predominantly axial along a cylindrical axis (i.e in the  $\hat{\boldsymbol{\zeta}}$  direction). All quantities designated as  $\perp$  will be assumed to be perpendicular to  $\hat{\boldsymbol{\zeta}}$  (not  $\mathbf{B}$ , as is often the convention). In this

case, it will be convenient to assume the form

$$\mathbf{B} = I \nabla \zeta + \mathbf{B}_\perp \quad (2.11)$$

where  $I \equiv RB_\zeta$ .

### 2.3.2 Asymptotic expansion of the Ideal MHD equations

We now proceed order by order systematically. The momentum equation starts at zero order, while all the other equations (density, Faradays law and the consistency conditions) start at  $2^{nd}$  order. Normalization parameters used are the minor radius, Alfvén speed and magnetic field:  $\{a, c_A, B_0\}$  respectively. These parameters will simply be set to unity. We do a perturbative expansion in the large aspect ratio parameter  $\epsilon \ll 1$  according to:

$$\begin{aligned} \mathbf{B} &= \mathbf{B}_0 + \epsilon \mathbf{B}_1 + \dots, \quad \psi = \psi_0 + \epsilon \psi_1 + \dots \\ I &= I_{-1}/\epsilon + I_0 + \epsilon I_1 + \dots, \quad \mathbf{j} = \mathbf{j}_0 + \epsilon \mathbf{j}_1 + \dots \\ R &= 1/\epsilon, \quad \mathbf{B} \cdot \nabla = \epsilon (\mathbf{B} \cdot \nabla)_1 + \epsilon^2 (\mathbf{B} \cdot \nabla)_2 + \dots, \\ d/dt &= \epsilon^2 d_t, \quad \varphi = \epsilon^2 \varphi_2 + \epsilon^3 \varphi_3 + \dots, \quad U_{||} = \epsilon^2 U_{||2} + \dots \\ n &= n_0 + \epsilon n_1 + \dots, \quad \beta \equiv \epsilon^2 \bar{\beta}, \quad p = \epsilon^2 n \bar{\beta}, \quad \eta \equiv \epsilon^2 \bar{\eta}, \quad \hat{s} = \epsilon \bar{s} \end{aligned}$$

where the magnetic flux  $\psi$  will be introduced below in Eq. (2.15). We have defined the quantities  $\bar{\beta}, \bar{\eta}$  so that these are  $O(1)$  quantities as opposed to  $\beta, \eta$  etc.

To lowest order,  $O(\epsilon^0)$ :

$$\mathbf{j}_0 \times \mathbf{B}_0 = 0, \quad \mathbf{j}_0 \equiv \nabla_\perp \times \mathbf{B}_0. \quad (2.12)$$

We assume that the magnetic field is purely axial to lowest order and thus  $\mathbf{B}_0 = \hat{\zeta}$ , and  $\mathbf{j}_0 = 0$ . From (2.11) we see that

$$\mathbf{B}_0 = \hat{\zeta}, \quad I_{-1} = 1, \quad (2.13)$$

where we use  $R = 1/\epsilon$ . To  $O(\epsilon^1)$ , we get

$$\mathbf{j}_1 \times \hat{\zeta} = 0 \quad \Rightarrow \quad \mathbf{j}_1 = J_1 \hat{\zeta}. \quad (2.14)$$

Now, from (2.2),  $\mathbf{j}_1 = \nabla_{\perp} \times \mathbf{B}_{\perp 1} + \nabla I_0 \times \hat{\zeta}$ . To first order, we also have  $\nabla \cdot \mathbf{B}_{\perp 1} = 0$  which implies  $\mathbf{B}_{\perp 1} = \hat{\zeta} \times \nabla \psi_0$ . Using these and condition (2.14) above, we get  $I_0 = \text{constant}$  and

$$\mathbf{B}_1 = \hat{\zeta} \times \nabla \psi_0, \quad J_1 = \nabla_{\perp}^2 \psi_0. \quad (2.15)$$

We further make the choice, for the predominantly axial geometry we are considering, that  $I_0 = 0$ .

We now proceed to  $O(\epsilon^2)$ . We first have the annihilation (2.9), which is second order at the lowest significant order. The only term that contributes at this order is the ‘‘field line bending term’’  $\mathbf{B} \cdot \nabla(j_{\parallel}/B)$ ; the other terms enter, at a minimum, at 4<sup>th</sup> order, given that  $I_0$  is zero. This results in

$$(\mathbf{B} \cdot \nabla)_1(j_{\parallel}/B)_1 = 0 \quad \Rightarrow \quad (j_{\parallel}/B)_1 = J_1(r) = \nabla_{\perp}^2 \psi_0. \quad (2.16)$$

The magnetic field at this order involves a constant axial field,  $B_0 = 1$  and an azimuthal field  $\hat{\zeta} \times \nabla \psi_0$ . We make the choice of a time independent  $\psi_0(r) = r^2/(2q_0)$ . This choice corresponds to a constant axial current  $J_1 = 2/q_0$  and implies a helical net field with the same winding number on each radial surface. In particular, the

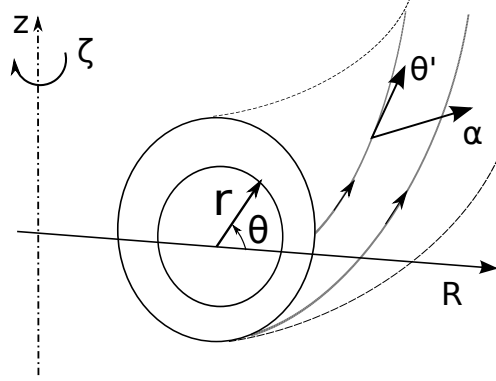


Figure 2.2: Field line following coordinate system

well-known tokamak safety factor,  $q(r) = rB_\zeta/RB_\theta$ , is a constant,  $q_0$ , and there is no magnetic shear. Additionally, we assume  $q_0$  is rational, and so we define a helical coordinate system with respect to the magnetic field given by the transformation

$$r' = r, \quad \theta' = \theta, \quad \alpha = \theta - (1/q_0)\zeta. \quad (2.17)$$

For the purposes of this chapter, we will assume that the magnetic shear is small, in the sense that any shear will be included as a correction term at the level of  $\psi_1$ . Likewise, we assume that any non-rational part of the magnetic field is also weak and enters at the  $\psi_1$  order. We will discuss later how these assumptions, while self-consistent, constrain our equations to apply only within a certain radial domain. We note that

$$(\mathbf{B} \cdot \nabla)_1 = (1/q_0) \partial_{\theta'} \quad (2.18)$$

in the helical coordinate system.

Continuing our expansion at 2nd order, we get, in addition to Eq. (2.16),

$$(\mathbf{j} \times \mathbf{B})_2 = \mathbf{j}_2 \times \hat{\boldsymbol{\zeta}} + \mathbf{j}_1 \times \mathbf{B}_{\perp 1} = \nabla_{\perp} p_2 = \bar{\beta} \nabla_{\perp} n_0. \quad (2.19)$$

Calculating  $\mathbf{j}$  to  $2^{nd}$  order using the form (2.11) for  $\mathbf{B}$ , and noting that  $\mathbf{B}_{\perp 1}$  is axisymmetric, we have  $\mathbf{j}_2 \times \hat{\boldsymbol{\zeta}} = -\nabla_{\perp} I_1$ . Using this in Eq (2.19), we can integrate (2.19) with respect to the perpendicular coordinates to get

$$\bar{\beta} n_0 + I_1 + \psi_0 \nabla_{\perp}^2 \psi_0 = 0. \quad (2.20)$$

This is the Grad-Shafranov equation. In our accounting, this is an equation for  $I_1$ : note that since  $n_0$  is not necessarily axisymmetric (we will describe this later),  $I_1$  is also in general non-axisymmetric (as by implication is the axial magnetic field, to  $2^{nd}$  order).

Next, we consider Eq (2.6) taken to second order. The time derivative term is zero since  $A_{\perp}^{(0)}$  is time independent, being proportional to  $I_{-1}$ . Using (2.5), we then deduce from the right hand side of (2.6) that

$$\mathbf{u}_2 = U_{||2} \hat{\boldsymbol{\zeta}} + \hat{\boldsymbol{\zeta}} \times \nabla \varphi_2. \quad (2.21)$$

Finally, at the  $O(\epsilon^2)$  order, we have from (2.1)

$$d_t n_0 = 0 \quad (2.22)$$

where  $d_t = \partial_t + \hat{\boldsymbol{\zeta}} \times \nabla \varphi_2 \cdot \nabla$ . We note also that the condition  $(\nabla \cdot \mathbf{B})_2 = 0$  becomes  $\nabla_{\perp} \cdot \mathbf{B}_{\perp 2} = 0$ , since  $I_0 = 0$ . This implies that  $\mathbf{B}_{\perp 2}$  can also be written in terms of the flux function  $\psi$ , viz.,

$$\mathbf{B}_{\perp 2} = \hat{\boldsymbol{\zeta}} \times \nabla \psi_1. \quad (2.23)$$

We now proceed to  $O(\epsilon^3)$ . The annihilation equation (2.9) becomes

$$(\mathbf{B} \cdot \nabla)_1 (j_{\parallel}/B)_2 + (\mathbf{B} \cdot \nabla)_2 (j_{\parallel}/B)_1 = 0 \quad (2.24)$$

where, again, we note that the remaining terms in the equation contribute only at 4<sup>th</sup> order. To calculate  $\mathbf{j} \cdot \mathbf{B}/B^2$  to 2<sup>nd</sup> order, we note that  $\mathbf{j}_{\perp} \cdot \mathbf{B}_{\perp}$  is of order  $\epsilon^3$  since  $\mathbf{j}_{\perp}$  is of 2<sup>nd</sup> order, at largest. Thus to the required order

$$(j_{\parallel}/B)_2 = (I \nabla \zeta \cdot (\nabla \times \mathbf{B})/B^2)_2 = \nabla_{\perp}^2 \psi_1 \quad (2.25)$$

Using this in the expression for  $j_{\parallel}/B$  above, we get the annihilation condition to be

$$(\mathbf{B} \cdot \nabla)_1 \nabla_{\perp}^2 \psi_1 = 0. \quad (2.26)$$

Thus,  $\psi_1$  is a “flute function”, that is to say it is constant along a twisted magnetic field line but not necessarily constant across the field lines, i.e.,  $\psi_1 = \psi_1(r, \alpha)$ . Hereon, we will suppress the prime on  $r$  as there is no ambiguity. We also find, from the annihilation equation (2.8),

$$(\mathbf{B} \cdot \nabla)_1 n_0 = 0. \quad (2.27)$$

We now write Eq (2.6) at 3<sup>rd</sup> order. An as yet unknown term,  $\mathbf{u}_3 \times \hat{\zeta}$ , appears on the RHS and can be annihilated by dotting with  $\hat{\zeta}$  (or, equivalently, using the annihilation equation Eq. (2.10)). Noting that  $\epsilon \mathbf{A}_1 = -\psi_0 \nabla \zeta$ , consistent with (2.15), and that  $\psi_0$  is self-consistently time independent, the annihilated equation becomes

$$(\mathbf{B} \cdot \nabla)_1 \varphi_2 = 0. \quad (2.28)$$

The foregoing three equations imply that all of the functions  $\{n_0, \varphi_2, \psi_1\}$  are flute functions. We denote  $\psi_1$  by  $\underline{\psi}_1$  just to emphasize its flute nature.

We pause here to collect the description for the  $\mathbf{B}$  field so far.  $\mathbf{B}$  is, in general written as (2.11). To the extent that we have obtained so far, to  $2^{nd}$  order in  $\epsilon$ , expressions for  $I_{-1}$ ,  $I_0$ , and  $I_1$ , and expressions for  $\psi_0$  and  $\underline{\psi}_1$ , (see equations (2.13), (2.20), (2.23), and (2.26)), we may write the  $B$  field from (2.11), in familiar form, as

$$\mathbf{B} = I\nabla\zeta + \nabla\zeta \times \nabla\psi + O(\epsilon^3) \quad (2.29)$$

where  $I = I_{-1} + I_1(r, \alpha)$ , and  $\psi = \psi_0(r) + \underline{\psi}_1(r, \alpha)$ . This expression for  $\mathbf{B}$  is familiar; it is correct to  $2^{nd}$  order in  $\epsilon$  and only  $3^{rd}$  order terms are dropped. Note, however, that the field is not axisymmetric (usually the form (2.29) is employed for axisymmetric fields). We will show in what follows that this is the only required precision in  $\mathbf{B}$  necessary to close our set of equations.

Finally, we go to fourth order. We first apply the  $E_{||} = 0$  annihilation condition (2.10). This gives us

$$(\mathbf{B} \cdot \nabla)_1 \varphi_3 + (\mathbf{B} \cdot \nabla)_2 \varphi_2 = \partial \underline{\psi}_1 / \partial t. \quad (2.30)$$

The  $\varphi_3$  term is higher order and not needed. This term can be annihilated by integrating over each separate closed field line for fixed  $\alpha$ , i.e., we use the condition  $\oint d\theta' (\mathbf{B} \cdot \nabla)_1 f = 0$ . We get

$$d_t \underline{\psi}_1 = 0. \quad (2.31)$$

We now proceed to the annihilation equation (2.9). The field line bending term,  $\mathbf{B} \cdot \nabla(j_{||}/B)$ , is the largest term. This term, to 4th order, is  $(\mathbf{B} \cdot \nabla)_1(j_{||}/B)_3 + (\mathbf{B} \cdot \nabla)_2(j_{||}/B)_2$ , since  $(j_{||}/B)_1$  is a constant. As above, we annihilate the  $(j_{||}/B)_3$  term by field line averaging. The remaining terms yield the vorticity equation (see 2.9),



viz.

$$\nabla_{\perp} \cdot (d_t n_0 \nabla_{\perp} \varphi_2) = \frac{2\bar{\beta}}{q_0} \partial_{\zeta} n_0 + (\mathbf{B} \cdot \nabla)_2 \nabla_{\perp}^2 \underline{\psi}_1. \quad (2.32)$$

Here, the LHS, being the “smallest” term, is calculated to lowest order in the cylindrical geometry. An expression for  $(j_{\parallel}/B)_2$  was previously obtained (see Eq (2.25)) and has been used to calculate the surviving field line bending term, where  $(\mathbf{B} \cdot \nabla)_2 = \hat{\zeta} \times \nabla \underline{\psi}_1 \cdot \nabla$ . The  $\mathbf{j} \cdot \nabla p = \mathbf{j}_2 \cdot \nabla p_2$  term is zero because of pressure balance condition, Eq.(2.19). The only nonzero contribution from the term proportional to  $\mathbf{B} \times \nabla p \cdot \nabla(1/B^2)$  is  $J_1 \hat{\zeta} \times \nabla \psi_0 \cdot \nabla n_0$  on account that  $I_0 = 0$  and that the non-constant part of  $I_1$  is equal to  $p_2$ , as seen from (2.20). Using Eq.(2.27), this term can be shown to give the first term on the RHS.

### 2.3.3 Summary: Closed set in a cylinder

The complete set for a cylinder that describes  $\{n_0, \varphi_2, \underline{\psi}_1\}$  is given by:

$$d_t n_0 = 0 \quad (2.33)$$

$$d_t \underline{\psi}_1 = 0 \quad (2.34)$$

$$\nabla_{\perp} \cdot (d_t n_0 \nabla_{\perp} \varphi_2) = \frac{2\bar{\beta}}{q_0} \partial_{\zeta} n_0 + \hat{\zeta} \times \nabla \underline{\psi}_1 \cdot \nabla \nabla_{\perp}^2 \underline{\psi}_1 \quad (2.35)$$

where,  $d_t = \partial_t + \hat{\zeta} \times \nabla \varphi_2 \cdot \nabla$ . Eqs (2.33), (2.34), and (2.35) now constitute a closed system for the flute functions  $n_0$ ,  $\varphi_2$ , and  $\underline{\psi}_1$ . These equations incorporate the cylindrical flute interchange, and also the shear Alfvén wave in the presence weak magnetic shear (or weakly off-rational fields). Together, these describe the low  $\beta$  interchange in a sheared field. Magnetic shear is introduced in the system in the  $\underline{\psi}_1$

field as follows: the usual tokamak safety factor  $q$  is defined as  $1/q(r) = RB_\theta/(rB_\zeta)$ , where  $B_\theta = (1/R)d\psi/dr$ . Thus, to lowest order in our expansion,

$$1/q_0 = d\psi_0/d(r^2/2)$$

where  $q_0$  is assumed rational which is consistent with the choice of  $\psi_0 = r^2/(2q_0)$ .

To first order then, we get then

$$q_0/q(r) - 1 = \epsilon d\underline{\psi}_1/d\psi_0$$

which defines  $q(r)$ . Per our expansion, the RHS must be small; thus, our system of equations is valid provided  $q$  is close to (but not equal to) rational. The magnetic shear parameter is defined in the usual way as  $\hat{s} = (r/q_0)(dq/dr)_0$ . The parallel wave number may be defined as  $\mathbf{k} \cdot \mathbf{B}/B$ . This can be calculated out to

$$k_{||} = (m/R)(1/q - 1/q_0) = \epsilon^2 \bar{k}_{||}$$

where  $\epsilon \bar{k}_{||} = m(1/q - 1/q_0)$  is an  $O(1)$  quantity in our ordering. For the full nonlinear equations above, the validity of our expansion can be checked by demanding  $k_{||}c_A \ll c_A/(qR)$ . This scales, using  $k_{||} \sim k'_{||}\Delta x$ , as  $\hat{s} \Delta x m \ll 1$ , where  $\Delta x$  is the radial extent from the rational surface and  $k'_{||} = m\hat{s}/(q_0R)$ . Thus, for a given  $m$  spectrum, this puts a restriction on the shear strength or the extent of the considered radial domain.

## 2.4 Reduction in Toroidal Geometry

We now derive sub-Alfvénic equations in toroidal geometry. The calculation parallels the cylindrical calculation closely. The primary difference is that the  $\hat{\zeta}$  unit vector is not constant in space, as in the cylindrical case, but points in the azimuthal direction of a toroidal geometry which can be described by the usual  $\{R, \zeta, z\}$  system. The curvature vector  $\hat{\zeta} \cdot \nabla \hat{\zeta}$  points in the  $\hat{R}$  direction, i.e.,  $\hat{\zeta} \cdot \nabla \hat{\zeta} = -\hat{R}/R$ . We will assume circular flux surfaces and use the toroidal coordinate system  $\{r, \theta, \zeta\}$ , where  $z = r \sin \theta$ , and  $R = 1/\epsilon + r \cos \theta$ . We will sometimes write  $R = 1/\epsilon + x$ , with  $x = r \cos \theta$ . The ordering is the same as given by (2.7). Again, we will use for  $\mathbf{B}$  the representation,  $\mathbf{B} = I\nabla\zeta + \mathbf{B}_\perp$ . Proceeding order by order as before, we recover, to  $O(\epsilon^2)$ , results identical to the cylindrical results as follows:

$$\mathbf{B}_0 = \hat{\zeta}, \quad \mathbf{j}_1 = J_1 \hat{\zeta}, \quad \text{with } J_1 = (1/r) \partial_r (r \psi'_0) = 2/q_0 \quad (2.36)$$

$$I_0 = 0 \quad (2.37)$$

$$(\mathbf{B} \cdot \nabla)_1 J_1 = 0 \quad (2.38)$$

$$\text{where } (\mathbf{B} \cdot \nabla)_1 = \partial_\zeta + \hat{\zeta} \times \nabla \psi_0 \cdot \nabla.$$

Here, we make the choice that  $\psi_0$  is axisymmetric and only a function of  $r$ ,  $\psi_0(r) = r^2/(2q_0)$ , as in the cylinder, and given the magnetic geometry under investigation. Again parallel to that shown in cylindrical geometry, we find that  $\mathbf{B}$  can be written, to  $O(\epsilon^2)$ , in the familiar form

$$\mathbf{B} = I\nabla\zeta + \nabla\zeta \times \nabla\psi + O(\epsilon^3) \quad (2.39)$$

with the important distinction that  $\nabla\zeta = \hat{\zeta}/R$  where  $R = 1/\epsilon + x$ , with  $x \ll 1/\epsilon$ . In this form,  $I = 1/\epsilon + \epsilon I_1$  and  $\psi = \psi_0 + \epsilon \psi_1$ , with (2.39) calculated to a precision no higher than  $O(\epsilon^2)$ . Given this form for  $\mathbf{B}$ , it can be deduced, from  $\mathbf{B} = \nabla \times \mathbf{A}$ , that  $\mathbf{A}$  to commensurate order is given as

$$\mathbf{A} = -\psi \nabla \zeta + \mathbf{A}_\perp. \quad (2.40)$$

The similarity to the cylindrical results continues to the Grad-Shafranov equation. As in the cylindrical calculation, to this order, we can show that  $\mathbf{j}_2 \times \hat{\zeta} = \nabla I_1$ . This leads to the same Grad-Shafranov equation as in cylindrical, viz.,

$$I_1 + J_1 \psi_0 + \bar{\beta} n_0 = 0 \quad (2.41)$$

and the flow velocity

$$\mathbf{U}_2 = U_{||2} + \hat{\zeta} \times \nabla \varphi_2. \quad (2.42)$$

Also, to this order, using the expression for  $\mathbf{u}_2$ , we find an evolution equation for  $n_0$  from the continuity equation, (2.1), viz.,

$$d_t n_0 = 0. \quad (2.43)$$

The equations are, however, modified at the  $O(\epsilon^3)$  and higher level. To  $O(\epsilon^3)$ , the annihilation equation (2.9) becomes

$$(\mathbf{B} \cdot \nabla)_1 (j_{||}/B)_2 + (\mathbf{B} \cdot \nabla)_2 (j_{||}/B)_1 = -\nabla \cdot (\mathbf{B} \times \nabla p/B^2) \quad (2.44)$$

where the inertial term is 4<sup>th</sup> order.  $(j_{||}/B)_1$  is a constant, thus the 2<sup>nd</sup> term does not contribute. To calculate  $\mathbf{j} \cdot \mathbf{B}/B^2$  to 2<sup>nd</sup> order, we note that  $\mathbf{j}_\perp \cdot \mathbf{B}_\perp$  is of order

$\epsilon^3$  since  $j_\perp$  is of  $2^{nd}$  order, at largest. The remaining term is  $I\nabla\zeta \cdot (\nabla \times \mathbf{B})/B^2$  which can be calculated to be  $\Delta_*\psi/I \equiv R^2\nabla_\perp \cdot (R^{-2}\nabla_\perp\psi)/I$ . This implies,

$$(j_{||}/B)_2 = (\Delta_*\psi/I)_2 = (\Delta_*\psi)_1 \quad (2.45)$$

where

$$(\Delta_*\psi)_1 = \Delta\psi_1 - \partial\psi_0/\partial R. \quad (2.46)$$

$$\text{and } \Delta = \partial_R^2 + \partial_z^2 = \frac{1}{r}\partial_r(r\partial_r) + \frac{1}{r^2}(\partial_\alpha + \partial_\theta)^2.$$

This provides the information needed to evaluate the line bending term. As far as the pressure term on the RHS, this can be decomposed as

$$\nabla \cdot (\mathbf{B} \times \nabla p/B^2) = \mathbf{B} \times \nabla p \cdot \nabla(1/B^2) + \mathbf{j} \cdot \nabla p. \quad (2.47)$$

Since  $\mathbf{j} \times \mathbf{B} = \nabla p$  up to  $O(\epsilon^3)$ ,  $\mathbf{j} \cdot \nabla p$  is at minimum of  $O(\epsilon^4)$ . Further, to the order required, the equilibrium equation,

$$\nabla(B^2/2 + p) = \mathbf{B} \cdot \nabla \mathbf{B} \quad (2.48)$$

can be used to insert for  $\nabla B^2$  into the pressure term in (2.47). The pressure term then becomes  $2\mathbf{B} \times \boldsymbol{\kappa} \cdot \nabla p/B^2$ , where  $\boldsymbol{\kappa} = \hat{\mathbf{b}} \cdot \nabla \hat{\mathbf{b}}$  is the field curvature. Evaluating the latter pressure term to  $3^{rd}$  order results in  $-2\partial p/\partial z$ . Collecting all terms, the annihilation equation (2.44), to  $O(\epsilon^3)$ , becomes

$$(\mathbf{B} \cdot \nabla)_1 (j_{||}/B)_2 = 2\partial p_2/\partial z, \quad (j_{||}/B)_2 = (\Delta_*\psi)_1. \quad (2.49)$$

We now note from (2.49) that  $\psi_1$  is driven by  $\beta$  and also driven by  $\partial\psi_0/\partial R$  (see also Eq. (2.46)). The homogenous solution for  $\psi_1$  is constant along field lines

and corresponds to the flute part of  $\psi_1$ , as in the cylindrical limit. The particular solutions correspond to the well-known Shafranov shift, a purely toroidal effect. The Shafranov shift has two components: the  $\cos \theta$  term in (2.46), proportional to  $\partial\psi_0/\partial R$ , gives a static shift,  $\Psi_{1x}$ , from the magnetics; while the  $\beta$  driver, the  $\partial p_2/\partial z$  term in (2.49), is time-dependent and, thus, gives a dynamic Shafranov shift,  $\Psi_{1\beta}$ . Further, while the equilibrium magnetic shift is toroidally in-out, the dynamic shift has both in-out and up-down components. Thus, in summary

$$\psi_1 = \underline{\psi}_1 + \Psi_1, \quad \text{where} \quad \Psi_1 = \Psi_{1x} + \Psi_{1\beta} \quad (2.50)$$

$$\Delta\Psi_{1x} = \partial_R\psi_0 \quad (2.51)$$

$$(\mathbf{B} \cdot \nabla)_1(\Delta\Psi_{1\beta}) = 2\bar{\beta} \partial_z n_0 \quad (2.52)$$

where  $\underline{\psi}_1$  is a flute function, and  $\Psi_1$  is harmonic.

Continuing further at  $3^{rd}$  order, we find from the annihilation equation (2.8)

$$(\mathbf{B} \cdot \nabla)_1 n_0 = 0. \quad (2.53)$$

We also write the annihilation Eq (2.10) at  $3^{rd}$  order. Noting that  $\epsilon\mathbf{A}_1 = -\psi_0\nabla\zeta$ , consistent with (2.39,2.40), and that  $\psi_0$  is time independent, the annihilated equation becomes

$$(\mathbf{B} \cdot \nabla)_1 \varphi_2 = 0. \quad (2.54)$$

In higher order, we will also need  $(\mathbf{B} \cdot \nabla)_2$ . This can be obtained starting from the expression (2.39) for  $\mathbf{B}$ . Using the result that  $I_0 = 0$ , we readily find

$$\begin{aligned} (\mathbf{B} \cdot \nabla)_2 &= ((I/R^2)\partial_\zeta + \nabla\zeta \times \nabla\psi \cdot \nabla)_2 \\ &= -2x \partial_\zeta - x \hat{\zeta} \times \nabla\psi_0 \cdot \nabla + \hat{\zeta} \times \nabla\psi_1 \cdot \nabla \end{aligned} \quad (2.55)$$

where,  $\nabla\zeta = \hat{\zeta}/R$ , and the various terms are to be evaluated to  $O(\epsilon^2)$ .

The foregoing equations imply that all of the functions  $\{n_0, \varphi_2, \underline{\psi}_1\}$  are flute functions, while  $\Psi_1$  is a harmonic function of  $\theta'$  and is obtained from Eqs. (2.50-2.52). At this stage, we have an evolution equation for  $n_0$ , Eq (2.43). To close the loop, we will need, as in the cylindrical case, a vorticity equation for  $\varphi_2$ , as well as an evolution equation for  $\underline{\psi}_1$ . To do this, we need to proceed to 4<sup>th</sup> order. First, we apply, at 4<sup>th</sup> order, the  $E_{||} = 0$  annihilation condition (2.10). This results in

$$(\mathbf{B} \cdot \nabla)_1 \varphi_3 + (\mathbf{B} \cdot \nabla)_2 \varphi_2 = \partial \psi_1 / \partial t. \quad (2.56)$$

We average this over each field line, viz.,  $\oint d\theta' (\mathbf{B} \cdot \nabla)_1 f = 0$ , to eliminate the  $(\mathbf{B} \cdot \nabla)_1 \varphi_3$  term. This gives us the evolution equation for  $\underline{\psi}_1$

$$d_t \underline{\psi}_1 = 0. \quad (2.57)$$

Next, we need an evolution equation for  $\varphi_2$ . This necessitates evaluating the annihilation equation (2.9) to 4<sup>th</sup> order. The line bending terms are to be calculated to this order as  $(\mathbf{B} \cdot \nabla)_1 (j_{||}/B)_3 + (\mathbf{B} \cdot \nabla)_2 (j_{||}/B)_2 + (\mathbf{B} \cdot \nabla)_3 (j_{||}/B)_1$ , and then averaged along the field lines. The first of these terms vanishes upon averaging, while the 3<sup>rd</sup> one is zero since  $(j_{||}/B)_1$  is a constant. The 2nd term survives; this is to be evaluated using the full expression for  $\psi_1$  defined in (2.50), where the terms  $(\mathbf{B} \cdot \nabla)_2$  and  $(j_{||}/B)_2$  are as defined in (2.55) and (2.45). It is natural to split  $\langle (\mathbf{B} \cdot \nabla)_2 (j_{||}/B)_2 \rangle$  into a piece independent of  $\theta'$ , ie, the flute part, and the remaining  $\theta'$ -dependent parts. The flute part can be written as  $\langle (\mathbf{B} \cdot \nabla)_2 \rangle \langle (j_{||}/B)_2 \rangle$  where  $\langle (\mathbf{B} \cdot \nabla)_2 \rangle = \zeta \times \nabla \underline{\psi}_1 \cdot \nabla$  and  $\langle (j_{||}/B)_2 \rangle = \underline{\Delta} \underline{\psi}_1$ , where  $\underline{\Delta} = (1/r) \partial_r (r \partial_r) + (1/r)^2 \partial_\alpha^2$

is the averaged Laplacian. This split is facilitated by the fact that  $\psi_1$  itself is decomposed as a linear combination of the flute part and harmonic part, as discussed in Eq. (2.50). Upon effecting this split, the harmonic terms in the line bending terms can be written as  $\langle d_2(j_{||}/B)_2 \rangle$ , where, using (2.55),

$$d_2 = -x(2\partial_\zeta + \hat{\zeta} \times \nabla \psi_0 \cdot \nabla) + \hat{\zeta} \times \nabla \Psi_1 \cdot \nabla. \quad (2.58)$$

We note that the operator  $d_2 \equiv (\mathbf{B} \cdot \nabla)_2 - \langle (\mathbf{B} \cdot \nabla)_2 \rangle$  has all harmonic terms. To calculate  $\mathbf{B} \times \nabla p \cdot \nabla B^2$ , we again use the equilibrium condition (2.48) above, still correct to the required order, to get a term proportional to  $\mathbf{B} \times \boldsymbol{\kappa}$ . To 2<sup>nd</sup> order, we readily find  $B\boldsymbol{\kappa} = \mathbf{B} \cdot \nabla(\mathbf{B}/B)$  becomes  $(\mathbf{B} \cdot \nabla)_1(\hat{\zeta} + \mathbf{B}_\perp) = -\hat{\mathbf{R}}/R + B_\theta^2 \hat{\mathbf{r}}/r$ . Thus, the required term becomes  $2\bar{\beta} \langle \partial_z n_1 \rangle$  plus the previously obtained cylindrical term  $2(\bar{\beta} \partial_\zeta n_0)/q_0$ .

Finally, we evaluate the inertial term  $\nabla \cdot (\mathbf{B} \times d\mathbf{U}/dt)$  to 4<sup>th</sup> order. This term is only cylindrical since  $d/dt$  and  $p$  are each of 2<sup>nd</sup> order. Thus, we get  $\nabla \cdot (\hat{\zeta} \times d\mathbf{U}_2/dt) = \nabla_\perp \cdot d_t \nabla_\perp \varphi_2$ . Collecting all the terms, we get the annihilated equation (2.9) to 4<sup>th</sup> order, the vorticity equation,

$$\nabla_\perp \cdot (d_t n_0 \nabla_\perp \varphi_2) = \frac{2\bar{\beta}}{q_0} \partial_\zeta n_0 + \hat{\zeta} \times \nabla \underline{\psi}_1 \cdot \nabla \nabla_\perp^2 \underline{\psi}_1 - 2\bar{\beta} \langle \partial_z n_1 \rangle + \langle d_2(j_{||}/B)_2 \rangle. \quad (2.59)$$

Between (2.43), (2.57), and (2.59), we now have a set of evolution equations for the flute variables  $n_0, \varphi_2, \underline{\psi}_1$ . However, unlike in the cylinder, the system is not closed, on account of the  $n_1$  term in (2.59). We thus write out the density equation



(2.1) to 3<sup>rd</sup> order:

$$\begin{aligned}
& d_t n_1 + x \hat{\boldsymbol{\zeta}} \times \nabla \varphi_2 \cdot \nabla n_0 + \hat{\boldsymbol{\zeta}} \times \nabla \varphi_3 \cdot \nabla n_0 \\
& + n_0 (\mathbf{B} \cdot \nabla)_1 U_{||2} - 2n_0 \partial_z \varphi_2 = 0.
\end{aligned} \tag{2.60}$$

We also need an equation for  $U_{||2}$ . We obtain this by evaluating (2.8) to 4<sup>th</sup> order:

$$(n_0 / \bar{\beta}) d_t U_{||2} + (\mathbf{B} \cdot \nabla)_1 n_1 + (\mathbf{B} \cdot \nabla)_2 n_0 = 0. \tag{2.61}$$

Thus, we have equations for  $n_1$  and  $U_{||2}$ . At first glance, it appears as though a vorticity equation like (2.59) would be needed to advance  $\varphi_3$ . However, examination of (2.59) reveals that in the averaged term  $\langle \partial_z n_1 \rangle$  only sine and cosine averages of  $n_1$  are needed. Further, the driving term for  $n_1$ , from the  $n_1$  equation (2.60), is the flute function  $\varphi_2$ , in particular the dot product  $\hat{\boldsymbol{z}} \cdot \nabla \varphi_2$ ; this term, in the circular surface geometry, has only  $\sin \theta$  and  $\cos \theta$  components. Thus, we only need the harmonic projections of the  $n_1$  equation (2.60). Further, in (2.56), we only need the first harmonics of  $\varphi_3$  to advance  $n_1$ . The system is now closed as we have evolution equations for the 3 flute functions  $n_0$ ,  $\varphi_2$ ,  $\underline{\psi}_1$ , and equations for the first harmonics of  $n_1$  and  $\varphi_3$ . In addition, the first harmonics of  $\psi_1$ , required in (2.56) to calculate  $\varphi_3$ , are obtained by inverting the Shafranov shift equation (2.49), as already discussed in Eqs. (2.51) and (2.52). Note that, on account the Shafranov shift is dynamic, the harmonics of  $\psi_1$  are time-dependent.

#### 2.4.1 Summary: closed set in a torus

In this section, we have derived closed equations Eqs. (2.43, 2.57, 2.59), in toroidal geometry for the flute variables  $\{n_0, \varphi_2, \underline{\psi}_1\}$  as coupled to the first harmonics

of  $n_1, U_{||2}, \varphi_3, \Psi_1$  given by Eqs. (2.60, 2.61, 2.56, 2.49) respectively. We now show a further simplification.

## 2.5 Further reduction

While we have a complete set of equations, which contains the physics of both interchange modes as well as sub-ballooning Alfvén modes, there are indications that further simplifications are likely. In this section, we rewrite the complete set using a more natural density variable to obtain simplified equations.

We begin by noting that in the complete set above there are 3 primary operators, which we will define as follows:  $d_1 = (\mathbf{B} \cdot \nabla)_1$ ,  $d_2 = (\mathbf{B} \cdot \nabla)_2 - \langle (\mathbf{B} \cdot \nabla)_2 \rangle$ , and  $\partial_z$ . These operators and their commutators are defined in Appendix A. Note that  $d_1 = (1/q)\partial_{\theta'}$  is the derivative along a cylindrical field line. We now show that there is a cancellation of two large terms in the vorticity equation (2.59), between the line bending term,  $d_2 (j_{||}/B)_2$ , and the  $\partial_z n_1$  term. We first observe that if the system is subsonic, then the  $\mathbf{B} \cdot \nabla n$  term in (2.61) must be zero in that limit. We are motivated by this to introduce a new density variable,  $N_1$ , defined according to

$$d_1 n_1 + d_2 n_0 = d_1 N_1. \quad (2.62)$$

Note that this equation is consistent under the field line averaging operation.  $N_1$  must be very small under subsonic conditions. From (2.62), using (A.9), we have

$$n_1 = N_1 + q_0^2 d_1 d_2 n_0. \quad (2.63)$$

We now insert this form of  $n_1$  into the  $\langle \partial_z n_1 \rangle$  term in (2.59), and insert  $(j_{||}/B)_2$  from (2.49) into the field line bending term  $\langle d_2 (j_{||}/B)_2 \rangle$  in (2.59). Upon these

insertions, and leaving aside for now the  $N_1$  term, the last two terms in (2.59) become proportional to

$$\langle d_2 d_1 \partial_z n_0 + \partial_z d_1 d_2 n_0 \rangle. \quad (2.64)$$

Given the symmetry in the operators in (2.64), a possibility for a cancellation is clearly evident. A cancellation becomes almost certain if one examines these terms in the WKB limit. Assuming solutions of the form  $\sim \exp(ik\alpha + \gamma t)$ , the linearized interchange mode is obtained from the continuity equation (2.43), which couples  $\gamma n_0$  to  $k\varphi_2$ , and from the vorticity equation (2.59), which couples  $\gamma k^2 \varphi_2$  to the RHS term involving the terms in  $n_0$  given in (2.64) above. Note now that the terms in (2.64) go as  $k^2$ , since both  $d_2$  and  $\partial_z$  go as  $k$ . The interchange dispersion then would result in  $\gamma^2 \propto k$ , which is clearly not consistent with the well-known Mercier interchange for which  $\gamma$  is independent of  $k$  in the large  $k$ , WKB limit. Thus, a cancellation is to be expected.

Indeed, we can show a nonlinear cancellation in (2.64) as follows. We note that  $d_2 d_1 \partial_z n_0 = d_2 [d_1, \partial_z] n_0$  since  $d_1 n_0 = 0$ ; and  $\langle \partial_z d_1 d_2 n_0 \rangle = \langle [\partial_z, d_1] d_2 n_0 \rangle$  since  $\langle d_1 f \rangle = 0$ . Here, for operators  $A$  and  $B$ , the commutator is defined as  $[A, B] = AB - BA$ . Definitions, properties and commutators of Poisson brackets and relevant operators are discussed in detail in Appendix A. Thus, expression (2.64) becomes

$$\langle d_2 [d_1, \partial_z] n_0 + [\partial_z, d_1] d_2 n_0 \rangle = \langle [d_2, [d_1, \partial_z]] n_0 \rangle \quad (2.65)$$

using  $[d_1, \partial_z] = -[\partial_z, d_1]$ . Further, as shown in Appendix A Eq.(A.10),  $q_0 [d_1, \partial_z] n_0 = \partial_R n_0$ . Thus, the expression (2.65) becomes  $(1/q_0) \langle [d_2, \partial_R] n_0 \rangle$ . The commutator

$[d_2, \partial_R]$  has been calculated in Appendix A, Eq.(A.15). We find

$$\langle [d_2, \partial_R] n_0 \rangle = \langle (x/q_0) \partial_z n_0 + \{\partial_R \Psi_1, n_0\} + \partial_\zeta n_0 \rangle. \quad (2.66)$$

To further evaluate (2.66), we note readily that the 1<sup>st</sup> term on the RHS, upon averaging, becomes  $(1/2)\partial_\alpha n_0$ , which then combines with the 3<sup>rd</sup> term. The 2<sup>nd</sup> term is evaluated in Appendix C: in brief, only the piece of  $\Psi_1$  that comes from the equilibrium magnetic Shafranov shift,  $\Psi_{1x}$ , survives the averaging, resulting in a term equal to  $(1/2)\partial_\alpha n_0$ , which simply combines with the other  $\partial_\alpha n_0$  terms already found; the piece of  $\Psi_1$  that comes from finite  $\beta$  terms,  $\Psi_{1\beta}$ , the dynamic Shafranov shift, simply averages to zero (shown in Appendix C). Altogether then, the expression  $\langle -2\bar{\beta} \partial_z n_1 + d_2 (j_{||}/B)_2 \rangle$  reduces to

$$-2\bar{\beta} (\langle \partial_z N_1 \rangle - \partial_\alpha n_0). \quad (2.67)$$

Note that this expression scales as  $\sim k$ , indicating a large cancellation from the original scaling of  $k^2$  terms in Eq.(2.64).

We thus have the RHS of the vorticity equation, greatly simplified. We now turn to the  $n_1$  equation, (2.60). This has to be rewritten in terms of the  $N_1$  variable, where  $N_1$  and  $n_1$  are related by the Eq. (2.63). Inserting for  $n_1$  from (2.63) into (2.60), we get

$$d_t N_1 - 2\partial_z \varphi_2 + n_0 d_1 U_{||2} + F = 0 \quad (2.68)$$

$$\text{where } F = q_0^2 d_t d_1 d_2 n_0 + \{n_0, \varphi_3\} + x \{n_0, \varphi_2\}.$$

We will now show that there is a large cancellation in (2.68), in that  $F$  is indeed equal to zero. To show this, it will be convenient to redefine the operator  $d_2$  (see

Eq.(2.55)) so as to split it into  $x$ -dependent and  $x$ -independent pieces according to

$$d_2 \equiv \mathcal{R}_1 + \{, \Psi_1\}, \quad \text{where } \mathcal{R}_1 \equiv -x(d_1 + \partial_\zeta). \quad (2.69)$$

We will also need the expression for  $\varphi_3$  as defined in Eq. (2.56). This expression can also be split into  $x$ -dependent and independent pieces, using (2.69), as

$$d_1\varphi_3 = d_t\Psi_1 - \mathcal{R}_1\varphi_2. \quad (2.70)$$

We now insert for  $d_2$  from (2.69) and for  $\varphi_3$  from (2.70) into the term  $F$  in (2.68) to get, upon separating out the  $R_1$  terms,

$$\begin{aligned} F = & q_0^2 (d_t d_1 \{n_0, \Psi_1\} - \{n_0, d_1 d_t \Psi_1\}) + \\ & q_0^2 (d_t d_1 \mathcal{R}_1 n_0 + \{n_0, d_1 \mathcal{R}_1 \varphi_2\}) + x \{n_0, \varphi_2\}. \end{aligned} \quad (2.71)$$

Using the commutation property of  $[d_1, d_t]$  from Eq.(A.14) in Appendix A, and  $d_1 n_0 = 0$  and  $d_t n_0 = 0$ , the 1<sup>st</sup> and 2<sup>nd</sup> terms can be seen to exactly cancel. The remaining  $x$ -terms in  $F$  can be expanded, using (A.6) and  $d_1 \mathcal{R}_1 n_0 = [d_1, \mathcal{R}_1] n_0 = (z/q_0) \partial_\zeta n_0$ , as

$$q_0 (z \partial_\zeta \partial_t n_0 + \{z \partial_\zeta n_0, \varphi_2\} + \{n_0, z \partial_\zeta \varphi_2\}) + x \{n_0, \varphi_2\}. \quad (2.72)$$

For the 2<sup>nd</sup> and 3<sup>rd</sup> terms in this equation, we use the identity (B.3) in Appendix B to rewrite (2.72) as

$$q_0 (z \partial_\zeta \partial_t n_0 + z \partial_\zeta \{n_0, \varphi_2\} - \{n_0, \varphi_2\}_{R,\zeta}) + x \{n_0, \varphi_2\}_{z,R}.$$

We see immediately that the first two terms cancel since  $d_t n_0 = 0$ . In addition, the 3<sup>rd</sup> and 4<sup>th</sup> terms cancel using the identity (B.1) in Appendix B.

### 2.5.1 Summary: closed set in a torus (in new variables)

The two large cancellations described above lead to a significant simplification, resulting in transparent equations for the vorticity and for the new density variable  $N_1$ . The equations for  $\{n_0, \varphi_2, \underline{\psi}_1, N_1, U_{||2}\}$  can be summarized as

$$d_t n_0 = 0 \tag{2.73}$$

$$d_t \underline{\psi}_1 = 0 \tag{2.74}$$

$$\begin{aligned} \nabla_{\perp} \cdot (d_t n_0 \nabla_{\perp} \varphi_2) &= -2\bar{\beta} \langle \partial_z N_1 \rangle \\ &- 2\bar{\beta} (1/q_0^2 - 1) \partial_{\alpha} n_0 + \frac{1}{r} \{\underline{\psi}_1, \underline{\Delta} \underline{\psi}_1\}_{(r,\alpha)} \end{aligned} \tag{2.75}$$

$$d_t N_1 - 2\partial_z \varphi_2 + n_0 d_1 U_{||2} = 0 \tag{2.76}$$

$$n_0 d_t U_{||2} + \bar{\beta} d_1 N_1 = 0. \tag{2.77}$$

## 2.6 Resistive MHD

In this section, we extend our sub-Alfvénic formalism to include non-ideal effects stemming from resistivity. We order resistivity such that  $\partial_t \sim \eta \nabla_{\perp}^2$ , i.e.,  $\eta = \bar{\eta} \epsilon^2 \sim O(\epsilon^2)$  Ohm's law in resistive MHD is

$$\mathbf{E} + \mathbf{u} \times \mathbf{B} = \eta \mathbf{j} + \mathbf{E}_{ext} \tag{2.78}$$

where  $\mathbf{E}_{ext} = E_{ext}(1/\epsilon) \nabla \zeta$  is an external inductive toroidal electric field needed to maintain a steady lowest order flux surface  $\psi_0$ . We note that resistivity will modify our previous reduced equation only through Faraday's law, Eqn. (2.3). Therefore,

here we will rederive only the terms in Faraday's law, order by order. First, Faraday's law to  $2^{nd}$  order is unchanged since  $\eta \mathbf{j}$  is of  $3^{rd}$  order at lowest. Thus, Eq. (2.77) for  $u_2$  remains unchanged. To  $3^{rd}$  order, we begin with the annihilated Faradays law, equation (2.10). This gives  $(\mathbf{B} \cdot \nabla)_1 \varphi_2 = \partial_t \psi_0 - \bar{\eta} J_1 - E_{ext}$ . Annihilating the  $\mathbf{B} \cdot \nabla f$  term in the usual manner, and assuming  $\partial_t \psi_0 = 0$ , we obtain  $E_{ext} = -\bar{\eta} J_1 = -\bar{\eta} \Delta \psi_0$ . This ensures  $\varphi_2$  remains a flute function.

To 4th order, we have

$$\begin{aligned} d_1 \varphi_3 + \mathcal{R}_1 \varphi_2 &= d_t \psi_1 - \bar{\eta} (\mathbf{j} \cdot \mathbf{B})_2 - x E_{ext} \\ &= d_t \psi_1 - \bar{\eta} \Delta \psi_1 - x \bar{\eta} / q_0. \end{aligned} \quad (2.79)$$

This equation is the analogue of Eq. (2.70). There are several  $x$  terms: obtained from the  $x$  correction to  $\mathbf{E}_{ext}$  and  $\bar{\eta} (\mathbf{j} \cdot \mathbf{B})_2$ . Before solving for  $\varphi_3$ , we annihilate the  $d_1$  operator. This results in the evolution equation for the flute part of the flux,  $\underline{\psi}_1$ , including the resistive diffusion term, viz.

$$d_t \underline{\psi}_1 = \bar{\eta} \underline{\Delta} \underline{\psi}_1 \quad (2.80)$$

$$d_1 \varphi_3 + \mathcal{R}_1 \varphi_2 = (d_t - \bar{\eta} \Delta) \Psi_1 - x \bar{\eta} / q_0. \quad (2.81)$$

The oscillatory part of  $\varphi_3$  can now be solved for. An examination of the terms that drive  $\varphi_3$  shows that resistivity enters only in the last two terms in Eq. (2.81). The remaining terms are all "ideal" terms that have been obtained before. In addition, all  $\psi_1$  terms are the same as in the ideal limit, since the Shafranov shifts, driven by  $n_0$  and  $\psi_0$ , are not affected by resistivity. We may thus separate out the ideal

and the resistive parts of  $\varphi_3$  as  $\varphi_3 = \varphi_3^I + \varphi_3^{PS}$  where  $\varphi_3^I$  satisfies the ideal equation (2.70) and  $\varphi_3^{PS}$  is the potential set up by Pfirsch-Schluter diffusion and is given by

$$\varphi_3^{PS} = \bar{\eta} q_0^2 d_1 (\Delta \Psi_1 + x/q_0) = -2\bar{\eta}(z - q_0^2 \bar{\beta} \partial_z n_0). \quad (2.82)$$

This separation between ideal and resistive parts of  $\varphi_3$  makes the transition to  $N_1$  from  $n_1$  transparent. In particular, the  $\varphi_3^I$  part cancels out exactly as in the ideal case but the  $\varphi_3^{PS}$  does not. Thus, the resistive  $N_1$  equation becomes

$$d_t N_1 + n_0 d_1 U_{||2} - 2\partial_z \varphi_2 + \mathbf{u}^{PS} \cdot \nabla n_0 = 0 \quad (2.83)$$

where

$$\mathbf{u}^{PS} = \hat{\zeta} \times \nabla \varphi_3^{PS}. \quad (2.84)$$

As noted earlier, the flow from  $\varphi_2$  is unaffected by the resistivity. All the extra flows, allowed by resistivity from frozen-in slippage, are now, to required order, captured by the (non-axisymmetric) Pfirsch-Schluter cells,  $\mathbf{u}^{PS}$ .

### 2.6.1 Summary: reduced Resistive MHD equations in a torus

In summary, we find that resistivity can be included in our formalism in a straightforward manner. The only modifications to the ideal toroidal system Eq.(2.73)-(2.77) are in the  $d_t \underline{\psi}_1$  and  $d_t N_1$  equations. The resistive version of these equations are given by Eq (2.76,2.74) replaced by (2.83,2.80).



## 2.7 Complete set of toroidal sub-Alfvénic equations

We summarize here the complete set of sub-Alfvénic resistive MHD equations. We drop without ambiguity all subscripts, for clarity. The toroidal nonlinear sub-Alfvénic equations for  $\{n, \varphi, \underline{\psi}, N, U_{\parallel}\}$  are:

$$d_t n = 0 \quad (2.85)$$

$$(d_t - \bar{\eta} \underline{\Delta}) \underline{\psi} = 0 \quad (2.86)$$

$$\begin{aligned} \nabla_{\perp} \cdot (d_t n \nabla_{\perp} \varphi) &= -\langle 2 \bar{\beta} \partial_z N \rangle \\ &- 2 \bar{\beta} (1/q_0^2 - 1) \partial_{\alpha} n + \frac{1}{r} \{\underline{\psi}, \underline{\Delta} \underline{\psi}\}_{(r, \alpha)} \end{aligned} \quad (2.87)$$

$$d_t N - 2n \partial_z \varphi + n d_1 U_{\parallel} + \mathbf{u}^{PS} \cdot \nabla n = 0 \quad (2.88)$$

$$n d_t U_{\parallel} + \bar{\beta} d_1 N = 0 \quad (2.89)$$

where,

$$\begin{aligned} d_t &= \partial_t + \hat{\zeta} \times \nabla \varphi \cdot \nabla = \partial_t + \frac{1}{r} (\{\varphi, \}_{(r, \alpha)} + \partial_r \varphi \partial_{\theta'}) \\ \underline{\Delta} &= (1/r) \partial_r (r \partial_r) + (1/r^2) \partial_{\alpha}^2 \\ \partial_z &= \sin \theta' \partial_r + (1/r) \cos \theta' (\partial_{\theta'} + \partial_{\alpha}) \\ d_1 &= (1/q_0) \partial_{\theta'}, \quad \langle \rangle = \oint \frac{d\theta'}{2\pi} \\ \mathbf{u}^{PS} &\equiv \hat{\zeta} \times \nabla \varphi^{PS}, \quad \varphi^{PS} = -2\bar{\eta} (z - q_0^2 \bar{\beta} \partial_z n). \end{aligned}$$

While these equations are complete, they are not manifestly 2D. As discussed, we only need the harmonic projections, as defined by  $X = X_s(r, \alpha) \sin \theta' + X_c(r, \alpha) \cos \theta'$ , for  $X = (N, U_{\parallel}, \varphi^{PS})$  with subscripts ‘c’ and ‘s’ denoting cosine and sine harmonics. To make the 2D nature of the equations explicit, we rewrite the above

complete set so that it only involves  $(r, \alpha)$  coordinates and the flute variables  $\{n, \underline{\psi}, \varphi, N_s, N_c, U_{\parallel s}, U_{\parallel c}\}$ . These equations are

$$\underline{d}_t n = 0 \quad (2.90)$$

$$(\underline{d}_t - \bar{\eta} \underline{\Delta}) \underline{\psi} = 0 \quad (2.91)$$

$$\begin{aligned} \nabla_{\perp} \cdot (\underline{d}_t n \nabla_{\perp} \varphi) &= -\langle 2 \bar{\beta} \partial_z N \rangle \\ -2 \bar{\beta} \left( \frac{1}{q_0^2} - 1 \right) \partial_{\alpha} n + \frac{1}{r} \{ \underline{\psi}, \underline{\Delta} \underline{\psi} \}_{(r, \alpha)} \end{aligned} \quad (2.92)$$

$$\underline{d}_t \begin{pmatrix} N_s \\ N_c \end{pmatrix} + \frac{1}{r} \partial_r \varphi \begin{pmatrix} -N_c \\ N_s \end{pmatrix} + \frac{n}{q_0} \begin{pmatrix} -U_{\parallel c} \\ U_{\parallel s} \end{pmatrix} = \begin{pmatrix} S_1 \\ S_2 \end{pmatrix} \quad (2.93)$$

$$n \underline{d}_t \begin{pmatrix} U_{\parallel s} \\ U_{\parallel c} \end{pmatrix} + \frac{n}{r} \partial_r \varphi \begin{pmatrix} -U_{\parallel c} \\ U_{\parallel s} \end{pmatrix} + \frac{\bar{\beta}}{q_0} \begin{pmatrix} -N_c \\ N_s \end{pmatrix} = 0 \quad (2.94)$$

where, all 7 variables are functions of  $(r, \alpha)$  and

$$\underline{d}_t = \partial_t + (1/r) \{ \varphi, \ }_{(r, \alpha)}$$

$$2 \langle \partial_z N \rangle = (\partial_r + 1/r) N_s + (1/r) \partial_{\alpha} N_c$$

$$\varphi_s^{PS} = -2\bar{\eta}(r - q_0^2 \bar{\beta} \partial_r n)$$

$$\varphi_c^{PS} = 2\bar{\eta}(q_0^2 \bar{\beta} \partial_{\alpha} n)/r$$

$$\begin{pmatrix} S_1 \\ S_2 \end{pmatrix} = \frac{1}{r} \begin{pmatrix} 2n r \partial_r \varphi + \{n, \varphi_s^{PS}\}_{r, \alpha} - \varphi_c^{PS} \partial_r n \\ 2n \partial_{\alpha} \varphi + \{n, \varphi_c^{PS}\}_{r, \alpha} + \varphi_s^{PS} \partial_r n \end{pmatrix}.$$

We restate here the normalizations: lengths are normalized to the minor radius  $a$ ; time rates are normalized to  $\epsilon^2 c_A/a \sim c_s/R$ ,  $\epsilon = a/R$ . The time-varying part of the magnetic field is defined according to  $\epsilon^2 \mathbf{B}_2 = \epsilon^2 \hat{\boldsymbol{\zeta}} \times \nabla \psi_1$ . In addition, the

complete density is given as  $n + \epsilon n_1$ , where  $n_1$  is defined in terms of  $N$  by Eq (2.63).

The operators  $d_1$  and  $d_2$  are defined in the Appendix, Eqs. (A.7) and (A.8).

## 2.8 Invariants of the Reduced system

Ideal MHD [1] satisfies a number of important conservation properties e.g conservation of mass, momentum, energy, flux, angular momentum, magnetic helicity, cross helicity etc. In this section we shall discuss the various quantities that are conserved by our reduced system of equations. The proofs are given in Appendix E. Besides mass and magnetic flux, Eqs (2.85,2.86,2.88), the following are also conserved:

1. Magnetic-helicity

$$\int r dr d\alpha d\theta' \psi \quad (2.95)$$

where  $\psi$  includes both the periodic and flute components of  $\psi_1$ .

2. Cross-helicity in a closed field line:

$$\int r dr d\alpha d\theta' U_{\parallel} \quad (2.96)$$

3. Angular momentum (in axisymmetry):

$$\int r dr \left( \left( U_{\parallel c} - \frac{1}{q_0} \partial_r \varphi \right) nr + \langle NU_{\parallel} \rangle \right) \quad (2.97)$$

4. Energy:

$$\int r dr d\alpha \left( \frac{1}{2} |\nabla \psi|^2 + \frac{1}{2} n |\nabla \varphi|^2 + \frac{1}{2} \left( \frac{\bar{\beta}}{n} \langle N^2 \rangle + n \langle U_{\parallel}^2 \rangle \right) - 2\bar{\beta} \left( \frac{1}{q_0^2} - 1 \right) rn \right) \quad (2.98)$$

where  $\langle NU_{\parallel} \rangle = (1/2) (N_s U_{\parallel s} + N_c U_{\parallel c})$  etc.

Let us now compare these with the corresponding quantities obtained from the full MHD system. The form of cross helicity in ideal MHD is  $\int dV \mathbf{U} \cdot \mathbf{B}$ . To required order we recover Eq.(2.96). The form for angular momentum is volume integral of  $nM \mathbf{u} \cdot \nabla \zeta R^2 = nM(RU_{\parallel} - (r/q_0)\partial_r \varphi)$ . Thus after averaging,  $U_{\parallel c}$  survives. The  $\langle NU_{\parallel} \rangle$  occurs because first order density and  $\parallel$  flow vary poloidally. Finally, from the energy density of isothermal ideal MHD [13],

$$\mathcal{E} = \frac{B^2}{2} + \frac{1}{2}nu^2 + nT \log(n)$$

we can see that the first term in Eq.(2.98) is the  $B_p^2$  energy, the flow energy is composed of averaged  $(n/2)(U_{\parallel}^2 + |\nabla \varphi|^2)$ . The logarithmic term  $nT \log n$ , which is a hallmark of a isothermal system, when expanded to required order gives the term quadratic [13] in  $N$  and finally we have an ‘‘effective gravity’’ like term  $\sim (1/q_0^2 - 1)rn$  due to the averaged curvature of  $\mathbf{B}$ .

## 2.9 Various sub-limits

The sub-Alfvénic equations, (2.85) to (2.89), can be examined in two illuminating limits, the axisymmetric limit, and the subsonic limit. We discuss these two limits in this section.

### 2.9.1 Axisymmetric limit

We discuss the axisymmetric ( $\partial_{\zeta} = 0 = \partial_{\alpha}, \partial_{\theta'} = \partial_{\theta}$ ) limit of the subalfvénic equations. In this limit, the flute functions are only functions of  $r$  and  $t$ . The  $E \times B$

flows are on a magnetic surface. Thus, the total time derivative is given by

$$d_t = \partial_t + \frac{1}{r} \frac{d\varphi(r, t)}{dr} \partial_\theta \quad (2.99)$$

and equation (2.73) becomes  $\partial_t n = 0$ , which yields  $n = n(r)$ .

In the vorticity equation we see that the only non zero contribution comes from the term  $\langle \partial_z N \rangle$  on the RHS of (2.75); the interchange and the field line bending terms vanish in the  $\partial_\alpha = 0$  limit, and  $\underline{\psi}_1$  is not needed. Thus, the axisymmetric reduced equations, which govern  $\varphi$ ,  $N$ , and  $U_{||}$ , are given by

$$\frac{1}{r} d_r \left( n r \frac{d}{dr} \partial_t \varphi \right) = -2\bar{\beta} \langle \partial_z N \rangle \quad (2.100)$$

$$d_t N - 2\partial_z \varphi + n d_1 U_{||} - \frac{q_0}{r} n'(r) d_1 \varphi^{PS} = 0 \quad (2.101)$$

$$n d_t U_{||} + \bar{\beta} d_1 N = 0 \quad (2.102)$$

where  $d_1 = (1/q_0)\partial_\theta$ ,  $\varphi^{PS} = -2\bar{\eta}z(1 - rn'\bar{\beta}_p)$ ,  $\beta_p = (q_0^2/r^2)\bar{\beta}$ .

In the limit of zero resistivity and  $\partial_r \gg 1/r$  these equations reduce to the nonlinear system of equations developed by Hassam-Drake [14] (HD). In that work, in-out asymmetric density source terms were included to show the existence of spontaneous poloidal spin-up. However, a spin-up can also be obtained from the resistive, Pfirsch-Schluter, flows. These terms appear in our  $N$  density equation and, as shown below, provide necessary source terms to drive spontaneous poloidal spin up.

From the axisymmetric equations (2.100) – (2.101), an equilibrium solution is:

$$\begin{aligned} n &= n(r), \quad N = \varphi = 0, \quad \Psi = \Psi_c \cos \theta' \\ U_{\parallel,s} &= -2\bar{\eta} q_0 \frac{n'}{n} (1 - \bar{\beta}_p r n') \end{aligned} \quad (2.103)$$

The parallel flows are in response to the toroidally outward resistive flow produced from the Pfirsch-Schluter potential  $\varphi^{PS}$ ; these are the well known Pfirsch-Schluter convection cells. Let us now linearize the system about this equilibrium. We shall assume that fluctuating gradients are much bigger than equilibrium gradients. We shall denote perturbations by overhead tildes. Assuming the perturbations  $\tilde{N}, \tilde{\varphi}, \tilde{U}_{\parallel}$ , to have a  $e^{\gamma t}$  dependence, we obtain the following dispersion relation (in agreement with Eq 41 in HD [14])

$$\gamma \left( 1 + 2q_0^2 + \frac{\gamma^2}{\bar{\beta}/q_0^2} \right) \approx \frac{q_0 U_{\parallel,s}}{r} \quad (2.104)$$

The parallel flow is resistive, thus small. As obtained in HD, the cubic equation yields GAMs and sound waves as the high frequency solution, and the Stringer-spinup with an effective mass as the low frequency solution.

We note that zero frequency incompressible zonal flows are also obtained from the set (2.100)-(2.102) by allowing  $\varphi(r)$  as part of the equilibrium. In this case,  $U_{\parallel}$  and  $\varphi$  are related by the incompressible condition  $U_{\parallel} = -2q \cos \theta d\varphi/dr$ .

## 2.9.2 Subsonic limit

It is instructive to study the sub-Alfvénic equations (2.85)-(2.89) in the limit that time variations are subsonic. This can happen, for example, when the Mercier

driving term is weak, or in the case of zonal flows. We study this by a subsidiary expansion with  $d_t \ll c_s/R$ . In this limit,  $d_t U_{\parallel}$  in Eq (2.77) is very small compared with the  $d_1 N$  term. Thus,  $N$  is a flute to lowest order and we can set this to zero. This implies we can ignore  $d_t N$  in equation (2.76). Denoting the subordered quantities by superscripts we obtain,

$$d_1 N^{(0)} = 0 \quad \Rightarrow \quad N^{(0)} = 0 \quad (2.105)$$

$$d_1 U_{\parallel}^{(0)} = 2\partial_z \varphi. \quad (2.106)$$

Thus, the flow is incompressible as expected. We substitute this in (2.77) to obtain the correction to  $N$ ,

$$d_1 N^{(1)} = -(n/\bar{\beta})d_t U_{\parallel}^{(0)} = (nq_0/\bar{\beta})d_t \partial_R \varphi. \quad (2.107)$$

Operating with  $d_1$  on this equation again and using the fact that  $[d_1, d_t] = 0$ , we obtain  $N^{(1)} = 2(q_0^2/\bar{\beta})d_t(n\partial_z \varphi)$ . From the vorticity equation (2.75) we observe that  $N$  enters through  $\langle \partial_z N \rangle$ . Using the expression for the latter from Appendix D we find that the subsonic vorticity equation takes the form of

$$(1 + 2q_0^2) d_t \Omega = -2 \left( \frac{1}{q_0^2} - 1 \right) \bar{\beta} \partial_\alpha n + \frac{1}{r} \{ \underline{\psi}, \underline{\Delta} \underline{\psi} \}_{(r,\alpha)}. \quad (2.108)$$

This clearly shows that in the ideal subsonic limit, the incompressible flows result in an ‘‘effective mass’’, leading to the Pfirsch-Schluter  $(1 + 2q^2)$  factor.

## 2.10 Linearized modes

In this section, we examine the linearized version of the full equation set (2.85-2.89), to effect a cross check with previous well known results. We consider the

axisymmetric equilibrium Eq.(2.103) about a rational surface  $q_0 = m/n$  with  $q(r)$  close to  $q_0$  and  $\underline{\psi}$  related to  $q(r)$  by  $(\epsilon/r)d\underline{\psi}/dr = (1/q(r) - 1/q_0)$ . We consider perturbations of the form  $\sim e^{\gamma t}e^{-im\alpha}$ . The linearized set is given by

$$\gamma \tilde{n} + \iota \frac{m}{r} n'_0 \tilde{\varphi} = 0 \quad (2.109)$$

$$(\gamma - \bar{\eta} \underline{\Delta}) \tilde{\underline{\psi}} + \iota \bar{k}_{||} \tilde{\varphi} = 0 \quad (2.110)$$

$$\begin{aligned} \gamma n \underline{\Delta} \tilde{\varphi} = & -2\bar{\beta} \langle \partial_z \tilde{N} \rangle + 2 (1/q_0^2 - 1) \bar{\beta} \iota m \tilde{n} \\ & + \frac{1}{r} \{ \widetilde{\underline{\psi}, \underline{\Delta} \underline{\psi}} \}_{(r,\alpha)} \end{aligned} \quad (2.111)$$

$$\gamma \tilde{N} + d_1(\widetilde{nU_{||}}) - 2n \partial_z \tilde{\varphi} + \{ \widetilde{n, \varphi^{PS}} \} = 0 \quad (2.112)$$

$$\gamma \widetilde{nU_{||}} + n \{ U_{||}, \tilde{\varphi} \} + \bar{\beta} d_1 \tilde{N} = 0 \quad (2.113)$$

where,

$$\bar{k}_{||} = (1/r) \{ \underline{\psi}, \ }_{(r,\alpha)} = (m/r)(d\underline{\psi}/dr) = (m/\epsilon)(1/q(r) - 1/q_0)$$

The general dispersion relation can be obtained in a straight forward manner.

Considering perturbed quantities to vary more rapidly than equilibrium quantities

we obtain

$$\begin{aligned} \gamma_s^2 \left( 1 + \frac{2q_0^2}{1 + \gamma_s^2} \right) \underline{\Delta} \tilde{\varphi} - 2(1 - q_0^2) \frac{r n'}{n} \left( \frac{m}{r} \right)^2 \tilde{\varphi} \\ = \frac{q_0^2}{n\bar{\beta}} \frac{\gamma}{r} \{ \widetilde{\underline{\psi}, \underline{\Delta} \underline{\psi}} \}_{(r,\alpha)} + \frac{\gamma_s^2}{1 + \gamma_s^2} \frac{q_0^2}{n} (\tilde{S}_N + \tilde{S}_U) \frac{1}{\gamma} \end{aligned} \quad (2.114)$$



where

$$\begin{aligned}\gamma_s^2 &= \frac{\gamma^2}{\bar{\beta}/q_0^2}, \quad \bar{\beta}_p = \frac{q_0^2}{r^2}\bar{\beta}, \quad U_{\parallel s} = -2\bar{\eta}q_0\frac{n'}{n}(1 - \bar{\beta}_p r n') \\ \tilde{S}_N &= \left\langle 2\gamma\partial_z\{\widetilde{n, \varphi^{PS}}\} \right\rangle \approx -2\bar{\eta}\bar{\beta}_p\left(\frac{m}{r}\right)^2 (r n')^2 \underline{\Delta}\tilde{\varphi} \\ \tilde{S}_U &= \left\langle 2\partial_z n\{-d_1 U_{\parallel}, \tilde{\varphi}\} \right\rangle \approx \frac{n}{q_0 r} (U_{\parallel s} \underline{\Delta}\tilde{\varphi})\end{aligned}$$

The source terms  $\tilde{S}_N, \tilde{S}_U$  are present only in the resistive case and shows the effect of ‘‘Pfirsch-Schluter’’ potential and flows respectively on the vorticity. Substituting for  $\tilde{S}_N, \tilde{S}_U$  in Eq. 2.114 we get

$$\begin{aligned}\gamma_s^2 \left(1 + \frac{2q_0^2}{1 + \gamma_s^2}(1 + \chi)\right) \underline{\Delta}\tilde{\varphi} = \\ 2q_0^2 \left(\frac{r n'}{n}\right) \left(\frac{1}{q_0^2} - 1\right) \left(\frac{m}{r}\right)^2 \tilde{\varphi} + \frac{q_0^2 \gamma}{n\beta r} \{\widetilde{\psi, \underline{\Delta}\psi}\}_{(r, \alpha)}\end{aligned}\quad (2.115)$$

where  $\chi = -\frac{1}{2\gamma} \left(\frac{U_{\parallel, s}}{q_0 r}\right) + \frac{\bar{\eta} \bar{\beta}_p n}{\gamma} \left(\frac{r n'}{n}\right)^2 \left(\frac{m}{r}\right)^2$ ,

If we put  $m = 0$  we immediately recover the axisymmetric dispersion relation (2.104) which describes Stringer spin-up. Next, we consider some other limiting cases.

### 2.10.1 Ideal MHD interchange modes without shear

For very weak magnetic shear, we may set  $k_{\parallel}$  to zero. Considering ideal modes only, and assuming elongated interchanges,  $\partial_\alpha \gg r\partial_r \gg 1$ , we obtain the dispersion:

$$\gamma_s^2 \left(1 + \frac{2q_0^2}{1 + \gamma_s^2}\right) = -2(1 - q_0^2) \frac{r n'}{n}, \quad \gamma_s^2 = \frac{\gamma^2}{\bar{\beta}/q_0^2}$$

The equation is bi-quadratic and we conclude instability if  $q < 1$  and for negative  $dn/dr$ . This is the well known ideal interchange instability first obtained by Mercier. If the instability driver term on the RHS is strong, i.e., very steep pressure gradients, the modes decouple into a supersonic interchange mode,  $\gamma_s^2 \approx -2(1 - q_0^2)(rn'/n)$ , and a sound wave  $\gamma_s^2 = 1$ . In the opposite limit, for weak gradients, the modes decouple into a subsonic interchange mode,  $\gamma_s^2 \approx -2(1 - q_0^2)(rn'/n)/(1 + 2q_0^2)$ , and the GAM  $\gamma_s^2 \approx -(1 + 2q_0^2)$ . The denominator in the interchange mode,  $(1 + 2q_0^2)$ , is the effective mass, discussed earlier. The GAM is of the same frequency as the GAM obtained in the axisymmetric limit Eq(2.104); however, the present calculation is for flute convection cells, elongated in radius and of high mode numbers. Thus, the GAM convection cells are isotropic and of unique frequency.

### 2.10.2 Ideal MHD Linear modes with shear

Using Eq (2.91) (with  $\eta = 0$ ) and  $(1/r)\{\underline{\psi}, \underline{\psi}\}_{(r,\alpha)} = \bar{k}_{||}$ , the shear term  $(1/r)\{\widetilde{\underline{\psi}}, \underline{\Delta}\underline{\psi}\}_{(r,\alpha)}$  can be written as

$$-(1/\gamma) (\bar{k}_{||} \underline{\Delta}\bar{k}_{||} \tilde{\varphi}) - \bar{k}_{||}\tilde{\varphi}(1/r)\partial_r ((1/r)\partial_r(r^2\bar{k}_{||})) .$$

It can further be shown that the resulting eigenvalue equation is

$$\begin{aligned} \frac{1}{r^2}\partial_r \left( \gamma_A^2 r^3 \partial_r \left( \frac{\tilde{\varphi}}{r} \right) \right) + \frac{1}{r^2}\gamma_A^2(1 - m^2)\tilde{\varphi} \\ = \frac{2m^2}{r^2}(1 - q_0^2)\frac{r}{n}\frac{n'}{n}\tilde{\varphi} \end{aligned} \quad (2.116)$$

where

$$\gamma_A^2 = \gamma_s^2 \left( 1 + \frac{2q_0^2}{1 + \gamma_s^2} \right) + \frac{\bar{k}_\parallel^2}{\bar{\beta}n/q_0^2}$$

This is the Shear-Alfvén law as discussed by Hazeltine et. al [15], that describes kink modes and interchange modes. In the case of constant  $k_\parallel$ , the Mercier dispersion obtained above contains an additional frequency, namely the Alfvén wave  $\omega = k_\parallel c_A$ , which is stabilizing for the Mercier mode.

In the marginal stability  $\omega \rightarrow 0$  case, the modes are highly localized near the mode rational surface. Expanding about the surface with  $r = r_0 + x$ , and  $\bar{k}_\parallel \approx \bar{k}'_\parallel x = -(m\hat{s}/q_0)(x/r_0)$ , we get

$$\frac{\partial}{\partial x} \left( -\frac{2\bar{\beta}}{\hat{s}^2} r n' (1 - q_0^2) \right) \tilde{\varphi} = 0$$

Newcomb's condition can be used on the above equation to obtain the Mercier criterion with shear, viz,

$$2\bar{\beta} (1 - q_0^2) r n' + \frac{1}{4} \hat{s}^2 > 0$$

### 2.10.3 Resistive ballooning without shear

Let us now include the effects of resistivity on the ideal mode of section 2.10.1 (no shear). In the limit  $m \sim \partial_\alpha \gg r \partial_r \gg 1$ , the term  $(\bar{\eta}/\gamma r^2)(r n'/n)m^2 r n' \bar{\beta}_p$  dominates over the term  $U_{\parallel,S}$  term in  $\chi$ . The linear dispersion relation can be shown from Eq. 2.115 to be

$$\gamma_s^2 \left( 1 + \frac{2q_0^2}{1 + \gamma_s^2} (1 + \chi) \right) = 2q_0^2 \left( \frac{r n'}{n} \right) \left( \frac{1}{q_0^2} - 1 \right) \quad (2.117)$$

For small  $\bar{\eta}$  and moderate mode numbers, the term in  $\chi$  can be neglected and the ideal interchange modes are recovered (stable or unstable). For large mode numbers, the  $\chi_1$  term can become large. This can only be balanced if  $\gamma_s^2$  itself is large, in which case  $1 = -2q_0^2\chi/\gamma_s^2$ . This results in a high  $m$  unstable mode, with  $\gamma \sim \bar{\eta}^{1/3}$ . This is the resistive ballooning mode which is unstable even if the RHS term is stabilizing, i.e, if the average curvature is stable. The mode localizes to the unfavorable curvature.

#### 2.10.4 Resistive MHD modes with shear

Let us now consider resistive modes with finite shear in the limit  $\gamma \ll \bar{\eta}\Delta$ . In this limit we have  $\bar{\eta}\Delta\tilde{\psi} = \iota k_{\parallel}\tilde{\varphi}$ . Expanding near the rational surface with  $r = r_0 + x$  we get  $\bar{k}_{\parallel} = \bar{k}'_{\parallel}x$ , with  $\bar{k}'_{\parallel}q_0r_0 = -m\hat{s}$ . The term  $\{\widetilde{\psi}, \widetilde{\Delta\psi}\}$  on the RHS of Eq. 2.115 can be shown to be  $\tilde{\varphi}(\bar{k}'_{\parallel}x)^2/\bar{\eta}$ . The vorticity equation now reduces to Webber's equation of the form

$$a_1 \frac{\partial^2 \tilde{\varphi}}{\partial x^2} = (a_2 + a_3 x^2) \tilde{\varphi} \quad \Rightarrow \quad \tilde{\varphi} \sim e^{-\alpha x^2/2} \quad (2.118)$$

where,

$$a_1 = \gamma_s^2 \left( 1 + \frac{2q_0^2}{1 + \gamma_s^2} (1 + \chi) \right), \quad a_2 = 2q_0^2 \left( \frac{r n'}{n} \right) \left( \frac{1}{q_0^2} - 1 \right), \quad a_3 = \frac{\gamma}{\bar{\eta}} \frac{\bar{k}'_{\parallel}{}^2}{n\bar{\beta}/q_0^2}$$

For an instability with a real growth rate to exist, the exponent  $\alpha$  must be real and positive. This is possible iff the conditions,  $a_2/a_1 < 0, a_1 a_3 = a_2^2$  are satisfied. The first of these conditions imply ideal stability and the second gives the dispersion relation

$$\frac{\gamma^3}{\bar{\eta}} \left( \frac{\bar{k}'_{\parallel}}{\bar{\beta}/q_0^2} \right)^2 \left( 1 + \frac{2q_0^2}{1 + \gamma_s^2} (1 + \chi) \right) = na_2^2 \quad \Rightarrow \quad \gamma \sim \bar{\eta}^{1/3}$$

Therefore we can see that the  $\gamma \sim \bar{\eta}^{1/3}$  scaling can be obtained both with and without shear.

## 2.11 Summary and Discussion

Reduced equations, at frequencies below the ballooning shear Alfvén frequency, have been derived for tokamak geometry. Because the field line structure guides the motion, the equations are 2-dimensional in space, though also nonlinear. While the calculation to reduction is involved and characterized by large cancellations, the resulting set of equations is quite intuitive and consistent with well known previous results in various sublimits.

Previously, Drake and Antonsen (DA) have also derived similar reduced equations. The DA ordering like our ordering, is also sub-Alfvénic. Accordingly, DA also incorporate a dynamic Shafranov shift in that  $\mathbf{j} \times \mathbf{B} \approx \nabla p$  to high order. Their ordering, in contrast to ours, is also subsonic: time rates  $\partial_t/(c_A/R)$  are ordered as  $\epsilon^2$ . By keeping higher order corrections, above the quasi static condition, they obtain general, 3D, sub-sonic equations, also applicable to low and intermediate mode numbers. DA show the necessity of 2 scales along  $\mathbf{B}$ , of order  $R$  and longer. This is similar to ours in that weak  $k_{\parallel}$  is retained. Our approach has many similarities except our equations optimally allow sonic frequencies. We also expand about a low order rational surface. This yields a set of 2D single helicity equations with

side band harmonic content, albeit restricting applicability to relatively short radial domains.

Our system is suited for regions where  $q(r)$  is close to rational and the shear is not too strong. One possible application is to the core of tokamaks, in regions where the safety factor  $q(r)$  stays close to unity. An important problem is to study the sawtooth phenomena in the core of tokamaks. When  $q(r)$  goes below unity, an  $m = 1$  tearing is precipitated at the  $q = 1$  surface. The ensuing reconnection is thought to be responsible for the well known sawtooth discharges which keep  $q$  close to unity. Nonlinearly, if  $q(r)$  stays self-consistently close to unity, our equations should be applicable. In particular, for regions where  $q < 1$ , the  $(1/q_0^2 - 1)$  term will destabilize Mercier modes, at growth rates of order  $(\Delta q)^{1/2}(c_s/R)$ . The Mercier interchanges would be macroscopic and would compete with the tearing mode whose intrinsic Alfvénic frequency could scale as  $\epsilon c_A/R$  or less. These unstable Mercier interchanges do not necessarily have to be high mode numbers. As has been pointed out by Ramos [16], for low shear and  $k_\perp \sim 1/a$  the interchange stability condition is independent of the toroidal wavenumber  $n$ . It would be very interesting to study the interaction of these two strong and long wavelength instabilities. As a caveat, we point out that our reduced equations, strictly, would have to be further reduced if  $q_0$  is exactly unity. However,  $q_0$  could evolve under slower transport time scales. Thus, by replacing  $q_0$  with  $q(r,t)$ , a model set of equations could be investigated. The results could be suggestive and provide guidance to a fully 3D code.

For high mode numbers, there will be strong overlap of sub-Alfvénic dynamics between mode rational surfaces. Our equations may not directly apply and a bal-

looning type formalism is more applicable. For low to intermediate mode numbers, however, as has also been pointed out by Hastie and Taylor [17, 18], the standard formalism breaks down. The failure shows up in the form of oscillations of local  $\omega^2$  with toroidal mode number. The main point is that the separation between successive rational surfaces increases, and the modes, instead of spreading over multiple surfaces, tend to localize near their respective mode rational surfaces. Thus, for low shear and finite to intermediate mode numbers, modes behave more like Fourier modes than ballooning modes as discussed by Connor et.al [19]. Hastie et al [17] modified the standard picture by making the ballooning coordinate finite and periodic in extent (as opposed to infinite in standard ballooning representation). Manickam et.al [20] later showed that even the modified ballooning formalism fails for certain modes labelled as “infernal” modes. These are sensitive to pressure and q profiles and can be unstable even though ballooning theory predicts complete stability. Our equations can allow ultra flat q profiles and could describe modes like “infernal modes”

# Part II

Kinetic MHD: Sub-Alfvénic and Kinetic MHD



## Chapter 3: Sub-Alfvénic and supersonic reduced Kinetic MHD

### 3.1 Overview

We generalize the previously derived sub-Alfvénic procedure to the collisionless limit described by kinetic MHD. Restricting to the supersonic limit, we systematically reduce the kinetic MHD system developed by Kulsrud [8]. For large  $q$ , one can achieve a self consistent supersonic regime where effects of sound waves are minimized. In this limit, the analysis is particularly simple because there are no trapped ions as the time rates exceed ion bounce frequency, and Kulsrud’s kinetic MHD system reduces to the CGL double adiabatic equations. Using methods analogous to Part I, especially as far as the cancellations, we present a complete set of nonlinear sub-Alfvénic reduced KMHD in the CGL limit. This is a direct generalization of the previous RMHD equations to a kinetic system which allows pressure anisotropy but, self-consistently not trapped dynamics.

### 3.2 Kinetic MHD Equations and ordering

We begin with the collisionless kinetic MHD equations written in

$\{v_{\parallel}, \mu = |\mathbf{v}_{\perp}|^2/2B, \mathbf{x}, t\}$  variables:

$$\partial_t n + \nabla \cdot (n\mathbf{u}) = 0 \quad (3.1)$$

$$\partial_t (nM\mathbf{u}) + \nabla \cdot \overleftrightarrow{\mathbf{P}} = \mathbf{j} \times \mathbf{B}, \quad \mathbf{j} \equiv \nabla \times \mathbf{B} \quad (3.2)$$

$$\partial_t \mathbf{B} = \nabla \times (\mathbf{u} \times \mathbf{B}) \quad (3.3)$$

$$\nabla \cdot \mathbf{B} = 0 \quad (3.4)$$

$$\partial_t f + (v_{\parallel} \nabla_{\parallel} + \mathbf{u}_E \cdot \nabla) f + \left( -\hat{\mathbf{b}} \cdot \frac{D\mathbf{u}_E}{Dt} - \mu \nabla_{\parallel} B + \frac{e}{M} E_{\parallel} \right) \partial_{v_{\parallel}} f = 0 \quad (3.5)$$

$$n_e = n_i \quad (3.6)$$

where,

$$\mathbf{u} = U_{\parallel} \hat{\mathbf{b}} + \mathbf{u}_E, \quad \mathbf{u}_E = \mathbf{E} \times \mathbf{B} / B^2 \quad (3.7)$$

$$D\mathbf{u}_E / Dt \equiv \partial_t \mathbf{u}_E + (\mathbf{u}_E + v_{\parallel} \hat{\mathbf{b}}) \cdot \nabla \mathbf{u}_E \quad (3.8)$$

$$\overleftrightarrow{\mathbf{P}} \equiv p_{\perp} \mathbb{I} + (p_{\parallel} - p_{\perp}) \mathbf{b}\mathbf{b}, \quad p_{\parallel} = M \int d^3v v_{\parallel}^2 f, \quad p_{\perp} = M \int d^3v \mu B f \quad (3.9)$$

$$(e/M)nE_{\parallel} = \hat{\mathbf{b}} \cdot \nabla \cdot (\overleftrightarrow{\mathbf{P}}_e - (m/M) \overleftrightarrow{\mathbf{P}}_i) / (1 + m/M) \quad (3.10)$$

Note that we have used Eq. (51) instead of Eq.(37) for our drift kinetic equation Eq.(3.5). Note also, that the distribution function is needed only to obtain the pressure tensor. The definition of pressures used here are different from Kulsrud [8] Eq. (44). Also, Kulsrud obtains  $\mathbf{E}$  from the perpendicular component of  $\mathbf{u}$  but we shall use  $\mathbf{E} = -\nabla\phi - \partial_t \mathbf{A}$  as before. We shall also assume adiabatic electrons. Therefore we shall use  $p_e = \bar{\beta}_e n$  order by order.

The standard annihilations corresponding to the fluid annihilations given by Eqs. (2.8,2.9,2.10) are

$$\mathbf{B} \cdot \left( \frac{\partial M_i n \mathbf{u}}{\partial t} + \nabla \cdot \mathbf{P} \right) = 0 \quad (3.11)$$

$$\begin{aligned} \partial_t \nabla \cdot \left( \frac{M_i n \mathbf{u} \times \hat{\mathbf{b}}}{B} \right) &= \mathbf{B} \cdot \nabla \left( \frac{j_{\parallel}}{B} \left( 1 + \frac{p_{\perp,e} + p_{\perp,i}}{B^2} \right) \right) + \\ &\quad \nabla \cdot \frac{\hat{\mathbf{b}}}{B} \times \left( 2 n T_e + \int d^3 v M (v_{\parallel}^2 \boldsymbol{\kappa} + \mu \nabla B) f_i \right) \end{aligned} \quad (3.12)$$

$$(e/M)n(\nabla_{\parallel} \phi + \hat{\mathbf{b}} \cdot \partial_t \mathbf{A}) = \hat{\mathbf{b}} \cdot \nabla \cdot \overleftrightarrow{\mathbf{P}}_e - (m/M) \hat{\mathbf{b}} \cdot \nabla \cdot (\overleftrightarrow{\mathbf{P}}_i + \overleftrightarrow{\mathbf{P}}_e) \quad (3.13)$$

For the asymptotic analysis we shall use the ordering similar to the fluid case

(2.7)

$$\frac{k_{\parallel}}{k_{\perp}} \sim \frac{\mathbf{u}_{\perp}}{c_s} \sim \frac{B_p}{B_T} \sim \frac{c_s}{c_A} \sim \sqrt{\beta} \sim \epsilon.$$

The main difference with the fluid ordering lies in the parallel flow which was chosen to be subsonic in the fluid case. However, in the axisymmetric limit, the trapped particles can have a large parallel flow  $\sim qu_E/\epsilon \approx c_s$  because of toroidal precession. Before proceeding further, let us simplify the basic equations for a low beta sub-Alfvénic system.

Let us first simplify the drift kinetic equation (DKE). Using Eq. (3.3,3.7,3.8), the term  $-\hat{\mathbf{b}} \cdot D\mathbf{u}_E/Dt$  can be shown to be

$$-\hat{\mathbf{b}} \cdot \frac{D\mathbf{u}_E}{Dt} - v_{\parallel} \mathbf{u}_E \cdot \boldsymbol{\kappa} = \mathbf{u}_E \cdot \partial_t \hat{\mathbf{b}} - \nabla_{\parallel} \frac{u_E^2}{2} + \frac{\mathbf{E}}{B} \cdot \nabla \times \mathbf{u}_E = \nabla_{\parallel} \frac{u_E^2}{2} \approx O(\epsilon^5).$$

Based on the fluid asymptotics, we need  $\partial_t f$  to a maximum of 3<sup>rd</sup> order, so  $-\hat{\mathbf{b}} \cdot D\mathbf{u}_E/Dt \approx v_{\parallel} \mathbf{u}_E \cdot \boldsymbol{\kappa}$ . Therefore, the DKE can be simplified to

$$\partial_t f + (v_{\parallel} \nabla_{\parallel} + \mathbf{u}_E \cdot \nabla) f + \left( v_{\parallel} \mathbf{u}_E \cdot \boldsymbol{\kappa} - \mu \nabla_{\parallel} B + \frac{e}{m} E_{\parallel} \right) \partial_{v_{\parallel}} f = 0 \quad (3.14)$$

Also, for a low beta system we shall find the following approximate form of the vorticity equation more useful

$$\nabla \cdot \left( M_i \partial_t (n \mathbf{u}) \times \frac{\hat{\mathbf{b}}}{B} \right) = \mathbf{B} \cdot \nabla \left( \frac{j_{\parallel}}{B} \left( 1 - \frac{p_{\parallel} - p_{\perp}}{B^2} \right) \right) + \hat{\mathbf{b}} \times \frac{\nabla B}{B^2} \cdot \nabla (p_{\parallel} + p_{\perp} + 2nT_e). \quad (3.15)$$

In the following, we shall use Eqs. (3.14,3.15) for the DKE and vorticity equations. It is important to note that Eq. (3.14) scales differently for the trapped and circulating particles since the velocity scales differently for these two species. For CPs,  $v_{\parallel} \sim c_s$ , while for TPs,  $v_{\parallel} \sim \sqrt{\epsilon} c_s$ . Assuming  $u_E \sim \epsilon c_s$  and defining  $\omega_s \equiv \omega / (c_s / qR)$ , we scale the DKE to obtain

$$\partial_t f + (v_{\parallel} \nabla_{\parallel} + \mathbf{U}_E \cdot \nabla) f + \left( v_{\parallel} \mathbf{U}_E \cdot \kappa - \mu \nabla_{\parallel} B + \frac{e}{m} E_{\parallel} \right) \partial_{v_{\parallel}} f = 0$$

$$\omega_s : \quad 1 : \quad q : \quad q \epsilon : \quad \epsilon : \quad 1 \quad (CP)$$

$$\omega_s : \quad \sqrt{\epsilon} : \quad q : \quad q \epsilon : \quad \sqrt{\epsilon} : \quad \sqrt{\epsilon} \quad (TP)$$

This means the trapped region is a boundary layer region in phase space of width  $\sqrt{\epsilon} c_s$ . In section 3.3 we shall consider the limit of large  $q$  and  $\omega \sim c_s / R$  so that the boundary layer can be avoided. In this super bounce limit the particles are no longer trapped and this simplifies the analysis considerably.

### 3.3 Supersonic limit

In the large  $q$  limit, we can neglect  $\nabla_{\parallel}$  terms and hence the DKE simplifies to

$$\partial_t f + \mathbf{u}_E \cdot \nabla f + (v_{\parallel} \mathbf{u}_E \cdot \kappa) \partial_{v_{\parallel}} f = 0 \quad (3.16)$$

Taking the density,  $p_{\parallel}$  and  $p_{\perp}$  moments of the above DKE with the volume integral given by  $d^3v = 2\pi B d\mu dv_{\parallel}$  we obtain

$$(\partial_t + \mathbf{u}_E \cdot \nabla)n - 2n(\mathbf{u}_E \cdot \nabla B/B) = 0 \quad (3.17)$$

$$(\partial_t + \mathbf{u}_E \cdot \nabla)p_{\parallel} - 4p_{\parallel}(\mathbf{u}_E \cdot \nabla B/B) = 0 \quad (3.18)$$

$$(\partial_t + \mathbf{u}_E \cdot \nabla)p_{\perp} - 3p_{\perp}(\mathbf{u}_E \cdot \nabla B/B) = 0 \quad (3.19)$$

These equations can be recast as the well known CGL equations as can be verified easily. Kulsrud's equations reduce to the CGL equations in the supersonic limit.

$$d_t \left( \frac{n}{B^2} \right) = 0, \quad d_t \left( \frac{p_{\parallel} B^2}{n^3} \right) = 0, \quad d_t \left( \frac{p_{\perp}}{n B} \right) = 0, \quad d_t = \partial_t + \mathbf{u}_E \cdot \nabla \quad (3.20)$$

We now proceed order by order and keep the calculation as close as possible to the collisional limit discussed in Chapter 2. However, we observe that it is more efficient to work directly with the distribution function,  $f$ , rather than its moments. This allows the same cancellations but at a more primitive level. We shall also take  $q \sim O(1)$  and take the large  $q$  limit only at the end. We shall highlight the main differences between the fluid and kinetics as we proceed.

The first two orders in the  $\epsilon$  expansion is completely identical to the fluid case. Note that the velocity space volume element  $d^3v$  has a factor of  $B$  in it and hence needs to be evaluated order by order too. To second order we have,

$$(\partial_t + \mathbf{u}_E^{(2)} \cdot \nabla)f_0 + v_{\parallel}d_1f_0 = 0$$

Since we ordered  $U_{\parallel} \sim \epsilon c_s$ ,  $f_0$  should not contribute to any parallel flows. This can be accomplished by making  $f_0$  a flute i.e  $d_1f_0 = 0$ . The lowest order DKE is then

given by,

$$(\partial_t + \mathbf{u}_E^{(2)} \cdot \nabla) f_0 = 0, \quad d_t n_0 = 0 \quad (3.21)$$

where  $d_t = \partial_t + \mathbf{u}_E^{(2)} \cdot \nabla$  and  $n_0 = \int B_0 d\mu dv_{\parallel} f_0$ .  $f_0$  stays a flute (i.e.  $(\mathbf{B} \cdot \nabla)_1 f_0 = 0$ ) and an even function of  $v_{\parallel}$  due to Eq. (3.21). We shall further choose  $f_0$  to be an isotropic function in velocity space so that  $p_{\parallel 0} = p_{\perp 0} = \bar{\beta} n_0$ . The Grad-Shafranov equation to  $2^{nd}$  order is therefore exactly the same as Eq. (2.41)

To  $3^{rd}$  order, the vorticity equation (3.15) reduces to (2.49)

$$(\mathbf{B} \cdot \nabla)_1 (j_{\parallel}/B)_2 = \partial_z (p_{\parallel 0} + p_{\perp 0} + 2n_0 T_e) = 2\bar{\beta}(1 + T_e/T_i) \partial_z n_0 \quad (3.22)$$

Thus, the choice of a Maxwellian, i.e

$$f_{0i} \propto n_0(\mathbf{x}, t) \exp\left(\frac{v_{\parallel}^2/2 + \mu B}{T_i/M_i}\right),$$

ensures that up to  $3^{rd}$  order, we have exactly the same equations (including the dynamic Shafranov Shifts) as the fluid system described in Chapter 2. This choice is not essential but is being made only to simplify the following analysis.

Taking Eq. (3.16) to  $3^{rd}$  order and using  $\kappa_1 \approx -\nabla_{\perp} B$  we get

$$\begin{aligned} (\partial_t + \mathbf{u}_E^{(2)} \cdot \nabla) f_1 + v_{\parallel} (d_1 f_1 + d_2 f_0) + (x \hat{\zeta} \times \nabla \phi_2 + \hat{\zeta} \times \nabla \phi_3) \cdot \nabla f_0 \\ + \left( v_{\parallel} \mathbf{u}_E^{(2)} \cdot \nabla B - \mu d_1 B \right) \partial_{v_{\parallel}} f_0 = 0 \end{aligned} \quad (3.23)$$

Density can be calculated using  $n_1 = \int dv_{\parallel} d\mu (B_0 f_1 + B_1 f_0)$  and can be shown to satisfy the corresponding collisional fluid Eq.(2.60). Similarly, the parallel flow can be obtained by taking the  $\int B_0 d\mu dv_{\parallel} v_{\parallel} f_1$  moment, since the contribution from  $f_0$  is zero. Once again the fluid result (2.61) is obtained.

We now proceed to  $O(\epsilon^4)$ . In ideal MHD  $E_{\parallel} = 0$  but in KMHD its given in terms of parallel pressure gradients. However in the large  $q$  limit it is negligible and hence we can recover the fluid result (2.56, 2.57). The vorticity equation is identical except for the first order pressure terms. Thus,

$$\begin{aligned} \nabla_{\perp} \cdot (d_t n_0 \nabla_{\perp} \varphi_2) &= \frac{2\bar{\beta}}{q_0} \partial_{\zeta} n_0 + \hat{\zeta} \times \nabla \underline{\psi}_1 \cdot \nabla \nabla_{\perp}^2 \underline{\psi}_1 \\ &\quad - \langle \partial_z (p_{\parallel 1} + p_{\perp 1} + 2n_1 T_e) \rangle + \langle d_2(j_{\parallel}/B)_2 \rangle. \end{aligned} \quad (3.24)$$

To efficiently effect the cancellations encountered in the fluid case, we define  $F_1$  in analogy with its fluid counterpart  $N_1$  such that

$$d_1 F_1 = d_1 f_1 + d_2 f_0, \quad F_1 = f_1 - q_0^2 d_1 d_2 f_0 \quad (3.25)$$

In exact analogy with the fluid case we find

$$d_t F_1 - d_t f_1 = -q_0^2 [d_1, [d_t, d_2]] f_0 = (x \hat{\zeta} \times \nabla \phi_2 + \hat{\zeta} \times \nabla \phi_3) \cdot \nabla f_0,$$

which allows us to write

$$d_t F_1 + v_{\parallel} d_1 F_1 + (v_{\parallel} \mathbf{u}_{\mathbf{E}}^{(2)} \cdot \nabla B_1 - \mu d_1 B_1) \partial_{v_{\parallel}} f_0. \quad (3.26)$$

The same cancellations can be shown to occur, and the vorticity equation in new variables is given by

$$\begin{aligned} \nabla_{\perp} \cdot (d_t n_0 \nabla_{\perp} \varphi_2) &= -2\bar{\beta} \left( \frac{1}{q_0^2} - 1 \right) \partial_{\alpha} n_0 + \frac{1}{r} \{ \underline{\psi}_1, \underline{\Delta} \underline{\psi}_1 \}_{(r, \alpha)} \\ &\quad - 2 \langle \partial_z P \rangle. \end{aligned} \quad (3.27)$$

where  $P_1 = (P_{\parallel 1} + P_{\perp 1})/2 + N_1 T_e$ . Let us now calculate the density, parallel and perpendicular pressures from  $F_1$  taking into account various powers of B in the integrals,

$$(N_1, P_{\parallel 1}) = \int d\mu dv_{\parallel} (1, v_{\parallel}^2) (F_1 + B_1 f_0), \quad P_{\perp 1} = \int d\mu dv_{\parallel} \mu B_0 (F_1 + 2B_1 f_0). \quad (3.28)$$

To obtain the equations for the parallel and perpendicular pressures we shall now use the large q limit so that the terms  $v_{\parallel} d_1 F_1, \mu d_1 B_1$  in Eq. (3.26) can be neglected.

Using  $\mathbf{u}_E^{(2)} \cdot \nabla B_1 = \partial_z \varphi_2$  we can simplify Eq.(3.26) to

$$d_t F_1 + \partial_z \phi_2 v_{\parallel} \partial_{v_{\parallel}} f_0 = 0. \quad (3.29)$$

Taking the density, parallel and perpendicular pressure moments, we obtain

$$\begin{aligned} d_t N_1 &= 2n \partial_z \varphi_2, & d_t P_{\parallel 1} &= 4\bar{\beta} n \partial_z \varphi_2, & d_t P_{\perp 1} &= 3\bar{\beta} n \partial_z \varphi_2 \\ \Rightarrow d_t P_1 &= d_t (P_{\parallel 1} + P_{\perp 1})/2 + T_e d_t N_1 = (7/2 + 2T_e/T_i) \bar{\beta} n_0 \partial_z \varphi_2 \end{aligned} \quad (3.30)$$

Thus we have a complete set of equation for the variables  $\{n_0, \varphi_2, \underline{\psi}_1, P_1\}$  which we summarize in the following.



### 3.4 Summary and discussion

We shall drop subscripts and summarize the equations for the complete set  $\{n, \varphi, \underline{\psi}, P\}$

$$d_t n = 0 \tag{3.31}$$

$$\nabla_{\perp} \cdot (d_t n_0 \nabla_{\perp} \varphi) = -2\bar{\beta} \partial_{\alpha} n + \frac{1}{r} \{\underline{\psi}, \underline{\Delta} \underline{\psi}\}_{(r,\alpha)} - 2\langle \partial_z P \rangle. \tag{3.32}$$

$$d_t \underline{\psi} = 0 \tag{3.33}$$

$$d_t P = 2(7/4 + T_e/T_i) \bar{\beta} n \partial_z \varphi. \tag{3.34}$$

The main point of this chapter is to show that the methodology that we developed in Part I applicable to collisional plasmas can also be suitably extended to collisionless plasmas described by kinetic equations. In the supersonic limit, we avoid the complications arising in the kinetic calculations due to trapped particles. In this limit, we can define  $F$  in analogy to  $N$  defined in Part I and show that the same nonlinear cancellations occur even in a sub-Alfvénic kinetic system. From  $F$  we can obtain  $P_{||1}, P_{\perp 1}$  which satisfy CGL equations. To keep the system close to the fluid system of Part I we have assumed that the lowest order pressure is isotropic. Keeping anisotropies to this level would have allowed us to retain firehose and mirror instabilities. The axisymmetric limit ( $\partial_{\alpha} = 0$ ) of the reduced system reproduces the CGL-GAM calculation of Hassam-Kleva [21].

# Part III

Kinetic MHD: Sub-sonic and Kinetic MHD

## Chapter 4: Sub-Alfvénic Axisymmetric Kinetic MHD

### 4.1 Overview

An initial radial electric field,  $E_r(0)$ , in an axisymmetric tokamak, results in geodesic acoustic mode [22] (GAM) oscillations. The GAMs Landau damp, resulting in a much smaller final residual electric field,  $E_r(\infty)$ , and accompanying parallel zonal flows [6]. The phenomenon exhibits a large effective mass (inertia due to flows), with an enhancement of order the well-known Rosenbluth-Hinton (RH) factor  $\approx 1+1.6q^2/\sqrt{\epsilon}$ . In apparent paradox, the final angular momentum in the RH parallel zonal flow is much smaller than the angular momentum expected from the well-known rapid precession of the trapped particle population in the final electric field. In addition, an effective mass calculated naively based on the rapid trapped particle (TP) precession is much larger than the RH factor. A drift kinetic calculation is presented showing a shift, proportional to  $E_r$ , of the usual energy coordinates in phase space. Importantly, this shift contributes to the effective mass even if the system is linearized in  $E_r$ , and can be interpreted as a first order linear shift in the Jacobian. Further, the Jacobian shift recovers the large TP precession flow and also uncovers the presence of reverse circulating particle flows that, to lowest order, are equal and opposite to the TP precession. A detailed calculation is presented.

## 4.2 Introduction

An initial radial electric field,  $E_r(0)$ , in an axisymmetric tokamak results in GAM oscillations. In a collisionless system, the GAMs Landau damp. However, it was shown by Rosenbluth and Hinton (RH) [6] that, in the asymptotic steady state, there persists a residual electric field,  $E_r(\infty)$ , and an associated parallel zonal flow. RH showed that the initial and final electric fields are related according to  $E_r(0) = (1 + \mathcal{D})E_r(\infty)$ , where  $\mathcal{D} \sim 1.6q^2/\sqrt{\epsilon}$ . Here,  $q$  is the tokamak safety factor and  $\epsilon \ll 1$  is the tokamak inverse aspect ratio. Since the initial  $\mathbf{E} \times \mathbf{B}$  flow,  $u_E(0)$ , has a toroidal component and, thus, an initial toroidal angular momentum, and the final  $\mathbf{E} \times \mathbf{B}$  flow is much smaller than the initial, a substantial parallel zonal flow must arise in order to preserve angular momentum (see Figure 4.1). The size of the parallel zonal flow, as found by RH, can be deduced from the geometry of Figure 4.1 to be of order  $(\epsilon/q)u_E(0)$ . Finally, as we will elaborate later, the term  $1 + \mathcal{D}$  is like an effective mass, arising from the inertia due to the parallel flows.

A question arises when one considers the individual contributions to the angular momentum of the trapped and circulating fractions of the plasma. It is well known that in the presence of a radial electric field, trapped particles precess toroidally. The speed of precession is of order  $(q/\epsilon)u_E$  and represents a rapid rate inasmuch as it is much larger than  $u_E$ . The reason behind the toroidal precession can be seen easily by going to a frame moving with speed  $\mathbf{U}$ , where the TPs are just bouncing back and forth in a magnetic well without feeling any net electric field. Such a frame exist only if  $\mathbf{E} + \mathbf{U} \times \mathbf{B} = 0$ . In an axisymmetric system, it can be

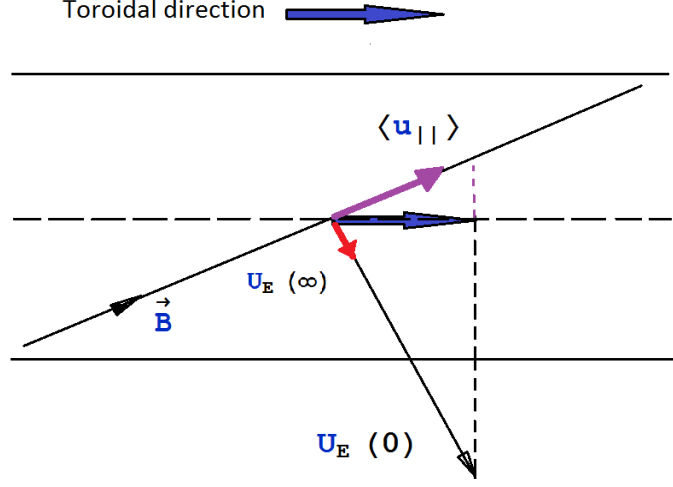


Figure 4.1: Comparison of initial and final RH flows

shown [23] that  $\mathbf{U} \approx \hat{\zeta} q u_E / \epsilon$ . In apparent paradox, one finds that the angular momentum in the TP population precessing in the final RH electric field is much larger than the total final RH angular momentum (the TP precession angular momentum is of order  $\sqrt{\epsilon}(q/\epsilon)u_E(\infty)$ , while the RH calculated final angular momentum is of order  $(\epsilon/q)u_E(0)$ , as discussed above. Here we have accounted for the lower density of the trapped fraction, i.e.  $n^{TP} \sim O(\sqrt{\epsilon})$ .) In addition, it is reasonable to expect (as we describe below) that such a large precession kinetic energy could result in a fractional effective mass factor of order  $\sim \left( \frac{1}{2}(nU_{\parallel}^2)^{TP} / \frac{1}{2}nu_E^2 \right) \sim O(n^{TP}q^2/\epsilon^2)$ . This factor is, in fact, larger than the RH mass factor, by  $1/\epsilon$ .

A simple toy model can be constructed to illustrate these points. We consider a massless rod and two beads of masses  $m_T, m_C$  that can slide freely, without interaction, along the rod; one of them ( $m_T$ ) is further constrained in that it can only move horizontally, that is to say it stays trapped inside a linear horizontal 1D

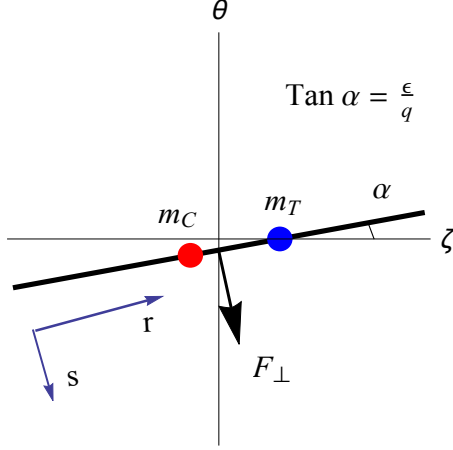


Figure 4.2: A toy model

channel. This system is depicted in Fig 4.2. The rod represents a magnetic field line;  $m_C$  represents circulating particles (CPs), while  $m_T$  represents deeply trapped particles. The rod is inclined at a small angle given by  $\sin \alpha = \epsilon/q \ll 1$ . Consider now an external perpendicular force,  $F_{\perp}$ , acting on the rod, as shown in the figure. We want to obtain the effective mass of the system defined according to the constrained Newton's equation  $M\ddot{s} = F_{\perp}$ , where  $s$  is the distance measured along  $F_{\perp}$  and  $\dot{s}$  is the speed of the rod in the lab frame. The Lagrangian for this system is

$$L(s, \dot{s}, \dot{r}) = \frac{1}{2 \sin^2 \alpha} (m_T + m_C) \dot{s}^2 + \frac{1}{2} m_C (\dot{r}^2 + 2\dot{s} \dot{r} \cot \alpha) + F_{\perp} s$$

leading to the equation of motion,

$$\ddot{s} = \frac{F_{\perp}}{m_C + m_T / \sin^2 \alpha} \Rightarrow M = m_C + m_T / \sin^2 \alpha = m_C + m_T \frac{q^2}{\epsilon^2}.$$

This shows that the effective mass from the constrained mass  $m_T$  is  $m_T(q^2/\epsilon^2)$ , illustrating our conjecture for TPs above.

This line of investigation raises further questions when one calculates sepa-

rately the CP and TP flows associated with the residual RH zonal flows: as we will show, by direct calculation [24] based on standard drift-kinetic theory, we find the RH parallel flow for the TP's to be of  $O(qu_E)$ , smaller than the precession drift by  $1/\epsilon$ . In addition, a direct calculation of the net flux surface averaged poloidal flow of the TP's surprisingly gives a nonzero result, namely, a net poloidal flow of  $O(qu_E)$ .

We note that the RH problem, as posed by Rosenbluth and Hinton, starts with an initial electric field that sets up GAMs, eventually settling to a steady residual flow. Our toy problem, as posed, does not incorporate GAMs, and is based on an external driver force  $F_\perp$ . Nonetheless, as we will show later, the externally driven problem is a relevant comparison. In particular, one may revisit the RH problem as the tokamak plasma response to a weak external perpendicular force; in that case, we will show that the same RH factor, or effective mass, is obtained. Such a force could arise from perpendicular neutral beams, for example: the force would provide toroidal torque that would slowly increase the angular momentum. There are accompanying GAMs, but of negligible amplitude. The final electric field is once again reduced by the same factor  $M = 1 + \mathcal{D}$ .

Our study in this chapter is motivated by an attempt to understand the discrepancy in the flows as well as in the naively expected effective mass of the RH problem. The discussion below is organized as follows: In section 4.3, we present the basic system of equations, consisting of the drift kinetic equation and the angular momentum conservation equation in axisymmetric toroidal geometry. We then solve the classic Rosenbluth-Hinton problem in section 4.4 and point out the aforementioned discrepancies in the flows. We introduce the shifted coordinates in section

4.5 and redo the RH problem in these new coordinates in section 4.6, to reconcile trapped particle toroidal precession in RH flows. In section 4.7, we illustrate the role of barely circulating particles in cancelling the large trapped particle precession and thereby explain the smaller overall RH effective mass. We summarize our results in section 4.9 and discuss future lines of research.

### 4.3 Kinetic Equations

We begin our calculation with the drift kinetic equation (DKE) as formulated by Kulsrud, Frieman, and Hinton-Wong [8, 25, 26]. The DKE is derived in “MHD ordering” and thus allows large, sonic level  $\mathbf{E} \times \mathbf{B}$  flows. A consistent ordering also requires that the parallel electric field  $E_{\parallel}$  be very small compared to  $E_{\perp}$ . In the electrostatic limit ( $\partial_t \ll V_A/L_{\parallel}$ ) the full DKE is given by

$$\frac{\partial f}{\partial t} + (\mathbf{u}_{\mathbf{E}} + v_{\parallel} \hat{b}) \cdot \nabla f + \left( -\hat{b} \cdot \left( (\mathbf{u}_{\mathbf{E}} + v_{\parallel} \hat{b}) \cdot \nabla \right) \mathbf{u}_{\mathbf{E}} + \mu B \nabla \cdot \hat{b} + \frac{e}{m} E_{\parallel} \right) \frac{\partial f}{\partial v_{\parallel}} = 0 \quad (4.1)$$

where,

$$\mathbf{u}_{\mathbf{E}} = \frac{\mathbf{B} \times \nabla \psi}{B^2} \varphi'(\psi) \quad (4.2)$$

is the  $\mathbf{E} \times \mathbf{B}$  flow and  $f = f(v_{\parallel}, \mu, \mathbf{x}, t)$ . The magnetic field  $\mathbf{B}$  is defined as usual by  $\mathbf{B} = I \hat{\zeta} + \hat{\zeta} \times \nabla \psi$ . Here, the  $E_{\parallel}$  force term is of the same order as the other parallel force terms (the mirror force and inertial forces) in the equation. The above DKE applies for both ions and electrons, though we will assume small electron mass and thus the electron response will be taken to be adiabatic. The full system in the electrostatic approximation consists of four variables, namely, the two distribution



functions, the potential  $\varphi$ , and  $E_{\parallel}$ . These four unknowns are governed by the two DKEs, the quasineutrality condition  $n_e = n_i$ , and the equation of conservation of angular momentum, namely [21]

$$M\partial_t \left\langle n\varphi' \frac{|\nabla\psi|^2}{B^2} - \int d^3v \frac{Iv_{\parallel}}{B} f \right\rangle = \tau_{\perp} \quad (4.3)$$

where  $\langle \cdot \rangle$  represents a flux surface average, and  $\tau_{\perp} = \left\langle n \frac{|\nabla\psi|}{B} F_{\perp} \right\rangle$  is a toroidal torque due to a perpendicular force  $F_{\perp}$ . The latter represents an external force, such as from a neutral beam, that could accelerate the  $\mathbf{E} \times \mathbf{B}$  flow. It can be shown that in axisymmetric geometry, the equation governing the angular momentum is identical to the radial current quasineutrality condition. This equivalence is shown in Appendix G. For the present purposes, we will find the former equation to be more convenient.

In this chapter, we will only be concerned with time scales which are subsonic, i.e.,  $d/dt \ll c_s/qR$ . In this limit, as we will show more precisely later,  $E_{\parallel}$  is small and can be neglected. In that case, the system can be closed by simply using the DKE for ions, Eq. (4.1), and the angular momentum conservation equation (4.3). As a further simplification, we will order  $q \gg 1$  but  $u_E \sim v_{th}/q$ . In this ordering, the nonlinear in  $u_E$  terms in the DKE can be neglected compared with cross terms in  $v_{\parallel}$  and  $u_E$ , since  $|v_{\parallel} \mathbf{b}\mathbf{b} : \nabla \mathbf{u}_E| : |\mathbf{b}\mathbf{u}_E : \nabla \mathbf{u}_E| \sim 1 : \frac{1}{q}$ . Given these orderings, Eq.(4.1) can be recast as

$$\frac{\partial f}{\partial t} + (\mathbf{u}_E + v_{\parallel} \hat{\mathbf{b}}) \cdot \nabla f + (v_{\parallel} \mathbf{u}_E \cdot \boldsymbol{\kappa} - \mu \nabla_{\parallel} B) \frac{\partial f}{\partial v_{\parallel}} = 0. \quad (4.4)$$

We now use the form for  $\mathbf{u}_E$ , Eq. (4.2), to simplify (4.1). In particular,  $\mathbf{u}_E \cdot \boldsymbol{\kappa} = \mathbf{u}_E \cdot \nabla B/B$ , in the low  $\beta$  limit. We also assume axisymmetry and thus  $\mathbf{B} \times \nabla \psi \cdot \nabla =$

$IB\nabla_{\parallel}$ . Given these, (2) can be recast to the form

$$\frac{\partial f}{\partial t} + \left(v_{\parallel} + \frac{I\varphi'}{B}\right) \nabla_{\parallel} f + \left(v_{\parallel} \frac{I\varphi'}{B} - \mu B\right) \frac{\nabla_{\parallel} B}{B} \frac{\partial f}{\partial v_{\parallel}} = 0. \quad (4.5)$$

where  $f = f(v_{\parallel}, \mu, \mathbf{x}, t)$ . We will now use (4.5) and (4.3) as the closed set of equations for the two variables  $f$  and  $\varphi$ .

#### 4.4 The classic Rosenbluth Hinton problem

We begin by reviewing the RH problem. We are interested mainly in the effective mass physics as derived by RH. This physics can be recovered by setting the field lines into motion by applying a weak perpendicular external force  $F_{\perp}$ . Since the force is weak, we look for a sub-bounce frequency solution according to the ordering  $\partial/\partial t \sim \mathbf{u}_{\mathbf{E}} \cdot \nabla \sim F_{\perp} \ll v_{\parallel} \nabla_{\parallel}$ . To lowest order from (4.5), we have

$$v_{\parallel} \nabla_{\parallel} f_0 - \mu \frac{\nabla_{\parallel} B}{B} \frac{\partial f_0}{\partial v_{\parallel}} = 0 \quad (4.6)$$

which yields  $f_0 = f_0(\mathcal{E}, \mu, \psi, t)$ , where  $\mathcal{E} = v_{\parallel}^2 + \mu B$  is the energy. The lowest order angular momentum equation from (4.3) is simply the 2nd term on the LHS set to zero. This is identically satisfied if we assume that  $f_0(\mathcal{E}, t)$  is symmetric in  $v_{\parallel}$  with respect to the circulating particles. To first order, Eq (4.5) becomes

$$\frac{\partial f_0}{\partial t} + v_{\parallel} \nabla'_{\parallel} f_1 = v_{\parallel} \nabla'_{\parallel} \left( \frac{I\varphi'}{B} v_{\parallel} \right) \frac{\partial f_0}{\partial \mathcal{E}} \quad (4.7)$$

where we have transformed from  $v_{\parallel}$  to  $\mathcal{E}$  coordinates with  $\nabla'_{\parallel}$  being the gradient operator at constant  $\mathcal{E}$ , and we have used  $v_{\parallel} \nabla'_{\parallel}(v_{\parallel}) = -\mu \nabla_{\parallel} B$ . Annihilating the  $f_1$  term by bounce averaging as in  $\bar{f} = \oint (df/v_{\parallel}) / \oint (dl/v_{\parallel})$ , we get  $f_0 = f_0(\mathcal{E})$  and

$$f_1 = I\varphi' \left( \frac{v_{\parallel}}{B} - g \right) f_0' \quad (4.8)$$

where  $g(\mathcal{E})$  is yet to be determined. To second order we have,

$$\frac{\partial f_1}{\partial t} + v_{\parallel} \nabla_{\parallel} f_2 = 0. \quad (4.9)$$

Annihilation of Eq.(4.9) yields  $\overline{\partial_t f_1} = 0$ , which gives  $g = \overline{(v_{\parallel}/B)}$ . Thus, we get the RH solution for  $f_1$  correct to first order [24], viz.

$$f_1 = \frac{I\varphi'}{B} \left( \frac{v_{\parallel}}{B} - \overline{\left( \frac{v_{\parallel}}{B} \right)} \right) f_0'. \quad (4.10)$$

We would now insert  $f_1$  into the second term of the angular momentum equation, Eq. (4.3). We would thus need to calculate the parallel flow to first order, viz.,

$$n_0 u_{\parallel 1} = \int d^3v v_{\parallel} f_0 = I\varphi' \int d^3v v_{\parallel} \left( \frac{v_{\parallel}}{B} - \overline{\left( \frac{v_{\parallel}}{B} \right)} \right) \frac{\partial f_0}{\partial \mathcal{E}} \quad (4.11)$$

Using an expansion in  $\epsilon$ , we find

$$u_{\parallel 1} = -[2\epsilon \cos \theta + 1.6\epsilon^{3/2} + O(\epsilon^2)] \frac{I\varphi'}{B}, \quad (4.12)$$

proportional to  $\varphi'$ . Inserting this into Eq. (4.3), we get the angular momentum equation in the form

$$\left( 1 + 2q^2 + 1.6 \frac{q^2}{\sqrt{\epsilon}} + O(q^2) \right) \partial_t u_E = F_{\perp}/M$$

from which the Rosenbluth-Hinton effective mass is seen to be the factor multiplying  $\partial_t u_E$ . The  $(1 + 2q^2)$  factor is the well known Pfirsch-Schluter factor [27] arising from the circulating particles response. We can see that the  $1.6q^2/\sqrt{\epsilon}$  is the dominant term.

#### 4.4.1 Rosenbluth-Hinton $\parallel$ flows

We note from the above that the effective mass is smaller than what we expect from the toy model, given the rapid TP toroidal precession. We also note that the parallel flow, (4.12), is much less than the toroidal precession speed expected of the TPs. In particular, given the large precession, we expect a much larger angular momentum contribution from the TPs (even given the lower density fraction of this species). To examine this further, we calculate separately for trapped and circulating species the parallel flows resulting from the RH solution. Using Eq. (4.11) and integrating only over  $\mathcal{E} > \mu B_{max}$ , we get for circulating particles (CP)

$$(nu_{\parallel})^{CP} = n_0[-2\epsilon \cos \theta + (-1.6 + (1 + \cos \theta)^{3/2})\epsilon^{3/2} + O(\epsilon^2)] \frac{I\varphi'}{B} \quad (4.13)$$

where we have used an expansion in  $\epsilon$ . This flow speed is as expected. Correspondingly, for the trapped particles (TP), we integrate inside the separatrix over  $\mu B_{min} < \mathcal{E} < \mu B_{max}$  to get for the parallel flow,

$$(nu_{\parallel})^{TP} = n_0 [-(1 + \cos \theta)^{3/2}\epsilon^{3/2} + O(\epsilon^{5/2})] \frac{I\varphi'}{B}. \quad (4.14)$$

The total parallel flow is obtained by summing these [24], giving

$$u_{\parallel} = -[2\epsilon \cos \theta + 1.6\epsilon^{3/2} + O(\epsilon^2)] \frac{I\varphi'}{B}, \quad (4.15)$$

in agreement with Eq. (4.12). We would expect to see a large toroidal precession from the TPs. Instead, we find the flow of the TP to be smaller than the toroidal precession drift of the TPs by a factor of  $\epsilon$ . Further, if we calculate the poloidal

velocity of the trapped particle fraction, we find

$$\mathbf{U}^{TP} \cdot \hat{\theta} = (u_{\parallel}^{TP} + \mathbf{U}_E) \cdot \hat{\theta} = \frac{B_p}{B} \left( u_{\parallel}^{TP} + \frac{I\varphi'}{B} \right) \approx \frac{B_p}{B} \frac{I\varphi'}{B_0} \approx u_E \quad (4.16)$$

the trapped particles seem to have a nonzero bounce averaged poloidal flow. This is puzzling, since for adiabatic changes we expect TPs to have a purely toroidal flow.

Incidentally, we can use  $f_0$  and  $f_1$  above to calculate the density. To lowest order, for  $f_0 = f_0(\mathcal{E})$ , the density is constant along the magnetic surface. To first order,  $f_1$  is antisymmetric in  $v_{\parallel}$ , yielding no change in the density. Likewise, changes in parallel and perpendicular pressures are also zero. The elements of the electron pressure tensor can be used to a posteriori calculate  $E_{\parallel}$ , as defined in Eq. (49) of the Kulsrud [8] manuscript. [For massless electrons,  $E_{\parallel}$  is given essentially by the generalized adiabatic electron response, viz.,  $neE_{\parallel} = -\mathbf{b}\nabla : \mathbf{P}_e$ .] We find that  $E_{\parallel} = 0$  to lowest order and also zero to first order given the  $f_1$  symmetry. This self-consistently justifies the neglect of  $E_{\parallel}$  in our calculation above.

In order to understand the discrepancy between the RH solution and the expected TP contribution to the flows and effective mass, we will now take a different approach to solve the low frequency RH problem.

## 4.5 Shifted coordinates

As shown earlier, assuming axisymmetry we can rewrite the DKE as

$$\frac{\partial f}{\partial t} + \left( v_{\parallel} + \frac{I\varphi'}{B} \right) \nabla_{\parallel} f + \left( v_{\parallel} \frac{I\varphi'}{B} - \mu B \right) \frac{\nabla_{\parallel} B}{B} \frac{\partial f}{\partial v_{\parallel}} = 0 \quad (4.17)$$

where  $f = f(v_{\parallel}, \mu, \mathbf{x}, t)$ . We reiterate that this equation is valid for large  $q$  and with  $u_E$  ordered to be commensurate with  $v_{th}/q$ . It can be deduced from this equation,

using the method of characteristics, that

$$\mathcal{E}_* = \frac{1}{2}v_{\parallel}^2 + \mu B + I\varphi' \frac{v_{\parallel}}{B}$$

is a constant of motion. In an axisymmetric system, conservation of the canonical angular momentum  $\psi_* = \psi - Iv_{\parallel}/(eB/m)$  implies that  $\mathcal{E}_* = \mathcal{E} + (e/m)(\phi(\psi) - \phi(\psi_*))$  is also conserved. It is to be noted that in Kinetic MHD ordering,  $\psi_* \approx \psi$ ,  $(e/T)\phi \gg 1$  and hence the  $\mathcal{E}_*$  can be interpreted as a shifted energy. (See references [23, 28–30] for further elaboration on this constant.) We shift to  $(\mathcal{E}_*, v_{\parallel*})$  coordinates, defined as follows:

$$\begin{aligned} \mathcal{E}_* = \frac{1}{2}v_{\parallel}^2 + \mu B + I\varphi' \frac{v_{\parallel}}{B} &= \mathcal{E} + \frac{I\varphi'v_{\parallel}}{B} \\ v_{\parallel*} = v_{\parallel} + \frac{I\varphi'}{B} \quad \mu \rightarrow \mu, \quad \mathbf{x} \rightarrow \mathbf{x} & \quad (4.18) \\ d^3v = \sum_{\sigma} \frac{B d\mu d\mathcal{E}_*}{|v_{\parallel*}|} . & \end{aligned}$$

Here,  $\sigma = \frac{v_{\parallel*}}{|v_{\parallel*}|}$  denotes the three regions in energy space, namely, the trapped population and the rightward and leftward moving circulating particle populations. The coordinate  $v_{\parallel*}$  is defined with respect to coordinates shifted downward in  $v_{\parallel}$ .  $\mathcal{E}_*$  is then a downshifted energy-like coordinate, centered about  $v_{\parallel*} = 0$ . This shift is depicted in Fig.[4.3b]. In  $\mathcal{E}_*$  coordinates, centered with respect to  $v_{\parallel*}$ , the DKE, Eq.(4.4), becomes

$$\frac{\partial f}{\partial t} + v_{\parallel*} \nabla_{\parallel} f + \frac{\partial I\varphi' v_{\parallel}}{\partial t} \frac{\partial f}{\partial \mathcal{E}_*} = 0 \quad (4.19)$$

where  $f = f(\mathcal{E}_*, \mu, \psi, \theta, t)$  and  $\partial/\partial t$  is at constant  $\mathcal{E}_*$ . The angular momentum equation, also recast in  $\mathcal{E}_*$  coordinates, is now given by

$$\partial_t \left\langle n_0 \varphi' \frac{|\nabla \psi|^2}{B^2} \right\rangle = \partial_t \left\langle \int \sum_{\sigma} \frac{B d\mu d\mathcal{E}_*}{|v_{\parallel*}|} \frac{Iv_{\parallel}}{B} f \right\rangle + \tau_{\perp}/M . \quad (4.20)$$

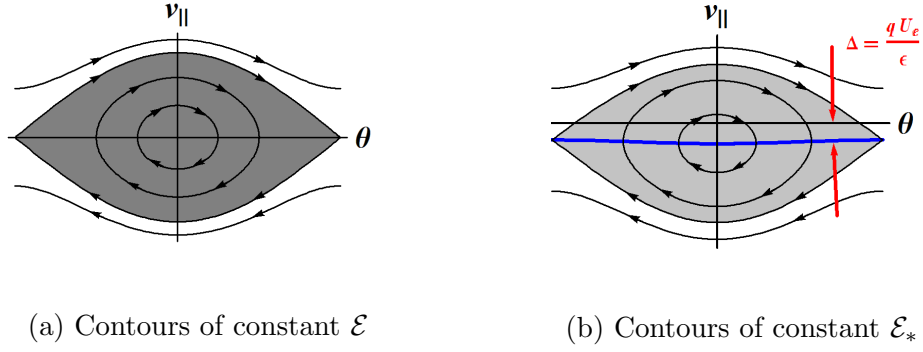


Figure 4.3: Comparison of the coordinate systems. [4.3a] standard energy coordinates  $(\text{sign}(v_{\parallel}), \mathcal{E}, \theta)$ . [4.3b] the shifted coordinates  $(\text{sign}(v_{\parallel*}), \mathcal{E}_*, \theta)$ . The shift is  $I\varphi'/B$

In what follows, we shall use equations (4.18),(4.19),(4.20).

## 4.6 The RH problem revisited

### 4.6.1 Sub-bounce limit

To make contact with the RH problem, we begin by performing a  $\partial_t \ll \omega_b$  expansion, but allowing a large  $u_E \sim v_{th}/q$ , which corresponds to a finite downward shift as shown in Fig(4.3b). This approach allows for a more transparent calculation.

To dominant order, we have from (4.19)

$$v_{\parallel*} \nabla_{\parallel} \Big|_{\mathcal{E}_*} f \approx 0 \quad \Rightarrow \quad f = f(\mathcal{E}_*, t). \quad (4.21)$$

Annihilating the  $\nabla_{\parallel \mathcal{E}_*}$  operator by bounce averaging gives a constraint equation for  $f(\mathcal{E}_*, t)$ , viz.

$$\frac{\partial f}{\partial t} + \frac{\partial I\varphi'}{\partial t} \overline{\left(\frac{v_{\parallel}}{B}\right)} \frac{\partial f}{\partial \mathcal{E}_*} = 0. \quad (4.22)$$

The constraint on  $f$  introduces a  $\sigma$  dependence. Eq. (4.22) and the angular momentum relation (4.20), with  $f = f(\mathcal{E}_*, t)$ , form a closed set for the nonlinear  $\{f, \varphi'\}$  system. We now do a subsidiary expansion in small  $\frac{I\varphi'}{B} \ll v_{th}$ , denoting  $f = f_0 + f_1 + \dots$  (here, the subscript indices are not the same expansion parameter as in earlier sections). From Eq.(4.22), the corresponding lowest and first order equations are

$$\left. \frac{\partial f_0}{\partial t} \right|_{\mathcal{E}_*} = 0 \quad \Rightarrow \quad f_0 = f_0(\mathcal{E}_*) \quad (4.23a)$$

$$\frac{\partial f_1}{\partial t} + \frac{\partial I\varphi'}{\partial t} \overline{\left(\frac{v_{||}}{B}\right)} \frac{\partial f_0}{\partial \mathcal{E}_*} = 0 \quad \Rightarrow \quad f_1 = -I\varphi' \overline{\left(\frac{v_{||*}}{B}\right)} \frac{\partial f_0}{\partial \mathcal{E}_*} \quad (4.23b)$$

where the overbar corresponds to the bounce average holding  $\mathcal{E}_*, \mu$  constant, and we note that  $\overline{(v_{||*}/B)} = 0$  for TPs.

## 4.6.2 RH flows

We can now calculate the RH flows from Eqs (4.23). For general  $(I\varphi'/B)/v_{th}$ , the dominant order parallel flow for either the TP or the CP populations (or both) is

$$(nU)_{||} = \int \sum_{\sigma} \frac{B d\mu d\mathcal{E}_*}{|v_{||*}|} v_{||} f = \int \sum_{\sigma} \frac{B d\mu d\mathcal{E}_*}{|v_{||*}|} \left( \sigma |v_{||*}| - \frac{I\varphi'}{B} \right) f \quad (4.24)$$

where, the integrals are to be taken over the appropriate populations and we have used the definition of  $v_{||*}$  as in Eq. (4.18). If we were to expand in small  $\varphi'$ , correct to first order, we would insert both  $f = f_0 + f_1$  in the right hand side integral in (4.24). However, since  $f_0$  is independent of  $\sigma$  for both species, the lowest order term, proportional to  $\sigma |v_{||*}| f_0$ , will vanish, by symmetry (with respect to the  $\mathcal{E}_*$  coordinates). To first order then, *two* terms must be retained: one from the  $\varphi$  term



in the parenthesis and the other from the  $f_1$  term. This yields the expression

$$(nU)_{\parallel} = \int \sum_{\sigma} \frac{B \, d\mu \, d\mathcal{E}_*}{|v_{\parallel*}|} \left( v_{\parallel*} f_1 - \frac{I\varphi'}{B} f_0 \right). \quad (4.25)$$

We emphasise that the second term in the integrand appears because of a ‘‘shift in the Jacobian’’, and acts on the lowest order  $f$ . In particular, even for small  $\varphi'$ , this term must be retained as it is of the same order as the preceding  $f_1$  term. Inserting for  $f_1$  in Eq. (4.25), we have

$$(nU)_{\parallel} = -I\varphi' \int \sum_{\sigma} B \, d\mu \, d\mathcal{E}_* \left( \overline{\left( \frac{v_{\parallel*}}{B} \right)} \frac{\partial f_0}{\partial \mathcal{E}_*} + \frac{1}{|v_{\parallel*}| B} f_0 \right) \quad (4.26)$$

where, for TPs, we recall that  $\overline{\left( \frac{v_{\parallel*}}{B} \right)} = 0$ . (Eq. (4.26) can be compared with Eq. (4.11), the corresponding equation from the previous section; the latter equation does not have a Jacobian shift term.)

Since  $\overline{\left( \frac{v_{\parallel*}}{B} \right)} = 0$  for TPs, the TP parallel flow from Eq. (4.26) is

$$(nU)_{\parallel}^{TP} = -\frac{I\varphi'}{B} \int_{TP} \sum_{\sigma} \frac{B \, d\mu \, d\mathcal{E}_*}{|v_{\parallel*}|} f_0^{TP}(\mathcal{E}_*, t) = -n^{TP} \frac{I\varphi'}{B} \quad (4.27)$$

where

$$n^{TP} = n_0 [\sqrt{\epsilon(1 + \cos \theta)} + O(\epsilon^{3/2})]$$

is the trapped particle density. This parallel flow is a rigid rotor flow and, we note, has an amplitude that corresponds precisely to the precession drift speed.

We can now also calculate the net poloidal velocity of the TP’s,

$$\mathbf{U}^{TP} \cdot \hat{\theta} = \int d^3v (\mathbf{b} v_{\parallel} + \mathbf{u}_{\mathbf{E}}) \cdot \hat{\theta}, \quad (4.28)$$

using Eq. (4.27), and we find

$$(n\mathbf{U})^{TP} \cdot \hat{\theta} = \frac{B_p}{B} \left( (nU)_{\parallel}^{TP} + n^{TP} \mathbf{u}_E \cdot \hat{\theta} \right) = \frac{\epsilon}{q} \left( (nU)_{\parallel}^{TP} + \frac{I\varphi'}{B} n^{TP} \right) = 0. \quad (4.29)$$

This is zero as expected. We note that the ‘‘Jacobian shift’’ is responsible for resolving the discrepancies.

The CP flow can be calculated from Eq. (4.26) assuming that the lowest order distribution function is a Maxwellian. This gives us

$$(nU)_{\parallel}^{CP} = n_0 \frac{I\varphi'}{B_0} \left[ \sqrt{\epsilon(1 + \cos \theta)} - 2\epsilon \cos \theta + O(\epsilon^{3/2}) \right]. \quad (4.30)$$

Note that, to lowest order, the CP flow is a rigid rotor flow, equal and opposite to the TP flow. Thus from Eqs (4.30),(4.27) we see that to dominant order,  $(nU)_{\parallel}^{CP} + (nU)_{\parallel}^{TP} \approx 0$ . This says that in the accounting of parallel flows for angular momentum, the large TP precession flow does not materialize as a large parallel flow since it is completely balanced by an oppositely directed CP flow. The  $\cos \theta$  term in the CP flow is the usual harmonic parallel flow.

The net poloidal velocity of the CP's is :

$$\mathbf{U}^{CP} \cdot \hat{\theta} = \int d^3v (\mathbf{b} v_{\parallel} + \mathbf{u}_E) \cdot \hat{\theta} = \frac{\epsilon}{q} \left( \frac{I\varphi'}{B_0} n^{CP} + O(\sqrt{\epsilon}) \right) \approx \mathbf{u}_E \cdot \hat{\theta} \quad (4.31)$$

Hence the poloidal velocity of the CPs is basically the  $\mathbf{E} \times \mathbf{B}$  flow, consistent with expectations.

Summing over the TP and CP flows, we get the total RH flow to be

$$(nU_{\parallel})^{TP+CP} = -\frac{I\varphi'}{B_0} (2\epsilon \cos \theta + 1.6\epsilon^{3/2} + O(\epsilon^2)) n_0. \quad (4.32)$$

Although the individual flows, Eqs. (4.27, 4.30), differ from the ones obtained using standard neoclassical methods, Eqs(4.14,4.13), the total flows, Eqs(4.32,4.15) from our calculation, match the RH solution. Remarkably, the large TP precession flow is balanced by an equally large and oppositely directed flow from the barely CPs.

### 4.6.3 RH Effective mass

We now consider the effective mass factor. For this, we would insert  $f_0 + f_1$  just found into the 2nd term of the angular momentum equation (4.20). The second term

$\partial_t \left\langle \int \sum_{\sigma} \frac{B d\mu d\mathcal{E}_*}{|v_{||*}|} \frac{I v_{||}}{B} f \right\rangle$  is just the time derivative of the parallel flow, viz.,  $\partial_t \left\langle \frac{I}{B} (n U_{||}^{\text{total}}) \right\rangle$ . A general expression for the parallel flow (for small  $\varphi'$ ) is given by Eq. (4.26). Inserting this expression as discussed, we obtain the angular momentum equation as

$$\partial_t \left\langle \varphi' \frac{|\nabla\psi|^2}{B^2} \right\rangle = -\partial_t \left\langle \left( \frac{I}{B} \right)^2 \varphi' \left( 1 + B \int_{CP} \sum_{\sigma} \frac{B d\mu d\mathcal{E}_*}{|v_{||*}| n_0} v_{||*} \overline{\left( \frac{v_{||*}}{B} \right)} \frac{\partial f_0}{\partial \mathcal{E}_*} \right) \right\rangle + \frac{\tau_{\perp}}{M}$$

Rearranging, we find

$$\partial_t u_E = \frac{F_{\perp}/m}{1 + \mathcal{D}}$$

where,

$$\begin{aligned} \mathcal{D} &= \left\langle \left( \frac{1}{B} \right)^2 \left( 1 + B \int_{CP} \sum_{\sigma} \frac{B d\mu d\mathcal{E}_*}{|v_{||*}| n_0} v_{||*} \overline{\left( \frac{v_{||*}}{B} \right)} \frac{\partial f_0}{\partial \mathcal{E}_*} \right) \right\rangle \left\langle \frac{|\nabla\psi|^2}{I^2 B^2} \right\rangle^{-1} \\ &\approx \frac{q^2}{\epsilon^2} \langle n U_{||}^{\text{total}} \rangle / (I \varphi' / B_0) \end{aligned} \quad (4.33)$$

represents the added effective mass.

To illuminate the role of each species in the effective mass, we consider the individual effective mass contributions from the TPs and CPs. The TP contribution to the effective mass factor is

$$\left\langle \left( n \frac{I}{B} U_{\parallel} \right)^{TP} \right\rangle = \partial_t \varphi' \left\langle n^{TP} \left( \frac{I}{B} \right)^2 \right\rangle = n_0 [0.9\sqrt{\epsilon} + 0.15\epsilon^{3/2}] \partial_t u_E \sim n_0 \sqrt{\epsilon} \frac{q^2}{\epsilon^2} \partial_t u_E. \quad (4.34)$$

Thus the effective mass contribution from the TPs is  $\sim O(q^2/\epsilon^{3/2}) \gg 1$  as expected from our toy model. The CP contribution to the effective mass factor is

$$\frac{q^2}{\epsilon^2} \langle n U_{\parallel}^{\text{total}} \rangle / (I\varphi'/B_0) \sim -\frac{q^2}{\epsilon^{3/2}} + 1.6 \frac{q^2}{\sqrt{\epsilon}} + O(q^2)$$

To lowest order this is equal and opposite to the TP effective mass. Thus the total effective mass is  $1 + 2q^2 + 1.6 \frac{q^2}{\sqrt{\epsilon}} + O(q^2)$ .

#### 4.6.4 Flows and effective masses for truncated distributions

We have seen that the cancellation of the rapid TP precession flow by an oppositely directed flow of barely CPs explains why the effective mass is smaller than that expected from the TPs alone. But this finding does not unequivocally address whether a distribution function of only TPs would result in the expected large effective mass. To address this, we consider the distribution function in (4.33) to be populated only for  $\mathcal{E}_* < \mu B_{max}$ . For this case, the TP contribution to the effective mass can be seen from Eq. (4.34) to be independent of the details of the distribution. The contribution is found to be  $\sim (q^2/\epsilon^2) n^{TP}$ . Since there are no CPs,  $n^{TP} = n$ . Therefore, we find the effective mass to be  $q^2/\epsilon^2$ , and the accompanying

TP flows to be

$$U_{\parallel}^{TP} = -\frac{I\varphi'}{B}, \quad \mathbf{U}^{TP} \cdot \hat{\theta} = 0.$$

These findings are completely consistent with our toy model.

To complete this line of reasoning, we consider a distribution function with only energetic circulating particles ECPs, i.e., all particles considered to lie well above the separatrix region ( $\mathcal{E}_* = \mu B_0(1 + \epsilon)$ ) in phase space (see solid curve in Fig.[4.4]). The distribution function  $f_0(\mathcal{E}_*)$  vanishes both at infinity and at the boundary  $\mathcal{E}_* = \mu \xi B_0$ , where,  $\xi$  is a parameter greater than 1, as shown in Fig. [4.4]. To calculate the response to this distribution, we use the following form of Eq. (4.26), obtained upon integrating the first term by parts:

$$(nU)_{\parallel} = -I\varphi' \left( \int B \, d\mu \, d\mathcal{E}_* \left( \frac{1}{|v_{\parallel*}|B} - \frac{\partial}{\partial \mathcal{E}_*} \overline{\left( \frac{v_{\parallel*}}{B} \right)} \right) f_0 - \int B \, d\mu \overline{\left( \frac{v_{\parallel*}}{B} \right)} f_0 \Big|_{\text{cutoff}} \right). \quad (4.35)$$

Using this form, the boundary term in Eq. (4.35) vanishes, and we get

$$(nU)_{\parallel} = -\frac{I\varphi'}{B_0} \int B_0 \, d\mu \, d\mathcal{E}_* \left( \frac{1}{|v_{\parallel*}|} - B \frac{\partial}{\partial \mathcal{E}_*} \overline{\left( \frac{v_{\parallel*}}{B} \right)} \right) f_0. \quad (4.36)$$

We evaluate this equation by an expansion in  $\epsilon$ . To lowest order in  $\epsilon$ , the RHS is

$$\frac{\partial}{\partial \mathcal{E}_*} \overline{\left( \frac{v_{\parallel*}}{B} \right)} \approx \frac{1}{B_0} \frac{1}{\sqrt{2(\mathcal{E}_* - \mu B_0)}} = \frac{1}{|v_{\parallel*}|B_0}.$$

Thus, the integral in (4.36) vanishes to lowest order, indicating that the parallel CP flow is smaller than the TP flow by at least  $O(\epsilon)$ . To evaluate this further, we consider the distribution to be of Maxwellian form but with a sharp cut-off at  $\mathcal{E}_* = \mu \xi B_0$  (as shown in Figure 4.4). We can then calculate the flows of the ECPs.

$$(nU_{\parallel})^{ECP} = -\frac{I\varphi'}{B_0} \left( \epsilon \cos \theta \, h_1(\xi) - (2 - \cos 2\theta) \, \epsilon^2 \, h_2(\xi) \right) \quad (4.37)$$

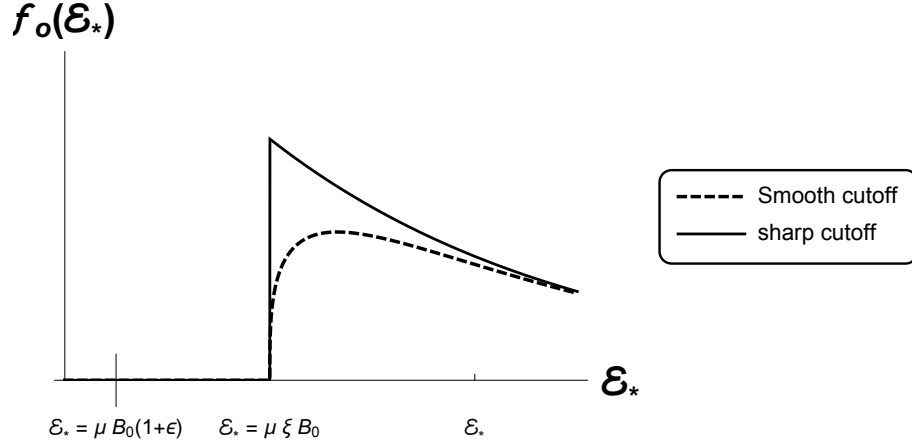


Figure 4.4: The distribution function is nonzero only well above the separatrix  $\mathcal{E}_* = \mu B_0(1 + \epsilon)$ .

where  $h_1, h_2$  are simple  $O(1)$  algebraic functions of  $\xi$ . Further approximating for large  $\xi$ , we get

$$U_{\parallel}^{ECP} = -\frac{I\varphi'}{B_0} (\epsilon \cos \theta + O(\epsilon^2)) \quad (4.38)$$

$$\mathbf{U}^{ECP} \cdot \hat{\theta} \approx \mathbf{u}_E \cdot \hat{\theta} . \quad (4.39)$$

The effective mass can be shown to be  $1 + O(q^2)$ . These results are consistent with fluid models where we get the oscillating Pfirsch-Schluter flows and the corresponding effective mass factor. Note that unless we approach the separatrix, there are no  $\sqrt{\epsilon}$  terms.

## 4.7 The role of the barely circulating particles

We have shown that the large trapped particle precession flow is cancelled to lowest order by an opposite flow from the circulating particles, so that there

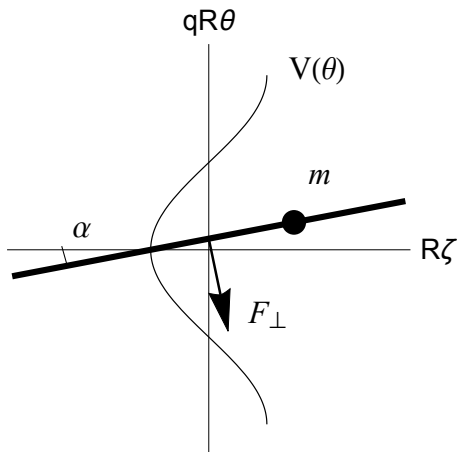


Figure 4.5: New toy model with potential  $V(\theta)$

are no large composite flows of order  $qu_E/\sqrt{\epsilon}$ . We would now like to understand the origin of the opposite flow. We show here that this flow is largely from a class of barely circulating particles. To demonstrate this, we begin with a more sophisticated toy model. Consider a particle on a rod as shown in figure[4.5]. The generalized coordinates are  $(x = R_0\zeta, y = qR_0\theta)$ , where  $\theta, \zeta$  are analogous to the poloidal and toroidal angles. In addition to being constrained to move only along the rod, the particle also feels a force due to an applied potential  $V(\theta) = \mu B(\theta) = \mu B_0(1 - \epsilon \cos \theta)$ . Thus, while our previous model allowed only freely circulating particles and deeply trapped particles, our new model allows these but also allows barely circulating particles.

The Lagrangian is given by,

$$L = \frac{1}{2} mR_0^2 \left( (q\dot{\theta})^2 + (\dot{\zeta} + q\dot{\theta} \cot \alpha)^2 \right) - \mu m B_0 (1 - \epsilon \cos \theta) - mR_0^2 c(t) \dot{\zeta}$$

where  $c = (\int F_{\perp} dt) \sin \alpha / (mR_0)$  is the impulse due to the applied force  $F_{\perp}$ .

The equation of motion is

$$\ddot{\theta} + \omega_b^2 \sin \theta = -\frac{F_{\perp} \cos \alpha}{qmR_0} \quad \text{where} \quad \omega_b = \sqrt{\mu B_0 \epsilon / qR_0}$$

which shows that our toy model is identical to a driven nonlinear pendulum. We can exploit this similarity to understand the particle trajectories in the presence of the external torque. Let's consider the case where  $F_{\perp}$  is time independent. In this case the work and energy  $\mathcal{E}$  of the driven pendulum is conserved. Thus,

$$\mathcal{E} = \frac{1}{2}\dot{\theta}^2 - \omega_b^2 \cos \theta + \frac{F_{\perp} \cos \alpha}{qmR_0} \theta = \text{constant}.$$

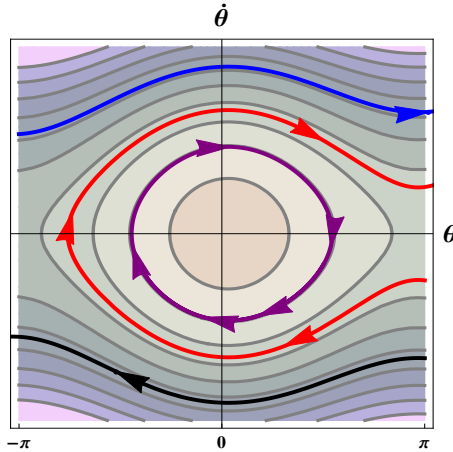


Figure 4.6: driven pendulum phase portrait

Figure (4.6) shows the contours of constant  $\mathcal{E}$  for nonzero  $F_{\perp}$ . Note that for small  $F_{\perp}$ , most of the trajectories resemble the original trajectories of a simple pendulum. However now there exists a group of particles near the separatrix which can change directions. In order to understand the change of direction (sign of  $\dot{\theta}$ ), we note that if we ignore the  $\omega_b^2$  term then the equation of motion is simply  $\ddot{\theta} = -g$ , where  $g \propto F_{\perp}$



is the effective gravity. This means that particles initially moving in the direction of “g” would not undergo a change in  $\dot{\theta}$ , but any particle moving opposite to the gravity would slow down and eventually change direction. Figure (4.6) shows a case where  $F_{\perp}, g < 0$  so that eventually  $\theta \approx -gt^2$  is positive. Thus we can understand how a small applied torque due to  $F_{\perp}$ , would generate a flow mostly due to the barely circulating particles. This is actually a very general phenomenon. A small perturbation (in this case  $F_{\perp}$ ) when added to a Hamiltonian system, keeps most of the original trajectories unchanged except for the ones near the separatrix.

In order to make contact with the drift kinetic system, let's now use the Hamiltonian description of the toy model. From the Lagrangian we calculate the canonical momenta,

$$\frac{P_{\theta}}{qmR_0^2} = \dot{\zeta} \cot \alpha + q\dot{\theta} / \sin^2 \alpha, \quad \frac{P_{\zeta}}{mR_0^2} = \dot{\zeta} - c + q\dot{\theta} \cot \alpha.$$

Since the Lagrangian is independent of  $\zeta$ , the “toroidal angle”,  $P_{\zeta}$  must be a constant. The Hamiltonian  $\mathcal{H}$ , can now be constructed,

$$\mathcal{H}/m - \frac{1}{2} \left( \frac{P_{\zeta}}{mR_0} + R_0 c \right)^2 = \frac{1}{2} v_{\parallel*}^2 + \mu B(\theta)$$

where,  $v_{\parallel*} \equiv qR_0\dot{\theta} = (P_{\theta} - q(P_{\zeta} + c mR_0^2) \cot \alpha)/qm$ . We can now define  $\mathcal{E}_* = \frac{1}{2} v_{\parallel*}^2 + \mu B(\theta)$  and write down Liouville's equation for this system in  $\{\theta, \zeta, \mathcal{E}_*, P_{\zeta}\}$  coordinates. We restrict ourselves to the “axisymmetric” problem by choosing  $\partial_{\zeta} = 0$ . Thus we have,

$$\frac{\partial f}{\partial t} + \frac{v_{\parallel*}}{qR_0} \frac{\partial f}{\partial \theta} - \frac{\partial}{\partial t} (R_0 c \cot \alpha) v_{\parallel*} \frac{\partial f}{\partial \mathcal{E}_*} = 0. \quad (4.40)$$

Let us compare the Liouville's equation (4.40) with the Drift kinetic equation (4.19).

We note that, by making the identification  $I\varphi'/B \iff -R_0 c \cot \alpha$ , we obtain a one-one relation. This is perhaps not surprising because both equations describe conservation of phase space volume.

Let us now try to understand the large cancellation of the RH flows. From the DKE-toy model equivalence, we see that  $I\varphi'/B \propto -F_\perp$ . Figure (4.6) now corresponds to the case where  $I\varphi'/B > 0$ . We have already seen that the trapped particles precess with speed  $u_{\parallel}^{TP} \approx qu_E/\epsilon$ . Their net flow from equation (4.27) is  $(nu_{\parallel})^{TP} = -n\sqrt{\epsilon}I\varphi'/B$  which is negative in this case. The barely circulating particles on the other hand, have a similar density,  $\sqrt{\epsilon}$ , but have an opposite flow  $n\sqrt{\epsilon}I\varphi'/B > 0$  (see Eq.(4.30)). Thus, the two flows cancel. A further explanation of the opposite flows are provided in the next section where we compare and contrast the collisional and the collisionless effective masses.

## 4.8 Effective mass factor in collisional and collisionless axisymmetric dynamics

The concept of “effective mass” or “added mass” is a very well known concept in fluid mechanics. It has important applications in naval architecture, since in ships the added mass can reach even a third of the mass of the ship. The physical reason behind the added mass is the fact that a body moving with non uniform speed through a fluid must also accelerate a volume of fluid surrounding it. Note that this concept is not related to buoyancy or viscosity.

We shall present a very simple derivation [31] of “effective mass” of a body

moving through an ideal fluid of density  $\rho$ . The flows shall be considered to be subsonic, incompressible, inviscid and potential, so that

$$\mathbf{U} = \nabla\phi, \quad \text{and} \quad \nabla \cdot \mathbf{U} = 0 \Rightarrow \nabla^2\phi = 0.$$

The force exerted on the moving body can be obtained from the hydrodynamic pressure through  $\mathbf{F} = -\nabla \int p dV$  and the pressure is given by  $p = \rho(\partial_t\phi + 1/2|\nabla\phi|^2)$ . When integrated over volume the second term vanishes owing to  $\nabla^2\phi = 0$  and we get  $\mathbf{F} = \partial_t \int \rho \mathbf{U} dV$ . This shows that the contribution of the flow adds up as an extra mass factor which depends on the geometry and shape of the body. We shall show next that this is exactly what happens in subsonic plasma dynamics.

Let us consider the adiabatically forced problem once again but this time assuming the plasma is described by ideal MHD. Instead of forcing a body we are forcing the flux tube which acts like a rigid “rod”. We shall also assume the flows to be subsonic and incompressible and given by  $\mathbf{U} = (U_{\parallel}/B)\mathbf{B} + u_E$ . In the subsonic limit,  $u_E = \mathbf{B} \times \nabla\varphi/B^2$ . In an axisymmetric system,  $\nabla \cdot \mathbf{U} = 0$  implies

$$\frac{U_{\parallel}}{B} = -\frac{I\varphi'}{B^2} + F(\psi) \tag{4.41}$$

where  $F(\psi)$  is an arbitrary flux function so that  $\mathbf{B} \cdot \nabla F = 0$ . We can write  $F$  in terms of the cross helicity  $\langle \int dV \mathbf{U} \cdot \mathbf{B} \rangle = \oint U_{\parallel} dl$  as,

$$F(\psi) = \oint dl U_{\parallel} + I\varphi' \frac{1}{\langle B^2 \rangle}, \quad \text{where} \quad \langle h \rangle \equiv \frac{\oint dl h/B}{\oint dl/B} \tag{4.42}$$

Let us now use angular momentum conservation to evaluate the effective mass. In axisymmetry it is given by

$$\partial_t \left\langle nM \left( \frac{IU_{\parallel}}{B} - \frac{|\nabla\psi|^2}{B^2} \right) \right\rangle = -\tau_{\perp}, \quad \tau_{\perp} = \left\langle n \frac{|\nabla\psi|}{B} F_{\perp} \right\rangle$$

Substituting for  $U_{\parallel}$  from Eq. (4.41) into Eq. (4.8) we get

$$\partial_t \varphi' \langle R^2 \rangle - I \partial_t F(\psi) = \frac{\tau}{nM} \quad (4.43)$$

In ideal MHD, cross-helicity is conserved. Choosing it to be zero initially implies

$$F(\psi) = I \varphi' \frac{1}{\langle B^2 \rangle}, \quad \frac{U_{\parallel}}{B} = I \varphi' \left( \frac{1}{\langle B^2 \rangle} - \frac{1}{B^2} \right) \quad (\text{MHD}). \quad (4.44)$$

In the large aspect limit this reduces to the well known Pfirsch-Schluter parallel flows  $U_{\parallel} \approx -2qu_E \cos \theta$ . Using this result in Eq. (4.43) gives

$$(1 + \mathcal{D}) \partial_t u_E = \frac{F_{\perp}}{M}, \quad \mathcal{D} = \left\langle \left( 1 - \frac{B^2}{\langle B^2 \rangle} \right) \right\rangle \left\langle \frac{|\nabla\psi|^2}{I^2 B^2} \right\rangle^{-1} \quad (4.45)$$

In the large aspect ratio, we recover the Pfirsch-Schluter effective mass factor:  $1 + \mathcal{D} \approx 1 + 2q^2$ .

Returning to the kinetic problem, it can be shown (Appendix H) that the second adiabatic invariant  $J_{\parallel} = \oint v_{\parallel} dl$  is conserved because the forcing is adiabatic. This is the kinetic analog of the cross helicity invariant of ideal MHD. Both  $F(\psi)$  and  $U_{\parallel}$  can be determined from conservation of  $J_{\parallel}$ . From the definition of  $U_{\parallel}$  we get,

$$\frac{U_{\parallel}}{B} = \int \frac{d^3v}{n} \frac{v_{\parallel}}{B} f = -\frac{I \varphi'}{B^2} + \int \frac{d^3v}{n} v_{\parallel*} f \quad (4.46)$$

where, we have used  $v_{\parallel*} = v_{\parallel} + I \varphi' / B$  and the symmetry property w.r.t  $v_{\parallel*} = 0$ .

This implies that,

$$F(\psi) = \int \frac{d^3v}{n} \frac{v_{\parallel*}}{B} f \quad (4.47)$$

Thus, for TPs,  $F(\psi)$  is always zero because the TP distribution function is an even function of  $v_{\parallel*}$ . For TPs, Eq. (4.43) therefore implies the large  $q^2/\epsilon^2$  effective mass. For CPs,  $F(\psi)$  is not necessarily zero. We obtain  $\partial_t F(\psi)$  from Eq. (H.5). Using angular momentum conservation Eq. (4.43) and Eq. (H.5), we recover Eq.(4.33).

Let us analyse the three cases that we just considered: the hydrodynamic problem, collisional and collisionless plasmas. In all these cases, the flows are time-dependent, subsonic and hence incompressible. The effective inertia arises in each case because the force on the body (“rod”) not only accelerates the body (“rod”) but also the associated flows in the surrounding liquid (parallel plasma flows).

Now let us try to understand the origin of the opposite flows from this point of view. In the fluid case, cross helicity is preserved and can be set to zero and stays zero. This completely determines  $F(\psi)$  for all time. In the kinetic problem, helicity evolves and has different values for different species of particles. Note that in the kinetic problem,  $F(\psi)$  is zero for TPs and the parallel flow is due to the fast precession. Thus, TPs always contribute the large  $q^2/\epsilon^2$  effective mass.  $F(\psi)$  is however nonzero and in fact different for the CPs above and below the separatrix. This breaks the up down symmetry dynamically, leading to differential parallel flow due to CPs. The fact that the CP flow must be opposite to the TPs also follow from the fact that  $J_{\parallel}$  must be conserved and  $J_{\parallel}$  is initially small because of the initial up down symmetry.

## 4.9 Summary

If a tokamak plasma is set into motion with an initial radial electric field  $E_r$ , the final state, after transients, is a much reduced  $E_r$  and a parallel zonal flow consistent with angular momentum conservation. However, the trapped particle precession angular momentum in the final  $E_r$  field is found to be much larger than the zonal flow. We have shown in this chapter that this discrepancy is resolved by the fact that there are reverse flows from the barely passing particles that cancel the large momentum from the TP precession momentum. Mathematically, we show that, even for small perturbations, there is a linear shift in the Jacobian of the phase space volume element, from  $E_r$ , that accounts for the reverse flows and the cancellation. The effective mass for this system is the same as that obtained by Rosenbluth and Hinton [6] and Xiao et.al [24]. However, the individual contributions from CPs and TPs to the effective mass are very different.

This calculation is done for the completely collisionless response. As is well-known, the separatrix plays an important role in this problem. In particular, the series expansion in  $\epsilon$  fails near the separatrix because of the logarithmic divergence in the bounce time. Discontinuous flows are obtained. This indicates an inner expansion in the separatrix region to fully understand the RH problem. In other work, we have shown we can use action angle coordinates to address the inner expansion. We have also shown that the RH effective mass can be obtained by simply conserving angular momentum and the second adiabatic invariant. Although, we used, MHD ordered drift kinetic equation, the results obtained here can be easily

generalized for the drift ordered axisymmetric system. Finally, as is well known [32], effects from collisions are also likely to play an important role and act to introduce friction between the large oppositely directed flows.

## Chapter 5: Conclusion

In Part I of this thesis we have carried out an analytical reduction scheme in a large aspect ratio tokamak to obtain a complete set of reduced sub-Alfvénic equations. We have shown that although the calculations are involved it is still possible to carry out a self consistent sub-Alfvénic asymptotic reduction. Salient features of our final reduced fluid equations are as follows. The complete set of equations derived for a large aspect ratio tokamak is self-consistent, nonlinear and sub-Alfvénic and includes dynamic Shafranov shifts. The modes are quasi-static and mostly flute-like and hence 2D. This is because the coordinate along the field line can be averaged out. Since these equations are 2D in space they offer a substantial advantage from the numerical standpoint. The modes that can be described are Mercier and Suydam interchange modes, GAMs, RH zonal flows, Stringer spin up, Resistive (but not ideal) Ballooning modes, 3D MHD “snake” equilibria and Pfirsch-Schluter cells. We do not expand in toroidal mode number, and unlike standard ballooning formalism, we can handle low shear and low to intermediate mode numbers. However, high mode numbers can not be described by our equations unless shear is very low.

In Part II, we have extended the methodology of Part I to sub-Alfvénic kinetic



MHD in the super-sonic limit. We have obtained a closed set of reduced kinetic equations which allow pressure anisotropy. These equations correctly reproduce the Mercier criterion and the GAM dynamics in the axisymmetric limit.

In Part III, we have studied the sub-Alfvénic dynamics in a collisionless axisymmetric tokamak using the kinetic MHD description due to Kulsrud. Our main result in this part is the analysis of trapped particle dynamics and their contribution to the effective inertia, which, in the fluid limit is given by the Pfirsch-Schluter factor. We have shown how the fast precession of trapped particles contribute to a large effective mass of order  $q^2/\epsilon^2$  but that is largely cancelled by a large opposite flow from the barely trapped particles. The resultant effective inertia is still large,  $\approx 1.6q^2/\sqrt{\epsilon}$  when compared to the Pfirsch-Schluter factor.

## Appendix 0: Various sub-Alfvénic modes

We shall discuss the various important sub-Alfvénic modes that can be described by the formalism developed in this thesis. Most of the description provided below is just to highlight the main features. A general description can be found in standard textbooks [1].

### Pressure driven modes

These are instabilities driven by the pressure gradient. The most unstable modes are internal modes which lie close to a rational surface where  $k_{\parallel} \Rightarrow 0$ . They can be further classified as Interchange modes and Ballooning modes.

### Interchange instabilities

They are the MHD equivalent of Rayleigh-Taylor instabilities observed in fluid dynamics. They occur when there is magnetic field curvature and the pressure gradient is sufficiently strong enough to overcome the restoring force from the magnetic line bending. An interchange of two flux tubes at two different radius in such cases lead to lowering of energy and hence an instability. Typically they are localized near a mode rational surface and they have large perpendicular wave numbers

and small parallel wave numbers giving them a “fluted” appearance. In a cylinder such modes are called Suydam modes while in toroidal geometry they are known as Mercier modes. Magnetic shear can stabilize interchange modes. Resistive interchange modes have slower growth rate compared to the ideal modes however typically resistive modes are always unstable [10].

## Ballooning modes

They occur only in toroidal geometry because toroidal coupling of modes on various rational surfaces allow a radially extended mode to exist. These modes set an upper limit on plasma beta. Ballooning modes occur near a region where the average magnetic curvature is unfavourable. They also have long parallel wavelengths and short perpendicular wavelengths like interchange modes. However they are not localized to any particular rational surface. There can be both ideal and resistive ballooning modes. In the sub-Alfvénic domain only weakly ballooning modes exist because the strongly ballooning limit excites Alfvén waves.

## Zonal flows

In plasma literature, the term zonal flow is generally used to describe a toroidally symmetric radial electric field perturbation, which is constant on a magnetic surface. It has been shown [33] that zonal flows can play important role in suppressing turbulence and in L-H transition. There are two important branches of zonal flows : Geodesic acoustic modes (GAMs) and the stationary zonal flows.

## GAMs

They are basically coherent nonlinear pendulum like oscillations of flux tubes in the “effective gravity” [14] due to toroidal curvature. The characteristic frequency is  $c_s/R$ . GAMs generate shear flows and hence are useful in suppression of turbulence. GAMs typically have a coupling of  $m = \pm 1$  poloidal modes. Linearly, collisionless GAMs are heavily Landau damped.

## Stationary Zonal flows

Studied theoretically by Rosenbluth-Hinton [6] and observed experimentally by Hillebrand et.al [34] in JET tokamak, the stationary zonal flows have been shown [33] to have a significant effect on turbulence saturation. They are the  $m = n = 0$  branch of the zonal flow modes. Sometimes in the literature the term zonal flow is used to describe only these modes.

## Various Resistive modes

In presence of finite resistivity, plasma is no longer ‘frozen-in’ and can diffuse past the magnetic fields. However charge/current neutrality requires a return parallel flow. This generates the so called “Pfirsch-Schluter” cells and the “Pfirsch-Schluter” flows.

Besides resistive interchange and ballooning modes there can be also other resistivity driven instability. The one that we shall find important in our discussion is the spontaneous poloidal spin-up mode also known as Stringer-spin up mode

[14]. These modes can exist if there is a poloidally asymmetric particle source but “Pfirsch-Schluter” flows can also self-consistently drive a poloidal-spin up.

## Appendix A: Operators and Commutators

### Definitions and properties of the operators

$$\partial_z = \sin \theta' \partial_r + \frac{1}{r} \cos \theta' \partial_\theta \quad (\text{A.1})$$

$$\partial_R = \cos \theta' \partial_r - \frac{1}{r} \sin \theta' \partial_\theta \quad (\text{A.2})$$

$$\partial_\theta = \partial_{\theta'} + \partial_\alpha, \quad \partial_\zeta = -(1/q_0) \partial_\alpha \quad (\text{A.3})$$

$$\{f, g\}_{z,R} = \partial_z f \partial_R g - \partial_R f \partial_z g = \hat{\zeta} \times \nabla g \cdot \nabla f \quad (\text{A.4})$$

$$\{f, g\}_{r,\theta} = \{f, g\}_{r,\theta'} + \{f, g\}_{r,\alpha} = -r \{f, g\}_{z,R} \quad (\text{A.5})$$

$$d_t = \partial_t + \{ \cdot, \varphi_2 \} \quad (\text{A.6})$$

$$d_1 = \partial_\zeta + \{ \cdot, \psi_0 \} = (1/q) \partial_{\theta'} \quad (\text{A.7})$$

$$d_2 = \{ \cdot, \Psi_1 \} + \mathcal{R}_1, \quad \mathcal{R}_1 = -x(d_1 + \partial_\zeta) \quad (\text{A.8})$$

$$d_1 f_0 = 0, \quad d_1^2 f_1 = -(1/q_0)^2 f_1 \quad (\text{A.9})$$

where,  $f_0, f_1$  demotes flute and first harmonic functions respectively and all Poisson brackets are assumed to be w.r.t  $(z,R)$  unless otherwise stated.

## Useful commutators

$$[d_1, \partial_z] = (1/q_0)\partial_R, \quad [d_1, \partial_R] = -(1/q_0)\partial_z \quad (\text{A.10})$$

$$[d_1, \partial_\zeta] = 0 \quad (\text{A.11})$$

$$[d_t, \partial_z] = \{\partial_z \varphi_2, \}, \quad [d_t, \partial_R] = \{\partial_R \varphi_2, \} \quad (\text{A.12})$$

$$[d_t, \partial_\zeta] = \{\partial_\zeta \varphi_2, \}, \quad (\text{A.13})$$

$$[d_t, d_1] = 0 \quad (\text{A.14})$$

$$[d_2, \partial_R] = (d_1 + \partial_\zeta) + (x/q_0)\partial_z - \{, \partial_R \Psi_1\} \quad (\text{A.15})$$

$$[d_2, \partial_z] = -(x/q_0)\partial_R - \{, \partial_z \Psi_1\} \quad (\text{A.16})$$

**Proofs:** We make use of the following identities:

$$[\hat{O}, \{f, \}] = \{\hat{O}f, \} \quad \text{where} \quad \hat{O} = (\partial_R, \partial_z, \partial_\zeta) \quad (\text{A.17})$$

$$[\{A, \}, \{B, \}] = \{\{A, B\}, \} \quad (\text{A.18})$$

The first identity follows from the fact that  $\hat{O}$  commutes past the Poisson bracket (in  $(z, R)$ ). The second identity follows from Jacobi's identity for Poisson brackets. Using the definition of  $d_1$  from (A.7),  $\partial_z \psi_0 = (z/q_0)$ ,  $\partial_R \psi_0 = (x/q_0)$ ,  $\partial_\zeta \psi_0 = 0$  and putting  $\hat{O} = (\partial_z, \partial_R, \partial_\zeta)$  we easily obtain (A.10, A.11). Similarly using the definition of  $d_t$  from (A.6) and the fact that  $\partial_t$  commutes with  $\partial_z, \partial_R, \partial_\zeta$  we obtain (A.12, A.13).

To prove (A.14) we first note that  $\partial_t$  does not contribute as  $\psi_0$  is time independent. Thus,  $[d_t, d_1] = \{\partial_\zeta \varphi_2, \} + [\{\psi_0, \}, \{\varphi_2, \}]$ . We can simplify the second term using (A.18) to obtain  $[d_t, d_1] = \{\partial_\zeta \varphi_2 + \{\varphi_2, \psi_0\}, \} = \{d_1 \varphi_2, \} = 0$ . Note that

the last equality follows from the fact that  $\varphi_2$  is a flute.

We shall now prove (A.15,A.16). From the definition of  $d_2$ , (A.8), we have  $[d_2, \hat{O}] = [\mathcal{R}_1, \hat{O}] + [\{ \cdot, \Psi_1 \}, \hat{O}]$  for  $\hat{O} = (\partial_R, \partial_z)$ . Using (A.17) we can simplify the second term to obtain  $-\{ \cdot, \hat{O}\Psi_1 \}$ . From the definition of  $\mathcal{R}_1$ , (A.8), we find that  $[\mathcal{R}_1, \hat{O}] = -[x, \hat{O}](d_1 + \partial_\zeta) - x[(d_1 + \partial_\zeta), \hat{O}]$ . Using the fact that  $\partial_\zeta$  commutes with  $\partial_z, \partial_R$ ,  $[x, \partial_R] = -1$ ,  $[x, \partial_z] = 0$  and (A.10) we finally obtain (A.15,A.16).



## Appendix B: Identities satisfied by flutes

For flutes  $f, g$ :

$$\{f, g\}_{R, \zeta} = (x/q_0)\{f, g\} \quad (\text{B.1})$$

$$d_t\{f, g\} = \{d_t f, g\} + \{f, d_t g\} \quad (\text{B.2})$$

$$z\partial_\zeta\{f, g\} = \{z\partial_\zeta f, g\} + \{f, z\partial_\zeta g\} + \{f, g\}_{R, \zeta} \quad (\text{B.3})$$

where  $\{f, g\} = \{f, g\}_{z, R}$  unless otherwise stated.

### Proofs:

For flute function  $f$ ,  $\partial_{\theta'} f = 0$  and (A.3) therefore implies  $\partial_\theta f = \partial_\alpha f = -q_0 \partial_\zeta f$ . From (A.5) we get  $\{f, g\} = -(1/r)\{f, g\}_{r, \alpha}$  for flutes  $f$  and  $g$ . Finally, expanding  $\{f, g\}_{R, \zeta}$  using (A.2, A.3) we find that the terms proportional to  $\sin \theta'$  cancel while the  $r \cos \theta' (= x)$  terms give  $\{f, g\}_{R, \zeta} = -(x/rq_0)\{f, g\}_{r, \alpha} = (x/q_0)\{f, g\}$ .

To prove (B.2) we shall use the fact that the  $\partial_t$  term in the expression for  $d_t$  commutes past the Poisson Brackets. Thus, from (A.6), we have  $d_t\{f, g\} = \{\partial_t f, g\} + \{f, \partial_t g\} - \{\varphi_2, \{f, g\}\}$ . We shall now use Jacobi's identity in the form  $\{\varphi_2, \{f, g\}\} = \{\{\varphi_2, f\}, g\} + \{f, \{\varphi_2, g\}\}$  to rewrite the second term. Collecting all the terms and using the definition of  $d_t$  leads to (B.2).

In (B.3) we first note that since  $\partial_\zeta$  commutes past the Poisson bracket, it is distributive just like  $\partial_t$ . Therefore,  $\{z\partial_\zeta f, g\} + \{f, z\partial_\zeta g\} - z\partial_\zeta\{f, g\} = \{z, g\}\partial_\zeta f +$

$\{f, z\}\partial_\zeta g = -\{f, g\}_{R, \zeta}$ , rearranging which leads to [B.3](#).

## Appendix C: Evaluation of $\{\langle \partial_R \Psi_1, n_0 \rangle\}$

Here, we show that the term  $\{\langle \partial_R \Psi_{1\beta}, n_0 \rangle\}$  in Eq (2.66) evaluates to zero.

Noting that  $-r\{, \}_{z,R} = \{, \}_{r,\theta}$  and using (A.5), we rewrite

$$\{\partial_R \Psi_1, n_0\}_{r,\theta} = \{\partial_R \Psi_1, n_0\}_{r,\theta'} + \{\partial_R \Psi_1, n_0\}_{r,\alpha}.$$

Noting that  $n_0$  is a flute function, the previous averaged Poisson bracket reduces to  $(1/r)\{\langle \partial_R \Psi_1 \rangle, n_0\}_{(r,\alpha)}$ . Thus, it remains to calculate  $\langle d_R \Psi_1 \rangle$ .

The complete  $\Psi_1$  equation is given by

$$\Delta \Psi_1 = \partial_R(\psi_0 - 2\bar{\beta}q_0n_0), \quad \Delta = \partial_R^2 + \partial_z^2 \quad (\text{C.1})$$

We first consider the particular solution for  $\Psi_{1x}$  as driven by  $\psi_0$ . Since we need  $\partial_R \Psi_{1x}$ , we rewrite the above equation as  $\Delta \partial_R \Psi_{1x} = \partial_R^2 \psi_0$ . However, since  $\psi_0 = \psi_0(r)$ , the RHS can be rewritten as  $(1/2)\Delta \psi_0$ . Thus,  $\partial_R^2 \Psi_{1x} = (1/2)\psi_0$  and, therefore,  $\{\langle \partial_R \Psi_{1x} \rangle, n_0\} = (1/2)\partial_\alpha n_0$ .

We now solve (C.1) for the particular solution proportional to  $\bar{\beta}$ . We proceed similarly as for  $\psi_0$ . First, we write  $\Delta$  in  $(\psi_0, \theta', \alpha)$  coordinates as

$$\Delta = \frac{1}{r}\partial_r(r\partial_r) + \frac{1}{r^2}\partial_\alpha^2 + \frac{1}{r^2}\partial_{\theta'}^2 + 2\frac{1}{r^2}\partial_\alpha\partial_{\theta'} \quad (\text{C.2})$$

from which we note that

$$\langle \Delta f \rangle = \left( \frac{1}{r}\partial_r(r\partial_r) + \frac{1}{r^2}\partial_\alpha^2 \right) \langle f \rangle = \underline{\Delta} \langle f \rangle \quad (\text{C.3})$$

We want the particular solution for  $\langle \partial_R \Psi_{1\beta} \rangle$  in the equation

$$\Delta \partial_R \Psi_{1\beta} = -2q_0 \bar{\beta} \partial_R^2 (n_0)$$

. Upon averaging, we have

$$\langle \Delta \partial_R \Psi_{1\beta} \rangle = \underline{\Delta} \langle \partial_R \Psi_{1\beta} \rangle \tag{C.4}$$

$$\langle \partial_R^2 \bar{\beta} n_0 \rangle = \frac{1}{2} \underline{\Delta} \bar{\beta} n_0 \tag{C.5}$$

whereupon,  $\langle \partial_R \Psi_{1\beta} \rangle = -\bar{\beta} n_0$ . It follows that  $\{\langle \partial_R \Psi_{1\beta} \rangle, n_0\} = 0$ .

## Appendix D: Evaluation of $\langle \partial_z N_1 \rangle$ in the subsonic limit

Starting from  $\partial_z N_1 = 2 (q_0^2 / \bar{\beta}) \partial_z (n_0 d_t \partial_z \varphi_2)$  and using  $[d_t, \partial_\zeta] = \{\partial_\zeta \varphi_2, \}$ , we obtain

$$\langle 2 \partial_z N_1 \rangle = (2q_0^2 / \bar{\beta}) \langle 2 d_t \partial_z (n_0 \partial_z \varphi_2) + \{n_0, (\partial_z \varphi_2)^2\} \rangle \quad (\text{D.1})$$

The second term is nonlinear and hence can be discarded. Using the fact that  $[d_t, d_t] = 0$  we can commute the  $d_t$  operator past the average along the field line denoted by angle brackets. Thus,

$$\begin{aligned} \langle 2 d_t \partial_z (n_0 \partial_z \varphi_2) \rangle &= 2 d_t \langle \partial_z (n_0 \partial_z \varphi_2) \rangle \\ &= d_t \left( \left( \partial_r + \frac{1}{r} \right) (n_0 \partial_r \varphi_2) + \frac{1}{r} \partial_\alpha \left( \frac{1}{r} n_0 \partial_\alpha \varphi_2 \right) \right) \end{aligned} \quad (\text{D.2})$$

$$= d_t \nabla_\perp \cdot (n_0 \nabla_\perp \varphi_2) \quad (\text{D.3})$$

Here we have used the expression for  $\partial_z$  as given in Appendix A and the fact that for a first harmonic quantity  $N = N_s \sin \theta' + N_c \cos \theta'$ , we have

$$2 \langle \partial_z N \rangle = \left( \partial_r + \frac{1}{r} \right) N_s + \frac{1}{r} \partial_\alpha N_c. \quad (\text{D.4})$$

Therefore,

$$\langle 2 \partial_z N_1 \rangle = \frac{2 q_0^2}{\bar{\beta}} d_t \nabla_\perp \cdot (n_0 \nabla_\perp \varphi_2) = \frac{2 q_0^2}{\bar{\beta}} d_t \Omega \quad (\text{D.5})$$

## Appendix E: Conserved quantities

### E.1 Flux and magnetic helicity conservation

Conservation of flux follows trivially from Eqn. 2.86 and the fact that  $\Psi$  vanishes upon  $\oint \partial_{\theta'}$ . Also  $\mathbf{A} \cdot \mathbf{B} = -(I\psi)/R^2 \sim -\psi$  to lowest order and is hence conserved.

### E.2 Cross helicity

Dividing the parallel flow equation (2.89) by  $n$  and performing the volume integral with  $rdrd\alpha d\theta'$  gives us  $\partial_t \int dV U_{\parallel} = 0$ .

### E.3 Angular momentum

In the axisymmetric limit  $\partial_{\alpha} = 0$  and  $\partial_t n = 0$ . Taking the  $r$  moment of the  $U_{\parallel c}$  equation (2.94) we get,

$$\partial_t \int r dr (nU_{\parallel c} r) + \int r dr n \partial_r \varphi U_{\parallel s} + (\bar{\beta}/q_0) \int r dr r N_s = 0 \quad (\text{E.1})$$

In order to evaluate the second term we multiply Eqn (2.93) by row vector

$(U_{\parallel s} \ U_{\parallel c})$  and Eqn (2.94) by  $(1/n)(N_s \ N_c)$  and add them to obtain

$$(1/2)\partial_t \int r dr (N_s U_{\parallel s} + N_c U_{\parallel c}) = n \partial_r \varphi U_{\parallel s} \quad (\text{E.2})$$

To evaluate the last term in (E.1), we multiply the vorticity equation Eqn(2.87) by  $r^2/(2q_0)$  and integrate over the volume. Integrating by parts we have

$$\partial_t \int r dr \frac{r}{q_0} n \partial_r \varphi + \frac{\bar{\beta}}{q_0} \int r dr r N_s = 0$$

Using all of the above, we finally obtain,

$$\partial_t \int r dr \left( nr(U_{\parallel c} - \frac{1}{q_0} \partial_r \varphi) + \frac{1}{2}(N_s U_{\parallel s} + N_c U_{\parallel c}) \right) = 0 \quad (\text{E.3})$$

## E.4 Energy

We shall start with the vorticity equation (2.87), multiply by  $\varphi$  and integrate over volume. The first term after integrating by parts in a straightforward manner produces  $-\partial_t \int r dr d\alpha (n/2) |\nabla \varphi|^2$ .

Similarly using  $d_t \underline{\psi} = 0$  the shear term can be massaged to give

$$\partial_t \int r dr d\alpha \frac{1}{2} |\nabla \underline{\psi}|^2.$$

The  $2\bar{\beta} \langle \partial_z N \rangle \varphi$  term can be simplified to obtain

$$\bar{\beta} \int r dr d\alpha \left( N_s \partial_r \varphi + \frac{1}{r} N_c \partial_\alpha \varphi \right).$$

Next, we multiply Eqn (2.93) by row vector  $(1/n)(N_s \ N_c)$  and Eqn (2.94)

by  $(U_{\parallel s} \ U_{\parallel c})$  and add them to obtain

$$\frac{1}{2}\partial_t \int r dr \left( \frac{\bar{\beta}}{n} \langle N^2 \rangle + n \langle U_{\parallel}^2 \rangle \right) = \bar{\beta} \int r dr d\alpha \left( N_s \partial_r \varphi + \frac{1}{r} N_c \partial_\alpha \varphi \right) \quad (\text{E.4})$$

$$\text{where } \langle U_{\parallel}^2 \rangle = \frac{1}{2}(U_{\parallel c}^2 + U_{\parallel s}^2), \langle N^2 \rangle = \frac{1}{2}(N_c^2 + N_s^2)$$

Finally, using  $\int r dr d\alpha (\partial_t(rn) + (1/r)\partial_\alpha n)$  we can rewrite the  $(1/q_0^2 - 1)$  term as  $-\partial_t \int r dr d\alpha (2\bar{\beta}(1/q_0^2 - 1)rn)$ . Thus,

$$\partial_t \int r dr d\alpha \left( \frac{1}{2}n|\nabla\varphi|^2 + \frac{1}{2}|\nabla\psi|^2 + \frac{1}{2} \left( \frac{\bar{\beta}}{n} \langle N^2 \rangle + n \langle U_{\parallel}^2 \rangle \right) - 2\bar{\beta} \left( \frac{1}{q_0^2} - 1 \right) rn \right) = 0 \quad (\text{E.5})$$



## Appendix F: Vorticity equation in $\mathcal{E}$ and $\mathcal{E}_*$ coordinates

We can derive the vorticity equation using  $\langle \mathbf{j} \cdot \nabla \psi \rangle = 0$ . From Kulsrud's Eqn [8] (46), It can be shown that

$$\partial_t \left\langle n \frac{|\nabla \psi|^2}{B^2} \varphi' \right\rangle = \left\langle \int d^3v \frac{e}{m} \vec{v}_d \cdot \nabla \psi f \right\rangle + \tau_\perp \quad (\text{F.1})$$

In axisymmetric system,

$$\vec{B} \times \nabla \psi \cdot \nabla B = I \vec{B} \cdot \nabla B, \quad \nabla_{\parallel} |_{\mathcal{E}} \left( \frac{1}{2} v_{\parallel}^2 \right) = -\mu \nabla_{\parallel} B$$

and we can show that

$$\frac{e}{m} \vec{v}_d \cdot \nabla \psi = v_{\parallel} \nabla_{\parallel} |_{\mathcal{E}} \left( \frac{I v_{\parallel}}{B} \right) = -(v_{\parallel}^2 + \mu B) I \frac{\nabla_{\parallel} B}{B^2}$$

Now,

$$\begin{aligned} \mathcal{E}_* &= \frac{1}{2} v_{\parallel}^2 + \mu B + I \varphi' \frac{v_{\parallel}}{B} = \frac{1}{2} v_{\parallel*}^2 + \mu B - \left( \frac{I \varphi'}{B} \right)^2 \\ \Rightarrow \nabla_{\parallel} |_{\mathcal{E}_*} \left( \frac{1}{2} v_{\parallel*}^2 \right) &= -\frac{\nabla_{\parallel} B}{B} \left( \mu B + \left( \frac{I \varphi'}{B} \right)^2 \right) \end{aligned}$$

So,

$$\begin{aligned} v_{\parallel*} \nabla_{\parallel} |_{\mathcal{E}_*} \frac{v_{\parallel}}{B} &= v_{\parallel*} \nabla_{\parallel} |_{\mathcal{E}_*} \left( \frac{v_{\parallel*}}{B} - \frac{I \varphi'}{B} \right) \\ &= -(v_{\parallel}^2 + \mu B) \frac{\nabla_{\parallel} B}{B^2} = v_{\parallel} \nabla_{\parallel} |_{\mathcal{E}} \left( \frac{v_{\parallel}}{B} \right) \end{aligned}$$

Appendix G: Proof of equivalence of Angular momentum and vorticity equation

Using the following identities,

$$\begin{aligned}\vec{B} &= I\nabla\zeta + \nabla\zeta \times \nabla\psi \\ R^2\vec{\nabla}\zeta \cdot \vec{U}_E &= -\frac{|\nabla\psi|^2}{B^2}\varphi', \quad R^2\vec{\nabla}\zeta \cdot \hat{b} = \frac{I}{B}\end{aligned}$$

the angular momentum conservation condition Eqn(4.20), simplifies to

$$\begin{aligned}\partial_t \left\langle n \frac{|\nabla\psi|^2}{B^2} \varphi' \right\rangle - \tau_\perp &= \partial_t \left\langle \int d^3v \frac{Iv_\parallel}{B} f \right\rangle \\ &= \left\langle \int d^3v \frac{Iv_\parallel}{B} \left( \frac{\partial}{\partial t} \Big|_{\mathcal{E}_*} + \frac{\partial I\varphi' v_\parallel}{\partial t} \frac{\partial}{B \partial \mathcal{E}_*} \right) f \right\rangle \\ &= \left\langle \int d^3v \frac{Iv_\parallel}{B} \left( -v_{\parallel*} \nabla_\parallel \Big|_{\mathcal{E}_*} f \right) \right\rangle \\ &= \left\langle \int d^3v \frac{e}{m} \vec{v}_d \cdot \nabla\psi f \right\rangle \quad (\text{By parts})\end{aligned}$$

## Appendix H: $J_{||}$ invariance

We shall now solve Eq. (4.22) without linearization. The second adiabatic invariant  $J_{||}$  is defined by

$$J_{||} = \oint_{\mathcal{E}_*} v_{||} dl = \oint_{\mathcal{E}_*} v_{||*} dl - \sigma q R \frac{I\varphi'}{B_0} \quad (\text{H.1})$$

Let us now show that Eq. (4.22) implies  $f_0 = f_0(J_{||})$ . Using  $\mathcal{E}_* = v_{||}^2/2 + \mu B + v_{||}I\varphi'/B$ , we can show that

$$\frac{\partial v_{||}}{\partial \mathcal{E}_*} = \frac{1}{v_{||*}} \quad \left. \frac{\partial v_{||}}{\partial t} \right|_{\mathcal{E}_*} = -\frac{1}{v_{||*}} \frac{v_{||}}{B} \partial_t I\varphi' \quad (\text{H.2})$$

$$\frac{\partial J_{||}}{\partial \mathcal{E}_*} = \oint_{\mathcal{E}_*} \frac{dl}{v_{||*}}, \quad \partial_t J_{||} = -\oint_{\mathcal{E}_*} \frac{1}{v_{||*}} \frac{v_{||}}{B} \partial_t I\varphi' \quad (\text{H.3})$$

Let us now simplify Eq. (4.22) using the above properties of  $J_{||}$ .

$$\frac{\partial f_0}{\partial t} + \frac{\partial I\varphi'}{\partial t} \left( \frac{v_{||}}{B} \right) \frac{\partial f_0}{\partial \mathcal{E}_*} = 0 \quad \Rightarrow \quad \frac{\partial f_0}{\partial t} \frac{\partial J_{||}}{\partial \mathcal{E}_*} - \frac{\partial J_{||}}{\partial t} \frac{\partial f_0}{\partial \mathcal{E}_*} = 0 \quad (\text{H.4})$$

The last equation implies  $f_0 = f_0(J_{||})$ .

Note the crucial sigma dependence in the expression for  $J_{||}$  as noted earlier by Taylor et al and Henrard [35,36]. There is no such sigma dependence in the trapped particle distribution because the second term averages out as  $\sigma = \pm 1$  for TPs. This means that the CP distribution is not symmetric with respect to  $v_{||*} = 0$  and this results in non zero CP flows from  $f_0$ .

Let us now obtain an evolution equation for the  $F(\psi)$ . Taking the  $v_{||*}$  moment of Eq. (4.22) and integrating over velocity space and along  $\mathbf{B}$ , we get

$$\partial_t F(\psi) = -\partial_t \varphi' \oint dl \int \frac{d\mu d\mathcal{E}_*}{|v_{||*}|} v_{||*} \overline{\left(\frac{v_{||}}{B}\right)} \frac{\partial f_0}{\partial \mathcal{E}} \quad (\text{H.5})$$

We can also calculate evolution of the cross-helicity by using

$$\partial_t \oint \nabla U_{||} = -I \partial_t \varphi' \oint \frac{dl}{B} + \partial_t F(\psi) \oint \frac{dl}{B} B^2$$

Thus although  $J_{||}$  is conserved, the cross-helicity moment need not be conserved in a kinetic system.

## Bibliography

- [1] Jeffrey P Freidberg. Ideal magnetohydrodynamic theory of magnetic fusion systems. *Reviews of Modern Physics*, 54(3):801, 1982.
- [2] R White, D Monticello, MN Rosenbluth, H Strauss, and BB Kadomtsev. Numerical study of nonlinear evolution of kink and tearing modes in tokamaks. In *International Conference of Plasma Physics, Tokyo*, pages 495–504, 1974.
- [3] Hank R Strauss. Nonlinear, three-dimensional magnetohydrodynamics of non-circular tokamaks. *Physics of Fluids (1958-1988)*, 19(1):134–140, 1976.
- [4] HR Strauss. Dynamics of high  $\beta$  tokamaks. *Physics of Fluids (1958-1988)*, 20(8):1354–1360, 1977.
- [5] HR Strauss. Finite-aspect-ratio mhd equations for tokamaks. *Nuclear Fusion*, 23(5):649, 1983.
- [6] MN Rosenbluth and FL Hinton. Poloidal flow driven by ion-temperature-gradient turbulence in tokamaks. *Physical review letters*, 80(4):724, 1998.
- [7] FL Waelbroeck. Models for sub-alfvénic magnetodynamics of fusion plasmas. *Fusion Science and Technology*, 59(3):499–518, 2011.
- [8] Russell M Kulsrud. *MHD description of plasma*. Princeton University, 1980.
- [9] GF Chew, ML Goldberger, FE Low, and Yoichiro Nambu. Relativistic dispersion relation approach to photomeson production. *Physical Review*, 106(6):1345, 1957.
- [10] James F Drake and Thomas M Antonsen Jr. Nonlinear reduced fluid equations for toroidal plasmas. *Physics of Fluids (1958-1988)*, 27(4):898–908, 1984.
- [11] R Schmalz. Reduced, three-dimensional, nonlinear equations for high- $\beta$  plasmas including toroidal effects. *Physics letters A*, 82(1):14–17, 1981.

- [12] R Izzo, DA Monticello, W Park, J Manickam, HR Strauss, R Grimm, and K McGuire. Effects of toroidicity on resistive tearing modes. *Physics of Fluids (1958-1988)*, 26(8):2240–2246, 1983.
- [13] RD Hazeltine, M Kotschenreuther, and PJ Morrison. A four-field model for tokamak plasma dynamics. *Physics of Fluids*, 28(8):2466, 1985.
- [14] AB Hassam and JF Drake. Spontaneous poloidal spin-up of tokamak plasmas: Reduced equations, physical mechanism, and sonic regimes. *Physics of Fluids B: Plasma Physics (1989-1993)*, 5(11):4022–4029, 1993.
- [15] Richard D Hazeltine and James D Meiss. Shear-alfvén dynamics of toroidally confined plasmas. *Physics Reports*, 121(1-2):1–164, 1985.
- [16] Jesus J Ramos. Theory of global interchange modes in shaped tokamaks with small central shear. *Physical review letters*, 60(6):523, 1988.
- [17] RJ Hastie and JB Taylor. Validity of ballooning representation and mode number dependence of stability. *Nuclear Fusion*, 21(2):187, 1981.
- [18] JW Connor, RJ Hastie, and JB Taylor. Stability of toroidal plasmas: the influence of magnetic shear, periodicity and rotation. *Plasma physics and controlled fusion*, 46(12B):B1, 2004.
- [19] JW Connor and JB Taylor. Ballooning modes or fourier modes in a toroidal plasma? *Physics of Fluids (1958-1988)*, 30(10):3180–3185, 1987.
- [20] J Manickam, N Pomphrey, and AMM Todd. Ideal mhd stability properties of pressure driven modes in low shear tokamaks. *Nuclear fusion*, 27(9):1461, 1987.
- [21] AB Hassam and RG Kleva. Double adiabatic theory of collisionless geodesic acoustic modes in tokamaks. *arXiv preprint arXiv:1109.0057*, 2011.
- [22] SV Novakovskii, CS Liu, RZ Sagdeev, and MN Rosenbluth. The radial electric field dynamics in the neoclassical plasmas. *Physics of Plasmas (1994-present)*, 4(12):4272–4282, 1997.
- [23] Per Helander and Dieter J Sigmar. *Collisional transport in magnetized plasmas*, volume 4. Cambridge University Press, 2005.
- [24] Yong Xiao, Peter J Catto, and Kim Molvig. Collisional damping for ion temperature gradient mode driven zonal flow. *Physics of Plasmas (1994-present)*, 14(3):032302, 2007.
- [25] Edward Frieman, Ronald Davidson, and Bruce Langdon. Higher-order corrections to the chew-goldberger-low theory. *Physics of Fluids (1958-1988)*, 9(8):1475–1482, 1966.
- [26] FL Hinton and SK Wong. Neoclassical ion transport in rotating axisymmetric plasmas. *Physics of Fluids (1958-1988)*, 28(10):3082–3098, 1985.

- [27] Adil B Hassam and Russell M Kulsrud. Time evolution of mass flows in a collisional tokamak. *Physics of Fluids (1958-1988)*, 21(12):2271–2279, 1978.
- [28] Grigory Kagan and Peter J Catto. Arbitrary poloidal gyroradius effects in tokamak pedestals and transport barriers. *Plasma Physics and Controlled Fusion*, 50(8):085010, 2008.
- [29] Matt Landreman and Peter J Catto. Effects of the radial electric field in a quasisymmetric stellarator. *Plasma Physics and Controlled Fusion*, 53(1):015004, 2010.
- [30] AB Hassam. Poloidal rotation of tokamak plasmas at super poloidal sonic speeds. *Nuclear fusion*, 36(6):707, 1996.
- [31] TR Auton, JCR Hunt, and M Prud’Homme. The force exerted on a body in inviscid unsteady non-uniform rotational flow. *Journal of Fluid Mechanics*, 197:241–257, 1988.
- [32] FL Hinton and MN Rosenbluth. The mechanism for toroidal momentum input to tokamak plasmas from neutral beams. *Physics Letters A*, 259(3):267–275, 1999.
- [33] PH Diamond, SI Itoh, K Itoh, and TS Hahm. Zonal flows in plasmas a review. *Plasma Physics and Controlled Fusion*, 47(5):R35, 2005.
- [34] JC Hillesheim, E Delabie, H Meyer, CF Maggi, L Meneses, E Poli, JET Contributors, EUROfusion Consortium, et al. Stationary zonal flows during the formation of the edge transport barrier in the jet tokamak. *Physical review letters*, 116(6):065002, 2016.
- [35] RJ Hastie, JB Taylor, and FA Haas. Adiabatic invariants and the equilibrium of magnetically trapped particles. *Annals of Physics*, 41(2):302–338, 1967.
- [36] Jacques Henrard. The adiabatic invariant theory and applications. In *Hamiltonian Dynamics. Theory and Applications*, pages 77–141. Springer, 2005.